Long-lived asymmetrically retained proteins and approaches to identify modulators of lifespan and age-associated phenotypes of budding yeast

Nathaniel Thayer

A dissertation

submitted in partial fulfillment of the

requirements for the degree of

Doctor of Philosophy

University of Washington

2016

Reading Committee:

Daniel E Gottschling, Chair

Celeste A Berg

Stanley Fields

Program Authorized to Offer Degree:

Molecular and Cellular Biology

University of Washington

Abstract

Long-lived asymmetrically retained proteins and approaches to identify modulators of lifespan and age-associated phenotypes of budding yeast

Nathaniel Thayer

Chair of the Supervisory Committee:
Dr. Daniel E Gottschling
Fred Hutchinson Cancer Research Center – Affiliate Investigator – Basic Sciences
University of Washington – Affiliate Professor – Genome Sciences

The budding yeast, *Saccharomyces cerevisiae*, is an excellent model for studying aging because it is a highly tractable, unicellular eukaryote that experiences a short, finite, replicative lifespan (RLS). Despite these advantages, genome-wide and unbiased approaches for studying aging in yeast have been hindered by technical difficulties in observing cells of any significant age. Using the previously described Mother Enrichment Program (MEP), our lab has recently been able to identify several age-associated phenotypes. In this dissertation, I will present three projects in which I adapted the MEP to study the replicative aging process and age-associated phenotypes. In the first project, I will present the identification and characterization of a novel type of protein that we have termed Long-lived Asymmetrically Retained Proteins (LARPs). Some of the proteins identified likely contribute to the aging process. In the

second project, I will present a lifespan assay that was designed to monitor the lifespan of aging yeast cells and require minimal experimentalist intervention during the aging process. The assay presented here should be amenable to high-throughput screening and allow unbiased screens for novel modulators of lifespan. In the third project, I will present an unbiased genome-wide screen for genetic suppressors of the age-associated loss of mitochondrial membrane potential. This screening strategy identified several effectors of this process and should be adaptable to study the genetic regulators of other age-associated processes.

TABLE OF CONTENTS

LIST OF FIGURES

LIST OF TABLES

ACKNOWLEDGEMENTS

First, I do not think that I can adequately thank everybody that contributed valuable support and encouragement throughout this process. My experiences and interactions with everybody at both the Fred Hutch and University of Washington made my time spent here easier, more valuable, and certainly more enjoyable. Specifically, I would like to thank my mentor, Dan Gottschling. In addition to showing me how to be a better scientist, thank you for showing me the importance of working on something in which you are interested (and giving me the freedom to do so). You provided an outstanding environment in which to learn by filling your lab with amazing people – again, I don't think I can thank all of the past and present members of the Gottschling Lab enough. I have to thank Christina Leverich – you were not only a great collaborator, but a truly good friend. And last, I must thank my wife, Mai. Simply, I would not have been able to do this without you.

Chapter 1. INTRODUCTION

1.1 How do I define aging?

Aging is the process of growing old. While seemingly simplistic, there is a lot contained within this definition. First, there is a state of 'old age' that nearly every individual is familiar with. While most are capable of describing some of the more obvious effects of growing old, this state can also be scientifically defined by the age-associated changes that occur in a number of specific cellular systems. Second, aging is a process. We, as humans, do not suddenly become aged. Aging is a gradual process in which there are a number of characterizable changes that occur that can be attributable to the state of 'old age'.

1.2 Lifespan, aging, and the known effectors of this process

There have been two ways to identify components of the aging process: identify modulators of lifespan and identify phenotypes of the aging process. It is not difficult to argue that there is a strong connection between the aging process and lifespan; altered lifespan could be caused by a change in either the rate of aging or the ability to tolerate advanced age. The stated goal of many research projects on aging is to identify ways to increase human lifespan or health span. As a result, many studies have focused on identifying modulators of lifespan in various model systems, rather than identifying phenotypes of advanced age. And while lifespan may be a tractable read-out for screening purposes, it may not be the most sensitive method to identify specific aging pathways.

Of the aging phenotypes observed in humans, many seem to be complex and highly variable across tissue types and even individuals (Finch and Kirkwood, 2000). The incidence rates and effects of cancers, cardiovascular diseases, and neurodegenation are not equal in everybody as they age. This variability likely indicates that there may not be one single aging pathway and that everyone experiences the onset/effects of various aging pathways with slightly different kinetics (Partridge, 2010). Simply, not everyone is dying for the same reasons at the same time. This variation is likely to occur in model

organisms as well and presents a complication when using altered lifespan to screen for effectors of aging pathways. Interventions that strongly suppress or increase some age-related phenotype may not actually dramatically alter the average lifespan of a population. Additionally, it is plausible that aging pathways may have varying levels of effect in different organisms. A pathway that has a small effect in determining the lifespan of a nematode could have a major role in determining the lifespan of mammals.

Additionally, caution should be used when using lifespan to establish epistasis of various modulators of lifespan. Often, if two interventions do not extend lifespan beyond either individual intervention, it is concluded that they likely act on the same aging pathways (Kennedy, 2008). While this interpretation is one possible scenario, it is also possible that each intervention does indeed act independently, but a third, unknown, aging process has now become limiting to lifespan. If acting strongly enough, this unknown limiter would mask the otherwise additive effects of the tested modulators of lifespan, indicating epistasis even if they affect lifespan by completely different mechanisms.

As technologies develop and various phenotypes of advanced age of several models are identified, these may allow for more sensitive screening methods for effectors of specific aging pathways. This additional dissection of the aging process will also allow for more accurate epistasis mapping of the known modulators of lifespan. Additionally, understanding age related phenotypes in model organisms would give insight into possible age-related diseases; they may identify particular tissues in metazoans that are sensitive to the aging process; and they may identify organelles or cellular processes that are sensitive to the aging process within individual cells.

Despite the concerns expressed above, altered lifespan has been a useful tool for identifying components of the aging process. In most model organisms, altered lifespan is a tractable readout for screening and several interventions have been found to drastically alter the lifespan in these systems (Kennedy, 2008).

Caloric (Dietary) Restriction -- 80 years ago, McCay et al. reported that the lifespan of laboratory rats could be increased by simply limiting their diet (McCay et al., 1935). Over the years, this observation was developed and expanded into the model of Dietary or Caloric Restriction (DR or CR) and shown to affect lifespan across nearly all organisms

(Kennedy et al., 2007). And while CR may be the most conserved and studied method to alter lifespan, the mechanism by which it does so is still unclear.

What is Dietary and Caloric Restriction? The terms CR and DR are often used interchangeably, but this has likely led to some confusion in the field. I will try to use CR when referring to experimental conditions thought to reduce total caloric intake, availability, or perception. I will use the term DR to refer to conditions that alter dietary composition. One of the most surprising aspects of the DR and CR models is that there is not a clear consensus as to what defines a restricted environment. While some of this disagreement can be explained by experimental differences between the various model organisms, the exact requirements of DR/CR within each system are still often unclear (Kennedy et al., 2007; Tatar, 2011; Walker et al., 2005). Initial DR studies simply limited or diluted the food available to the subject animals. While this may be sufficient for rodents, it has been debated whether dilution of nutrients reduces the final caloric intake of worms and flies (Gershon and Gershon, 2002; Tatar, 2011). Some of these concerns have been addressed with careful administration of experimental diets, but there remains considerable variance between DR/CR regimens and protocols. In flies, this variation can be lab-to-lab differences in the concentrations of yeast and sugars in the media (Tatar, 2007). In worms, DR/CR can be administered by dilution of bacterial food or genetics, but each concentration or mutant could potentially have unique effects (Walker et al., 2005). And in yeast several different concentrations of sugars, and even dilutions of nitrogen sources, have been used to study the effects of DR/CR (Jiang et al., 2000; Steinkraus et al., 2008).

Recent work from the Partridge Lab has explored the exact requirements of DR and has shown that restriction of a single essential amino acid, methionine, is both necessary and sufficient to cause lifespan extension by DR in *Drosophila* (Grandison et al., 2009). Reports from mouse models have also implicated specific amino acids during DR (Miller et al., 2005; Richie et al., 2004; Zimmerman et al., 2003). While general nitrogen limitation has been shown to extend lifespan in the budding yeast model, carbon source manipulation has been the dominant method of administering CR (Jiang et al., 2000; Kaeberlein et al., 2004). Yeast cells are traditionally grown on 2% glucose, a

concentration optimized for maximum growth rate of a culture (Amberg et al., 2005). Strikingly, this 2% concentration seems to represent a local minimum for lifespan, where either a decrease or increase can lead to an extension of lifespan (Kaeberlein et al., 2002). Many single gene mutations have been made that alter the yeast cells' ability to metabolize or sense nutrients correctly and are thought to alter lifespan in a manner similar to CR (Kaeberlein et al., 2005a). Similarly, single genes mutations are thought to mimic or induce CR in other model organisms, e.g. *eat-2*, a mutation limits a nematode's ability to ingest food (Lakowski and Hekimi, 1998).

The role of Dietary/Caloric Restriction in aging and lifespan: Despite extensive research on the subject, the mechanism by which DR or CR extend lifespan has remained elusive (Kennedy et al., 2007). It was initially thought that limiting nutrients slowed the metabolic rate of the organisms and reduced damaging by-products of metabolism, like Reactive Oxygen Species (ROS). While this was an attractive theory, some restricted organisms actually have increased metabolic rates and increased levels of ROS (Houthoofd et al., 2002a, 2002b). To complicate the matter further, the direct effect of nutrient limitations on aging cells is starting to be doubted (Durieux et al., 2011). Recent reports have shown that the sensory system plays a crucial role of CR, where simply the exposure to odorants of nutrients may be sufficient to eliminate the effects in CR (Libert et al., 2007). Additionally, CR may be more important for determining lifespan than altering the aging process. Flies that are switched between CR and non-CR diets immediately adapt to the mortality rates of flies that have been on that diet their entire life (Mair et al., 2003). This intriguing result argues that the CR state is more important for tolerating old age rather than altering the rate of aging. If CR was altering the aging process, the time spent under CR conditions should leave an organism effectively younger, even once transferred to normal conditions. This result was particularly exciting because it suggests that interventions affecting lifespan can be made in already aged organisms. While the exact mechanism by which CR extends lifespan remains unclear, many studies have tested its effects on known aging pathways.

Insulin signaling and lifespan: age-1 was one of the first single-gene mutations discovered that could dramatically alter lifespan in *C. elegans* (Johnson, 1990). Later, this gene was

found to encode a PI3 kinase downstream of the insulin receptor, DAF-2 (Fig 1.1) (Kimura, 1997; Morris et al., 1996). As these genes of the insulin-signaling pathway were further characterized, it appeared that any reduction of insulin signaling could increase lifespan; loss of signaling molecule, receptor, and several downstream kinases all lead to lifespan extension (Schaffitzel and Hertweck, 2006). DAF-16, the FOXO transcription factor normally under negative control of the insulin-signaling cascade, is required for lifespan extension by decreased insulin signaling; *daf-16* mutants eliminate any lifespan extension by mutations in the signaling pathway (Ogg et al., 1997). The effects of insulin signaling on lifespan have been extended to *Drosophila* and mouse models, indicating that this may be an evolutionarily conserved longevity pathway (Partridge et al., 2011; Selman et al., 2008). Even mutants of *SCH9*, which encodes the budding yeast homolog of the AKT kinase in the insulin- signaling cascade, have been shown to affect lifespan of yeast cells(Kaeberlein et al., 2005a).

Insulin-signaling and dietary restriction: Because it was known that insulin signaling responds to nutrients levels, once the importance of insulin-signaling in affecting lifespan was discovered, it was proposed that CR could be acting through the insulin-signaling pathway to extend lifespan. While a plausible hypothesis, this is unlikely to be the case in nematodes or mice because of two experimental results. First, CR is able to further extend the lifespan and modulate aging phenotypes in insulin-signaling mutants(Al-Regaiey et al., 2005; Lakowski and Hekimi, 1998). Second and more convincingly, lifespan extension by CR is not dependent on DAF-16 (Lakowski and Hekimi, 1998). These results are contradicted by experiments performed in flies and mice, where CR is unable to further extend the lifespan of insulin signaling mutants (Clancy et al., 2002).

Insulin-signaling effects on lifespan and aging: The insulin-pathway is a relatively general nutrient sensing pathway and DAF-16 is known to regulate many genes (Carter and Brunet, 2005). Some target genes play roles in sugar metabolism, DNA damage response, ROS detoxification, cell cycle arrest and energy homeostasis. While the diverse effects of this pathway could explain some of the differences between *Drosophila* and *C. elegans,* where all downstream targets are unlikely to be conserved, they also raise the question if these each represent aging pathways or processes that allow the

organisms to tolerate old age. In preliminary experiments, when the activity of components of the signaling pathway are altered during the aging process, there seems to be an immediate shift in mortality rates (Giannakou et al., 2007). Similar to CR, this result indicates that this pathway is controlling sensitivity to age rather than altering the rate of aging. Although intriguing, additional experiments will help to confirm this result and to test specific downstream targets of the pathway individually.

TOR signaling and lifespan: Target of rapamycin (TOR) is part of a signaling pathway that is thought to play a role in amino acid sensing (Fig 1.1)(Hay and Sonenberg, 2004; Oldham and Hafen, 2003). Signaling through the TOR pathway regulates translation initiation, ribosome biosynthesis, autophagy and protein degradation. Mutations in this pathway alter lifespan in several organisms, e.g. worms, flies, and yeast (Guarente and Kenyon, 2000).

Multiple effectors of the TOR signaling pathway: In *Drosophila*, individually inhibiting downstream signals is enough to block the lifespan extension caused by reduced TOR signaling (e.g. regulation of autophagy and translation) (Partridge et al., 2011). This result is slightly surprising, where it might be expected that downstream effects are additive and might indicate that the multiple outputs of TOR signaling act together to extend lifespan. And although similar results have been found in *C. elegans,* it is still unclear whether all of these downstream targets act together or individually to affect lifespan (Hansen et al., 2007).

The TOR pathways and dietary restriction: It was plausible that CR could be acting through this nutrient-sensing pathway to alter lifespan, but again, the experimental results show that it is not that simple. In *Drosophila,* CR is able to further extend the lifespan of TOR-signaling mutants(Kapahi et al., 2004). This result is contrary to experiments in *C. elegans*, where CR is not thought to further extend lifespan of animals with decreased TOR signaling (Hansen et al., 2007). The same is found in yeast, where low glucose concentrations do not further extend the lifespan of TOR mutants (Kaeberlein et al., 2005a).

Insulin signaling and TOR pathways overlap: There is both documented and proposed overlaps between the TOR and insulin-signaling pathways. PEP-2, an oligopeptide

transporter under the transcriptional control of DAF-16 and insulin signaling, is thought to be upstream of TOR signaling (Fig 1.1). In *C. elegans* a *pep-2* mutant enhances the phenotype of partial RNAi knockdown of TOR, but does change the lifespan of a more efficient knockdown (Meissner et al., 2004; Walker et al., 2005). Indicating further overlap of the two pathways, DAF-16 is reported to be required for full lifespan extension by mutants in downstream targets of TOR in *C. elegans* (Hansen et al., 2008; Henderson et al., 2006). This result further argues that the multiple downstream targets of TOR may interact to affect lifespan, however is somewhat surprising because the initial lifespan extension by knockdown of TOR was thought to be DAF-16 independent (Hansen et al., 2007)

The controversial sirtuins: Another class of genes that have been proposed to affect aging and lifespan are the sirtuins, or specifically Sir2, a NAD+-dependent histone deacetylase (North and Verdin, 2004). While the proteins seem to be conserved across many organisms, their effects on lifespan of these organisms has been a subject of controversy.

The discovery of sirtuins: The initial observation that sirtuins affect lifespan was made in yeast. Lifespan is difficult to screen for in the yeast system. In an attempt to identify mutants with altered lifespan, stress resistance in young cells was used as a surrogate phenotype to quickly screen mutants because it was noticed to correlate with longevity. An allele was identified, *sir4-42*, that caused a 45% increase in lifespan(Kennedy et al., 1995). Upon further characterization, this mutation was shown to cause relocalization of the sirtuin complex to the rDNA, effectively increasing Sir2 activity at this site (Kennedy et al., 1997; Smith et al., 1998; Steinkraus et al., 2008). Subsequently, deletion of *SIR*2 caused a dramatic decrease in lifespan, while overexpression of *SIR2* increased lifespan (Kaeberlein et al., 1999, 2005b). The mechanism by which Sir2 affects lifespan is primarily thought to be from its role at the rDNA locus, a repetitive segment of the genome that is susceptible to recombination and genome instability. Cells lacking Sir2 are thought to accumulate Extra-chromosomal RNA Circles (ERCs), a byproduct of recombination events, which are proposed to have a negative impact on lifespan (Kaeberlein et al., 1999; Sinclair and Guarente, 1997). This mechanism is supported by the finding that loss of Fob1, a component of the replication-fork barrier at the rDNA that facilitates the

recombination event, restores the lifespan of a *sir2Δ* (Kaeberlein et al., 1999). However, the *sir2Δ fob1Δ* double-mutant is not as long-lived as the *fob1Δ* single-mutant, possibly indicating an additional role for Sir2 regulating lifespan.

In addition to Sir2, there are a number of other proteins in this class, globally referred to as the sirtuins (North and Verdin, 2004). These proteins all share an NAD-dependent deacylase activity and regulate many metabolic processes in the cell. Several members of this class have been implicated in the aging process in metazoans. Specifically, SIRT3, a mitochondrial-localized sirtuin, modulates several age-associated processes and its underexpression was reported to be seemingly incompatible with longevity in humans (Brown et al., 2013; Finkel et al., 2009; Rose et al., 2003).

Caloric restriction and sirtuins: One proposed mechanism of CR in yeast cells has been that an altered metabolic state under CR leads to a change in NAD/NADH ratios (Lin et al., 2002). An increase in NAD levels could activate the NAD-dependent histone deacetylases and increase their apparent beneficial effects on lifespan. Although it was originally reported that Sir2 activity is increased under CR, this finding has been contradicted in subsequent reports (Riesen and Morgan, 2009; Smith et al., 2009b). Additionally, lifespan extension by CR was originally reported to be Sir2 dependent, but again this finding has been contradicted in subsequent reports (Kaeberlein, 2010; Kaeberlein et al., 2004). The original finding is thought to be dependent on the strain used in the study, arguing that there are strain-to-strain differences in the effects of Sir2 on lifespan and this is only the beginning of the controversy surrounding sirtuins.

Is Sir2 a yeast specific modulator of lifespan?: ERCs do not appear to be a phenotype of aging in any other organism, so it is unlikely that sirtuins affect lifespan in other organisms by regulating ERC formation (Laun et al., 2007). However, deletions of sirtuins can cause a decrease in lifespan in *Drosophila*, possibly indicating an importance during aging (Aström et al., 2003). And it was originally reported that over-expression of Sir2 could also extend lifespan in worms and flies, generating excitement for possible drug interventions that could activate sirtuins and extend lifespan (Rogina and Helfand, 2004; Tissenbaum and Guarente, 2001). Recently, a contradictory finding was published, reporting the absence of lifespan extension due to *SIR2* overexpression in these same

animals (Burnett et al., 2011). In *C. elegans,* the lifespan was shown to segregate with a separate locus, possibly affecting sensory neurons, not *SIR2* overexpression. In *Drosophila,* neither the original transgenic line, nor a stronger overexpression line, were long-lived when compared to a transgenic control. These overexpression lines were only long-lived when inappropriately compared to a complete WT strain. Despite the controversy, reports continue to be published claiming lifespan extension by overexpression of various sirtuin proteins in higher eukaryotes (Kanfi et al., 2012). It will be interesting to see how the role of sirtuins in the aging of these various models is resolved.

1.3 WHY DOES AN ORGANISM AGE?

Evolution and aging. One theory as to why an organism ages is that there is not a substantial selective pressure for an organism that does not age (Kirkwood, 2002). Once an individual reproduces, successfully passing on its genetic information to the next generation, there is no longer any evolutionary benefit to survive. Furthermore, any selective pressure for longevity decreases after each round of reproduction. Therefore, it makes sense that evolution has selected for organisms that are able to successfully reproduce, rather than for longevity. There are a number of proposed mechanisms for how this, or similar principles, translate into the aging process that we observe in many organisms (Austad, 2010; Croft et al., 2015; Gershon and Gershon, 2001; Hamilton, 1966; Kirkwood and Melov, 2011; Stumpferl et al., 2012). Most of these hypotheses are just an extension of the same basic observation and are beyond the scope of this study. I will simply state that there does not appear to be an evolutionary pressure for an organism that does not age.

Accumulation of damage and its consequences. Organisms are constantly subject to various forms of damage (Medvedev, 1990). The sources of this damage are sometimes intrinsic, byproducts of basic biochemical processes required for life. Some sources of damage are environmental, like solar radiation or ingestion of reactive chemicals. Almost no matter the source of the damage, the longer the lifespan of an organism, the longer it is exposed to each of these stressors. Cellular damage can manifest in a number of forms

in aged cells:

Damaged proteins – Proteins are known to experience several forms of damage (Chondrogianni et al., 2014) – oxidation, glycosylation, aggregation, among others. These damaged proteins could alter function in a number of ways. First, a damaged protein could lose function or activity. Second, a damaged protein could gain function, possibly by altering regulatory interactions. Damaged proteins are likely a contributing factor to the aging process.

Damaged DNA – There is a large correlation between cancer and increased age(Stewart et al., 2003). Various forms of DNA damage are likely responsible for this link (Garinis et al., 2008; Veatch et al., 2009). Damaged DNA can lead to gene dysregulation, segregation defects leading to further damage, and the induction of stress responses.

Damaged lipids – While relatively understudied, compared to protein and DNA, lipids are known to accumulate age-associated damage (Rikans and Hornbrook, 1997). Additionally, stressors known to modify lipids can have dramatic effects on lifespan. Oxidative and other damages alter biochemical properties of lipids that are responsible for establishing membrane fluidity, permeability and signaling capabilities.

Damaged organelles – Altered organelle function is likely the results of the damage to its components, some of which are listed above. The mitochondrion (discussed in more detail below) has likely received the most attention, but many organelles and cellular structures have shown age-associated changes to form and function – e.g. peroxisome, nucleolus, nuclear pore complex, extracellular matrix (Bratic and Larsson, 2013; Kurtz and Oh, 2012; Manivannan et al., 2012; Savas et al., 2012).

Seemingly, every macromolecule in the cell has the potential to experience age-associated damage. And the accumulation of these damaged molecules may lead to the many phenotypes of the aging process, both on the organismal and cellular levels.

Many sources of cellular damage are known to affect how an organism ages, and modulating exposure to these damaging agents is known to modulate lifespan(Medvedev, 1990). At times this correlation has led to confusion in the field – when an agent is suggested to be *a* cause of aging, this association is misinterpreted (or overstated) to be *the* cause of aging. In reality, cells are constantly and simultaneously coping with many sources of damage, each with the potential of shortening lifespan. Eventually, the cumulative consequences from each of these damaged systems becomes overwhelming, and the cell is no longer able to maintain viability, resulting in the end of lifespan.

Asymmetrical distribution of damage. By definition, age-associated damage must be distributed asymmetrically between each generation. Unless the rate of reproduction is sufficient to prevent damage from accumulating, eventually all individuals in the population would die of 'old age', if it is not somehow partitioned (Coelho et al., 2013). However, if one cell/organism retains a majority of the damage, this is the one that ages, whereas the cell/organism that does not inherit damage is then rejuvenated, able to live a full lifespan. In most mammals, it appears that this asymmetry and rejuvenation is accomplished at the germline. In yeast, it appears that this asymmetry and rejuvenation occurs between mother and daughter cells.

Some damage can be repaired. A cell is not passive and can actively respond to many of the forms of damage it faces. Additionally, some systems are inherently resistant to accumulating damaged components. There are a number of ways an organism can cope with age-associated damage:

> *A cell can repair the damaged molecule, restoring function.* A cell has several systems in place designed to repair damaged proteins, lipids and DNA (Chondrogianni et al., 2014; Pacifici and Davies, 1991). For example, proteins can be refolded by chaperones to cope with aggregation, reduced by reductases after certain types of oxidative damage, or deglycosylated after certain types of glycosylations (Kim et al., 2013; Squier, 2001).
>
> *A cell can replace (turn over) a damaged molecule.* Some types of damage are irreversible, or, it is easier to degrade and replace the damaged molecule. A cell can target damaged proteins for either lysosomal (vacuole in yeast) or proteosomal

degradation and replace the damaged molecule with a newly synthesized protein in order to maintain function (Goldberg, 2003). Additionally, some molecules are constantly subject to turn-over and replacement (irrespective of damage), possibly a passive system to limit the amount of damaged molecule present at any given time.

A cell can target organelles for repair/degradation. There are even a number of quality control pathways on the organelle level. For example, the PINK1/PARKIN system is thought to be responsible for monitoring the fitness of the mitochondria within the cell (Poole et al., 2008). If mitochondrial dysfunction is sensed in the organelle, phosphorylation and ubiquitination events target the organelle for degradation.

Repair pathways may not be sufficient to prevent aging. Despite the existence of several pathways that should be capable of responding to many sources of damage, it appears that these responses are not sufficient to prevent the aging process. Most simplistically, the rate of damage may exceed the rate at which a cell is able to repair or replace a damaged molecule, leading to an eventual accumulation of damage. Supporting this hypothesis, Kruegel et al. reported that simply upregulating the proteasome, one of the cellular pathways responsible for degradation of damaged proteins, is sufficient to extend lifespan in budding yeast (Kruegel et al., 2011).

There are a number of things that could impair a cell's ability to replace/repair damage. Some proteins just may be inaccessible for exchange with a newly synthesized version. Large complexes tend to consist of proteins with long half-lives, predicted to be due to an inability to exchange components and to the energy cost associated with assembling the complex (Toyama and Hetzer, 2013). This property may put these types of complexes at particular risk for age-associated dysfunction. For example, the nuclear pore complex is known to both have extremely low turnover and to experience an age-associated decline in function (D'Angelo et al., 2009; Savas et al., 2012; Toyama et al., 2013).

It is possible that the damage itself is toxic to the cell, such that it is not the loss of function of the damaged cellular component, but the damage itself that leads to various aging phenotypes. For example, aggregated proteins are capable of inducing aggregation of

healthy protein (Stefani and Dobson, 2003). Additionally, certain types of reactive oxygen species are self-propagating, generating more reactive molecules (Dickinson and Chang, 2011). If the cell is not able to remove the damaged molecules and the damage is toxic, this could lead to age-associated accumulation of this toxin. Likely, several of these, and other factors, limit an organism's ability to cope with age-associated damage, ultimately leading to the end of lifespan.

Aging is complex because the cellular network is complex. Several years ago, Constanzo et al., published the global genetic interaction network for the cellular processes in a yeast cell (Costanzo et al., 2010). One conclusion from this study was that the network is highly interconnected. Every cellular process or component interacts with many other processes. This observation supported previous global protein-protein interaction studies that found a number of physical interactions between components of seemingly independent cellular processes (Schwikowski et al., 2000). The network of genetic and physical interactions in a cell is undeniably complex. When one activity of the cell is impaired, these effects extend to the other interacting processes throughout the network. These interactions are likely maintained (or new interactions develop) as an organism ages, suggesting that as one function or process is affected by age, it likely affects the activity of other interacting processes.

One crucial step to understanding the aging process is to understand which processes are directly affected by age and which are affected through their interactions in the network. There may be a handful of initiating events, each responsible for several independent aging cascades, each that may be independently modulated. Identifying the causal and reactive components of the aging process could have large implications in how we think about the process.

1.4 YEAST AS A MODEL FOR AGING RESEARCH

Yeast as a model system. The budding yeast, *Saccharomyces cerevisiae,* is a tractable model system that has been used to study many different aspects of biology and human disease (Botstein and Fink, 2011). There are a number of traits that make yeast an exceptional model system to understand the basic processes that govern the aging

process and they have been well reviewed elsewhere (Denoth Lippuner et al., 2014; Kaeberlein et al., 2007; Sinclair et al., 1998; Steinkraus et al., 2008; Tissenbaum and Guarente, 2002). However, I do want to point out the abundance of genetic tools and knowledge available in the yeast system. The yeast genome is extremely well characterized and a number of collections have been created that have systematically deleted or overexpressed every gene in the yeast genome (Giaever et al., 2002; Ho et al., 2009). Because of these tools, and several reasons listed below, yeast is an ideal organism to understand the genetics that govern the aging process.

How yeast cells age. Yeast is a single-cell eukaryotic cell that experiences a short and finite lifespan (Kaeberlein, 2010). Because it is a single-cell organism, we can study how a single cell experiences the aging process, outside of the potentially complicating factors of a multicellular organism. There are two models to study aging in yeast, chronological and replicative lifespan. Chronological lifespan is the length of time a single cell can survive in a non-dividing state (Fabrizio and Longo, 2007). Replicative lifespan is defined by the number of daughter cells a single mother cell can produce prior to senescence and death (Mortimer and Johnston, 1959). Both models of lifespan show several characteristics of an age-associated decline and are thought to be models of aging cells in either a dividing or non-dividing state. Both models have contributed to the understanding of the overall aging process (Kaeberlein et al., 2007). I have focused on the replicative aging model because it provides a unique opportunity to study the aging process specifically in dividing cells, which is not possible in other model systems.

The need for technology and recent innovations. While the initial observation that yeast cells have a finite replicative lifespan was made nearly 60 years ago, work to understand this phenomenon has been limited by technological hurdles (Mortimer and Johnston, 1959). These technical limitations primarily stem from the fact that old cells are exceedingly rare in a population of cells. Theoretically, if a single cell was used to start a culture, this cell will divide and age. However, the daughter cells produced during each division will also start to divide, creating daughter cells of their own. After just 7 cell divisions, no where near the average lifespan for most strains, the oldest cells comprise only <1% of the population. After, 25 divisions, approaching the average lifespan for our

lab strain, the oldest cells are about .000003% of all the cells of the culture. Simply, cells of significant age are difficult to observe. Furthermore, a significant number of cells cannot feasibly be cultured long enough before cells start dying of old age. If 10^7 cells (required for many biochemical techniques) were to be aged for 25 divisions, without any type of intervention, a researcher would need thousands of liters of media to prevent the culture from saturating and exhausting the available nutrients.

In order to isolate aging mother cells and measure the lifespan of a cell, researchers have traditionally relied on a micromanipulation assay (Steffen et al., 2009). This assay requires a researcher to use a micro-dissection needle to physically remove a daughter cell after each cell division. This technique, while functional, is extremely tedious and not amenable to high-throughput studies. It is also very difficult to identify and quantify aging phenotypes using this assay. Manual intervention is required for every cell, after every cell division, and such that only a very limited number of aged cells can be isolated. Also, dissections must be performed on an agar plate, where high-resolution imaging of subcellular components is impossible.

The technological limitations of the micromanipulation technique are well understood, and a number of groups have developed alternative techniques in order to study old cells. Magnetic purification protocols have been developed to quickly purify large quantities of aged cells for biochemical studies of the aging process(Sinclair and Guarente, 1997; Smeal et al., 1996). Genetic tools have been developed in attempts to selectively prevent daughter cells from dividing(Jarolim et al., 2004). One example which I used throughout my work is the Mother Enrichment Program (MEP)(Lindstrom and Gottschling, 2009). The MEP is an inducible genetic system that selectively arrests daughter cells, making cells of significant age far more common in the population. The MEP is a tractable method that allows researchers to culture a significant number of cells (10^7-10^8) for their entire lifespan with minimal intervention during the aging process. A number of other techniques have been developed attempting to make studying the aging process more amenable. I will introduce various techniques throughout this dissertation and discuss how they were used or why alternative approaches were taken.

Studies using the micromanipulation assay to measure the lifespan have identified several important regulators of the aging process (Kaeberlein et al., 2005a; McCormick et al., 2015). The contributions from these studies should not be overlooked. However, due to the limitations of the assay, only certain processes could be screened for potential effects on the aging process, or compromises had to be made to make the experiments feasible. During an initial screen of the yeast deletion collection for modulators of lifespan, only fives cells of each genotype could be assayed for lifespan in order to complete the screen. This cursory screening approach identified several of the most severe modulators of lifespan, but had a high number of false-negative results likely occurred simply because of low sample number. New technology is still required to fully explore and identify possible effectors of the aging process.

Age is asymmetrically distributed between mother and daughter cells. Each cell division of a budding yeast cell is asymmetric. There are known asymmetries of several cellular components and properties, some as simple and obvious as the size difference between a mother and daughter cell (Kennedy et al., 1994). Others are complex and regulated pathways to establish asymmetry of specific proteins and RNAs. Ace2 is a transcription factor that is preferentially enriched in daughter-cell nuclei, initiating daughter-cell-specific transcription profiles (Laabs et al., 2003). A number of mother-enriched proteins have been identified, tending to have roles at the vacuole or plasma membrane, yet a number of these asymmetries are of unknown consequence(Eldakak et al., 2010; Yang et al., 2015).

Age is also asymmetrically distributed during each cell division (Mortimer and Johnston, 1959). The mother cell ages, but produces a rejuvenated daughter that has a full replicative potential of its own. This asymmetry in the aging process, coupled with the observation age acts dominantly during cell-fusion assays, has led to the idea of a putative ‘aging factor’ that is asymmetrically retained in the aged mother cell (Egilmez and Jazwinski, 1989; Müller, 1985). While reviewed in detail elsewhere, there have been a number of suggestions of putative aging factors that are retained in a mother cell throughout successive cell divisions (Henderson and Gottschling, 2008). The

identification of potentially novel aging factors that cause a mother cell to age is an important step to understanding the aging process in yeast.

Aging phenotypes of the mitochondria and other organelles. The simple question of what an old cell 'looks like' is still not fully understood. Our lab and others are attempting to define the physiological state of various organelles, proteins, and metabolic processes in old cells. However, a number of age-associated changes to cellular morphology, physiology, and metabolism have been reported(Falcón and Aris, 2003; Hughes and Gottschling, 2012; Smeal et al., 1996). One organelle that has been implicated both in age-associated disease and general age-associated dysfunction is the mitochondrion (Hughes and Gottschling, 2012; Lam et al., 2011; McFaline-Figueroa et al., 2011; Scheckhuber et al., 2011; Veatch et al., 2009). While the age-associated mitochondrial dysfunction will be a focus of this dissertation, characterizing all of the age-associated changes to various organelles and cellular processes will be vital to better understanding the aging process. Identifying specific regulators of these age-associated phenotypes will help identify regulators of the aging process in general, potentially identifying modulators of lifespan.

1.5 Unbiased screening techniques for effectors of the aging process

In this dissertation, I will present several techniques that I used to further explore the aging process in budding yeast. The studies presented here are designed to screen (or facilitate screening) for effectors of the aging process in an unbiased way. As discussed above, the aging process is incredibly complex and it is still unknown which cellular processes will be capable of altering how a cell grows old.

I will first present our attempts to identify long-lived proteins that are asymmetrically retained in aging mother cells. Long-lived proteins have long been implicated in the aging process of other organisms and we posited that they may contribute to the suggested aging factor in yeast (Toyama and Hetzer, 2013; Verzijl et al., 2000). Our characterization identified a number of proteins that exhibit this behavior, each possibly contributing to the aging process. We also identified a novel class of fragmented proteins that are apparently

retained throughout the lifespan of a cell. These fragmented proteins may exist in other organisms and contribute to the overall aging process.

In Chapter III of this dissertation, I will discuss a lifespan assay that I developed in order to quickly and easily identify mutants and conditions that alter lifespan. Contrary to many existing techniques, this assay was designed to required minimal intervention during the aging process and use relatively accessible technology. The assay was able to replicate the effects of several previously reported modulators of lifespan, but it was not able to detect lifespan extension by CR.

In Chapter IV of this dissertation, I will present an unbiased genetic screen for effectors of the age-associated loss of mitochondrial membrane potential. Discussed in more detail in this chapter, mitochondrial dysfunction is a conserved aging phenotype, observed across several organisms (Bratic and Larsson, 2013). The screen identified several genetic regulators of this process that will warrant further investigation.

The work in this dissertation has identified several causal factors in the aging process in addition to identifying genetic regulators of known age-associated phenotypes. It is likely that some of these effectors would not have been identified by targeted studies of the aging phenotypes as they alter the dynamics of these aging processes by some unknown mechanism. The techniques presented here are meant to be adaptable to further study the aging process under other conditions and other age-associated phenotypes. It is my hope that the techniques and approaches presented here will contribute and facilitate a better understanding of the aging process in budding yeast and other organisms.

1.6 TABLES AND FIGURES

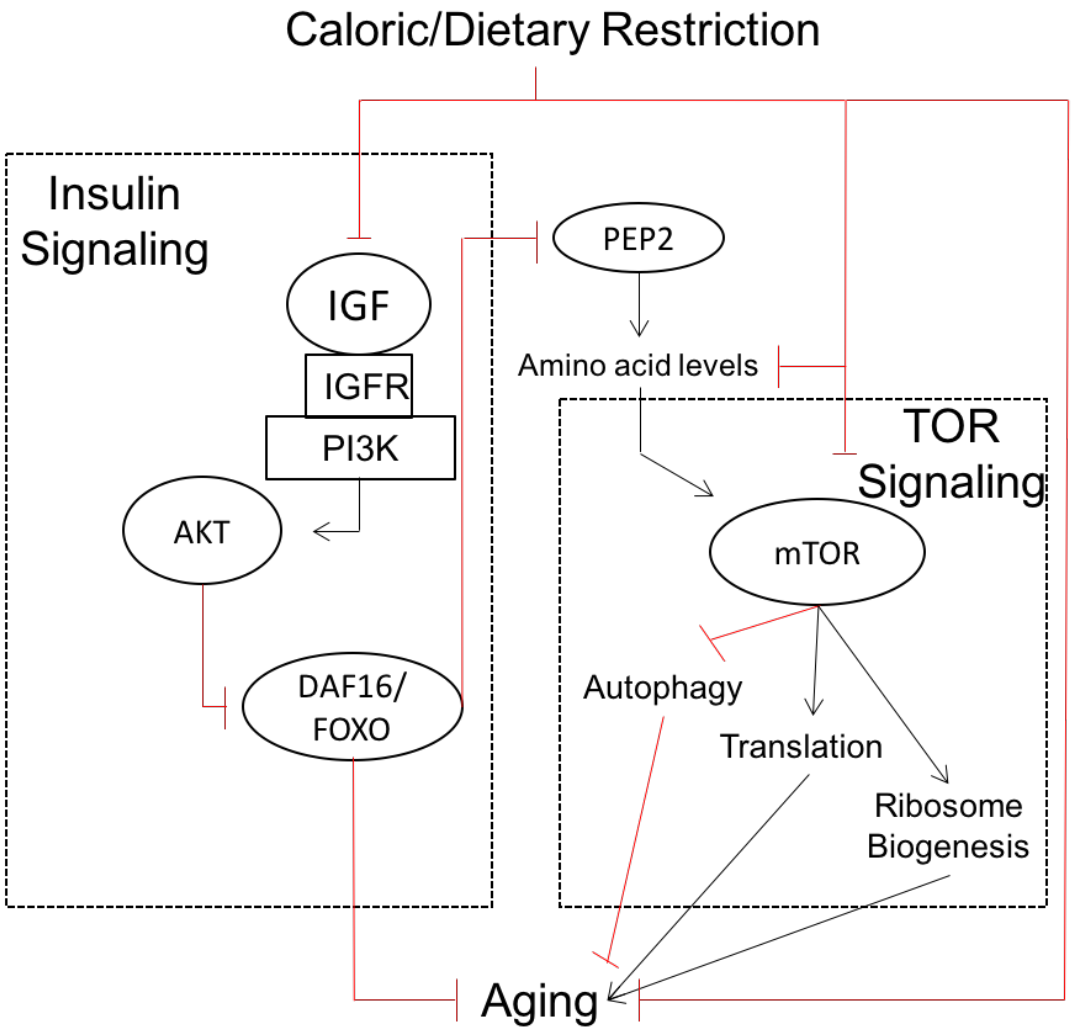

Figure 1.1. Insulin signaling and TOR signaling modulate lifespan

Mutations in in the insulin signaling pathway have strong effects on lifespan. Mutations that alter TOR activity (and its regulated processes) can also strongly modulate lifespan. There is evidence that caloric/dietary restriction acts through insulin signaling, TOR signaling and independent mechanisms to affect lifespan. Additionally, there is some evidence that there is cross-talk between insulin and TOR signaling pathways (e.g. PEP2). However, adding to the complexity of these signaling pathways, many details, interactions, ant their effects on lifespan and aging vary between model organisms.

Chapter 2. IDENTIFICATION OF LONG-LIVED PROTEINS RETAINED IN CELLS UNDERGOING REPEATED ASYMMETRIC CELLS DIVISIONS

The work described in this chapter has been previously published and description of specific author contributions is provided in section 2.5.

Thayer NH, Leverich CK, Fitzgibbon MP, Nelson ZW, Henderson KA, Gafken PR, Hsu JJ, Gottschling DE. *Identification of long-lived proteins retained in cells undergoing repeated asymmetric divisions*. *PNAS. 2014* doi: 10.1073/pnas.1416079111.

2.1 INTRODUCTION

Long-lived proteins have a well-documented impact on age-associated decline. In mammals, extracellular proteins, such as elastin and collagen, or those within specialized nondividing cells, such as the lens crystalline proteins, are turned over slowly or not at all (Bank et al., 1998; Lynnerup et al., 2008; Shapiro et al., 1991; Toyama and Hetzer, 2013; Truscott, 2010). Consequently, these proteins are susceptible to a lifetime of damage or other changes, which contribute to reduced elasticity of tissues and vision problems. More recently, the long-lived nuclear pore proteins within metabolically active, postmitotic neurons have been implicated in nuclear “leakiness” with increasing age (D’Angelo et al., 2009; Savas et al., 2012). These examples indicate that long-lived proteins can contribute to the aging process, but this evidence has been limited to situations that occur in the absence of cellular division.

Many molecular studies of the aging process have been limited to nondividing cell types; however, dividing cells also age. This finding was first demonstrated in the budding yeast, *Saccharomyces cerevisiae*, where the number of daughter cells produced by a single mother cell is finite, typically 25–30 cell divisions (Mortimer and Johnston, 1959). Since that time, limited replicative potential of cells has been observed across species; and similar to budding yeast, repeated asymmetric cell divisions have been reported to lead

to dysfunction of the progenitor cell in bacteria and metazoan stem cells (reviewed in refs. (Jones and Rando, 2011; Kysela et al., 2013; Signer and Morrison, 2013)).

Asymmetry is a fundamental property of cell divisions across species. It creates differentiated cells, maintains germ lineages and stem cells, generates phenotypic diversity, and is fundamental to species that propagate by polarized cell growth. Even in cells that morphologically appear to divide symmetrically, there is asymmetry in molecular constituents, for example proteins, RNA, and lipids (Kysela et al., 2013; Li, 2013; Macara and Mili, 2008). In budding yeast, the limited lifespan of mother cells has provided fundamental insights about how repeated asymmetric cell divisions may lead to cellular aging. Multiple studies have led to the idea that a “senescence factor” accumulates in a mother cell through her successive cell divisions, whereas the daughter cell is rejuvenated for a full lifespan (Steinkraus et al., 2008). Candidate senescence factors include extrachromosomal ribosomal DNA circles, damaged proteins or proteins that are not renewed, dysfunctional mitochondria, and increases in vacuolar pH (reviewed in ref. (Nyström and Liu, 2014)). Each of these entities or events is reported to accumulate or change over time, preferentially in the mother cell. Although there is support for each playing a role in the determination of lifespan, how they become senescence factors and contribute to aging phenotypes, or whether a common mechanism or process underlies all these hypotheses, remains unclear.

The apparent links between long-lived proteins and aging in postmitotic cells or extracellular compartments (Toyama and Hetzer, 2013; Truscott, 2011) have led us to ask whether long-lived proteins might contribute to aging in a cell that goes through repeated asymmetric divisions. It is technically challenging to explore this idea in metazoan stem cells. Therefore, we have taken a first step to explore this idea in *S. cerevisiae* by applying recent technology we developed (Lindstrom and Gottschling, 2009) to identify long-lived proteins that reside and persist in budding yeast mother cells as they go through repeated asymmetric cell divisions. Our approach to identify long-lived proteins in this asymmetric dividing cell type, and our findings, are presented herein.

2.2 RESULTS

2.2.1 Approach to Identify Long-Lived Asymmetrically Retained Proteins.

To identify long-lived proteins that are retained in yeast mother cells, we combined a method developed in our laboratory [the Mother Enrichment Program: MEP(Lindstrom and Gottschling, 2009)] with a pulse-chase protocol using total proteome analysis (outlined in Fig. 2.1A). Cells were initially grown in medium with stable heavy-isotope amino acids to label proteins. The cells were then switched into media containing light-isotope amino acids and cultured for an additional ~18 cell divisions with the MEP engaged. Finally, we determined whether any of the original heavy-labeled proteins were still present in the aged mother cells.

We did this by purifying these aged mother cells, extracting total cellular proteins, and separating them by SDS/PAGE. The gel was cut into slices spanning apparent molecular weights of ~200–8 kDa, and each slice was treated with trypsin and the eluted peptides were subjected to LC-MS/MS analysis.

Peptides from ~3,200 total proteins were identified with high confidence (described in Materials and Methods). This number represents over 50% of known ORFs and afforded comparable coverage to the number of total yeast proteins identified previously by LC-MS (de Godoy et al., 2008). Of all of the high-confidence peptides identified, 1,581 had both heavy- and light-labeled forms (13C- and 12C-labeled, respectively) in any given gel slice; this corresponded to 465 proteins (Dataset S1). We limited further analysis to proteins in which peptide pairs with both heavy- and light-labeled events in a gel slice had an 13C/12C ratio ≥ 0.1. (This cut-off was chosen to reduce the frequency of inaccurate assignments and provide a reasonable number of candidates for further analysis described below.) For these 136 proteins, we considered all high-confidence peptide sequences and mapped their position within the SDS/PAGE gel slices. This assignment allowed us to assess the apparent molecular weight (MW) of proteins that were heavy-labeled. The median 13C/12C ratio of the peptides in each gel slice was then calculated and plotted for each protein (Fig. 2.1B and Datasets S1 and S2).

2.2.2 Two Classes of Long-Lived Asymmetrically Retained Proteins: Full-Length and Fragmented.

Analysis of these data divided the long-lived proteins into two categories: those in which the high 13C/12C ratios were present in peptides identified from full-length versions of the protein, and those in which the high 13C/12C ratio peptides migrated with apparent MW that was smaller than the expected full-length protein. For proteins in the first category, we hypothesized that the heavy-labeled peptides represent proteins synthesized very early in the lifespan of the mother cell, and that a significant fraction of each protein was still present in a full-length form after ~18 cell divisions. Twenty-one proteins were in this category (Table 2.1) and were enriched in several classes. These classes included: plasma membrane proteins (Mrh1, Pma1, Snq2, and Sur7), proteins secreted into the cell wall (Bgl2, Exg1, Pho5, Pho11), and proteins involved in sulfur metabolism (Met3, Met5, Met6, Met10, Sam2, Thr1). The cell wall and proteins comprising it remain with the mother cell through her lifespan (Orlean, 2012; Smeal et al., 1996). Thus, the presence of Bgl2, Exg1, Pho5, and Pho11 in our dataset provided support that the isotopic pulse-labeling/MS method could indeed identify proteins retained by mother cells.

The “full-length” category could be subdivided further by examining where each of the high 13C/12C ratio peptides for a particular protein migrated in the gel. Some proteins with high 13C/12C ratios had isoforms that migrated exceptionally slowly through the SDS/PAGE gel (e.g., Pho5, Pho11, Pma1, Mrh1) (Fig. 2.1B and Dataset S2), suggesting that they were posttranslationally modified or in an SDS-resistant aggregated form. Consistent with this idea, Pho11 and Pho5 are glycoproteins and known to run aberrantly on SDS/PAGE (Shnyreva et al., 1996), and Pma1 and Mrh1 are integral membrane proteins and are modified or prone to aggregation (Rath et al., 2009).

2.2.3 Fragmented Long-Lived Asymmetrically Retained Proteins.

The majority of proteins with peptide pairs ratios ≥0.1 13C/12C contrasted with those described above. In this larger group the predicted full-length isoforms had 13C/12C ratio peptides below the 0.1 threshold. In fact, the majority of the peptides corresponding to

these full-length isoforms were light-labeled (Fig. 2.1B and Dataset S2). Instead, the peptide pairs with ≥0.1 13C/12C ratios mapped to apparent MWs that were much smaller than the predicted MW of their respective protein. We speculate that these proteins were synthesized early in the life of the mother cell but were partially degraded into stable truncated isoforms during the next ~18 cell divisions. These smaller fragments persist in the mother cell. The full-length version of each protein was also present; however, it was represented by few or no heavy-labeled peptides, suggesting that the full-length protein was the result of more recent synthesis that occurred as the mother cell went through successive cell divisions. Many of the proteins in this class were components of protein translation and folding (~60%) or glycolytic enzymes (~15%). The reason these truncated proteins were present in the mother cell after ~18 cell divisions requires further investigation, but their detection may reflect that the full-length proteins are quite abundant (Ghaemmaghami et al., 2003).

2.2.4 Examination of Prospective Full-Length Long-Lived Asymmetrically Retained Proteins by Recombination-Induced Tag-Exchange Tagging.

To independently assess whether the full-length proteins identified above were indeed long-lived and retained in mother cells, fluorescence microscopy was combined with a protein-tagging method: the recombination-induced tag-exchange (RITE) system (Verzijlbergen et al., 2010). Tagging a protein of interest with the RITE system creates a fusion protein, which initially expresses protein-GFP, then through an estradiol-inducible recombination event, expresses protein-RFP. The original ("old") protein is labeled green, and after the switch, all subsequent ("new") protein synthesis are labeled red. (Fig. 2.2A)

We successfully RITE-labeled 10 of the 21 candidate proteins (Table 2.1) (many were mislocalized). As will be presented below, five of the full-length candidates were verified by RITE-tagging to be long-lived and asymmetrically retained in mother cells. We refer to these proteins as "long-lived asymmetrically retained proteins" (LARPs).

2.2.5 **Plasma Membrane LARPs.**

The cells containing RITE-tagged proteins were monitored by time-lapse fluorescence microscopy beginning ~2 h after their respective RITE-tags were switched from green to red fusion proteins. The analysis of the integral plasma membrane proteins Mrh1, Pma1, and Sur7 revealed that these proteins were exceptionally long-lived and asymmetrically retained in the mother cells. For these proteins the perimeter of every original mother cell remained green for the entire period of observation (seven to eight cell divisions), with no detectable amount of the plasma membrane “old” green protein observed in daughter cells. These observations are consistent with all three of these integral plasma membrane proteins being long-lived and asymmetrically retained in the mother cell; little or none was distributed to the daughter cells (Fig. 2.2B and Movies S1–S3).

2.2.6 **LARPs in Large Cytoplasmic Structures.**

Thr1 and Hsp26 are cytoplasmic proteins that were identified as LARPs by the isotopic/MS method. These proteins also appeared to be long-lived and preferentially retained in mother cells by RITE-tagging, although differently than the plasma membrane proteins. In contrast, these cytoplasmic proteins were diffusely cytoplasmic or undetectable in most cells, but in a subpopulation of mother cells they formed distinct structures. Thr1 formed a cytoplasmic, short rod-like structure, consistent with previous reports of this metabolic enzyme forming filaments in vivo (Noree et al., 2010). However, the RITE-tagged Thr1 revealed that the original GFP-labeled protein in the filament was long-lived and had a very strong bias to remain in the mother cell. We monitored 24 cells over a total of ~135 divisions and in only three instances (2%) did the filament transfer from the mother to the daughter. Although filaments were typically retained in mother cells, we observed small fragments of the Thr1-GFP filament break off and segregate into daughter cells during 12% of cell divisions (16 of 135). These small fragments of the original filament remained in daughter cells and appeared to serve as seeds for further filament formation once these daughters became mother cells (Fig. 2.3A and Movie S4). Similarly, in old mother cells the old Thr1-GFP filament appears to be a site for further deposition of newly synthesized Thr1-mRFP; the green filament was surrounded by red

(Fig. 2.4A and Movie S4). These observations suggest that newly synthesized Thr1 was added to the old structure with increasing age.

Hsp26 is a small heat-shock chaperone that is involved in protein homeostasis and associates with a variety of proteins that are prone to aggregation (Cashikar et al., 2005; Haslbeck et al., 2005). One or two distinct green Hsp26 RITE-tagged foci of variable size were observed in a number of mother cells, and like Thr1, had a strong bias to remain in the mother (Fig. 2.4B and Movie S5). Sixty-two cells were monitored over ~275 cell divisions, and in only 30 divisions was the Hsp26-GFP focus transferred to the daughter cell (11%). In nearly all cases, the initial Hsp26-GFP focus remained green throughout the observation of the aging mother cell. However, in one mother, the focus became a composite of green and red after several cell divisions, consistent with newly synthesized Hsp26-RFP being added to the original Hsp26-GFP focus (Movie S6). Taken together, these results suggest that Hsp26 foci and Thr1 filaments are long-lived proteins with a propensity for asymmetric retention in the mother cell.

2.2.7 **Plasma Membrane LARPs Remain, Whereas Partner Proteins Exchange.**

One of the plasma membrane proteins examined, Sur7, is part of a multiprotein complex: the eisosome (reviewed in refs.(Douglas et al., 2011; Merzendorfer and Heinisch, 2013)). The eisosome, whose role remains enigmatic, is defined by dozens of cortical structures distributed around the plasma membrane. In addition to the integral membrane protein Sur7, other important components of eisosomes include Lsp1. Although it is not an integral membrane protein, Lsp1 is deposited early in the bud and can assemble into a membrane scaffold (Karotki et al., 2011; Moreira et al., 2012). Another important eisosome component is Nce102 which, like Sur7, is an integral membrane protein with four transmembrane domains (Fröhlich et al., 2009; Grossmann et al., 2008). We tested whether these components of the eisosome were as stable as Sur7 by examining their localization with the RITE tag system. In contrast to Sur7, Lsp1, and Nce102 were replaced with newly synthesized protein. For both of these proteins the mother's eisosomes turned from GFP to RFP within a few cell divisions (Fig. 2.5 and Movies S7 and S8). This distinction between Sur7 and Lsp1 or Nce102 was further supported by the

MS data; neither Lsp1 nor Nce102 had full-length proteins with a high 13C/12C ratio (Datasets S1 and S3). These results suggest that although Lsp1 and Nce102 are required for normal eisosome formation and structure, Sur7 may function as an anchor to ensure eisosome position within the plasma membrane as the cell repeatedly divides.

2.2.8 LARPs Change in the Mother Cell with Successive Cell Divisions.

A consequence of little or no protein turnover of the LARPs is that they may accumulate in the mother cell if they continue to be synthesized. In fact, this appeared to be so in some cells for the cytoplasmic LARPs (Hsp26 and Thr1) that served as seeds (see above and Fig. 2.4). Examination of the plasma membrane LARPs, which are expressed in all mother cells, suggested that they might also accumulate: during the time-lapse analysis of the plasma membrane-associated RITE-tagged proteins (e.g., Mrh1) mother cells appeared yellow because of expression of Mrh1-RFP, whereas Mrh1-GFP was still present in the mother cell (Movie S1).

We further characterized two plasma membrane LARPs to determine if their accumulation continued through the life of the mother cell. This possibility was explored by examining the level of fluorescence at the plasma membrane of a relatively fast-folding GFP (matures within minutes, without a switchable RITE-tag) fused to Mrh1 or Sur7 in cells from birth through ~20 divisions. For each of these GFP fusion proteins, there was little to no fluorescence in a small bud, but by the time the daughter had separated from the mother cell, a large increase in GFP fluorescence was evident (Fig. 2.7A) (e.g., Mrh1). For Sur7-GFP the total fluorescence increased a modest ~50% over the next 15–20 divisions (Fig. 2.5B). Mrh1-GFP increased over the next ~15 cell divisions as well, but it plateaued with ~2.5-fold greater fluorescence than in a newborn mother cell (Fig. 2.7B). Thus, it appears that Sur7 and Mrh1 are initially deposited into the plasma membrane around the time a daughter cell matures into a mother cell, and continue to be deposited and accumulate through many cell divisions.

A hallmark of some long-lived proteins that are extracellular or reside in nondividing cells is that they become modified over time (Toyama and Hetzer, 2013). Therefore, we examined several of the LARPs by western analysis, comparing their migration by

SDS/PAGE as a function of mother cell replicative age. For the two plasma membrane proteins examined (Pma1 and Mrh1), increasing amounts of the protein showed reduced mobility in the gel as the cell aged (Fig. 2.7C). The nature of this altered mobility requires further characterization, but suggests that there is an age-dependent change in both of these LARPs. Taken together, these results indicate that plasma membrane LARPs can be both modified and increase in levels with successive cell divisions.

2.3 DISCUSSION

In this study we identified long-lived proteins that are retained within yeast mother cells as they undergo repeated asymmetric cell divisions. We designate these proteins as LARPs. Although very long-lived or mother-retained proteins have been previously identified in budding yeast (Belle et al., 2006; Eldakak et al., 2010; Khmelinskii et al., 2012), the combination of these properties in the LARPs represents a class of proteins that has not been specifically investigated. We suggest that LARPs play a role in age-associated phenotypes as a yeast mother cell transits through repeated asymmetric cell divisions.

2.3.1 **Strengths and Limitations of the Method Used.**

The ability to identify LARPs by LC-MS/MS combined several technologies, but two were uniquely important to this study. First, the MEP (Lindstrom and Gottschling, 2009) permitted us to isolate a sufficient quantity of aged yeast mother cells for the analysis. The ability to isolate a sufficiently large population of cells that have undergone ~18 asymmetric cell divisions is not otherwise possible. Second, the fractionation of the old cell proteins by SDS/PAGE before LC-MS/MS allowed us to discriminate between full-length and fragmented LARPs. This process allowed us to not only readily identify the best full-length candidates for testing via the RITE-tagging assay, but also to identify the fragmented class of LARPs despite the simultaneous presence of the full-length protein within the cell. The identification of this fragmented class leaves many questions to explore in the future.

We used stringent criteria in our classification of proteins as LARPs. This classification started with requirements of high confidence in MS sequencing calls, insistence of a 13C/12C isotope ratio $\geq$ 0.1, and finally with independent testing by RITE-tagging for the full-length LARPs. Consequently, we suspect that the proteins reported here are representatives of a larger class of proteins. For example, we would not have included proteins that were very stable and retained in the mother cell, but had 10-fold more protein synthesis during the light isotope-labeling period. Additionally, our method would not be sensitive to detecting long-lived proteins that had a modest bias to remain in the mother cell. For example, ~60% of stable nuclear pore proteins are retained in the mother each cell division (Khmelinskii et al., 2010; Menendez-Benito et al., 2013; Shcheprova et al., 2008). Assuming an extreme case in which these proteins are infinitely long-lived, then after 18 cell divisions the expected 13C/12C ratio would be ~10−4, well below our cut-off threshold. A recent report using LC-MS/MS to identify long-lived proteins in nondividing mammalian tissues used a 13C/12C ratio cut-off of ~0.05 (Toyama et al., 2013). Nevertheless, our more stringent cut-off and analysis provided a view of a new spectrum of proteins. With increased experimental sensitivity and accuracy in the future, our approach may allow higher confidence in detecting more subtle mother-biased retention.

The proteins classified as LARPs had a very robust GFP signal over the course of more than eight cell divisions when analyzed by RITE-tagging. This screening tool required that the proteins be abundant and exceptionally stable (as a GFP fusion protein). Thus, less-abundant or shorter-lived proteins would be overlooked. We therefore included candidates that could not be verified by RITE-tagging in Table 2.1, with the expectation that more sensitive assays in the future will confirm these proteins as true LARPs. We do note, however, that several LARP candidates by MS criteria may be false-positives because of the constraints of the stable isotope-labeling protocol. For example, six proteins involved in methionine biosynthesis passed the initial MS criteria, but were not considered LARPs when analyzed by RITE-tagging. Further analysis revealed that some of these proteins were highly induced under the growth conditions of heavy-isotope labeling, but substantially repressed in the media used for the light-label chase (Fig. 2.8). This finding suggests that the 13C/12C ratio of these proteins was artificially high: with

little light protein synthesized, the denominator of the 13C/12C ratio was quite small, even though the heavy, old protein was being distributed to the daughter cell at each division.

Our approach was also capable of identifying LARPs with variable expression in the population of cells. The plasma membrane LARPs gave a very robust MS and RITE-tagging signal, in large part because they were present in every cell and highly retained in the mother cell. In contrast, the two cytoplasmic LARPs, Hsp26 and Thr1, were present in a subset of original mother cells and had some probability of being passed onto daughter cells, albeit at a low frequency.

2.3.2 What Makes LARPS Long-Lived?

There are two traits that define a LARP: being long-lived and retained in the mother cell for many cell divisions. Although understanding the molecular basis of these traits will require further analysis, we can speculate about how they might be long-lived. The full-length LARPs appear to be immune from the normal pathways of protein turnover under the conditions examined. For those associated with the plasma membrane (e.g., Pma1, Mrh1, Sur7), they may lack or structurally occlude motifs necessary for the endocytic turnover of plasma membrane integral membrane proteins (reviewed in (MacGurn et al., 2012)). Similarly, the cytoplasmic LARPs may elude the ubiquitin-proteasome system, cytoplasmic proteases, and autophagy (Schreiber and Peter, 2014). It is worth noting that one of the LARPs is Hsp26, which contains the conserved α-crystallin domain (Horwitz, 1992). In eye tissues, this domain is associated with proteins that are among the most stable proteins in the human body (Lynnerup et al., 2008).

Localization of the LARP (e.g., the plasma membrane or a filamentous structure) appears to be an important contributor to a LARP's stability. For example, in movies of RITE-tagged Mrh1, a fraction of the protein made early in the life of the mother cell can be observed within the vacuole, whereas that located at the plasma membrane is incredibly stable (Fig. 2.2B and Movie S1). This finding is consistent with LARPs being sensitive to quality-control mechanisms along their transit to the plasma membrane (MacGurn et al., 2012), but once properly inserted into the plasma membrane they appear to be largely resistant to degradation.

The fragmented class of LARPs represents an interesting group of stable peptides in the mother cell. Proteins with long half-lives have been previously observed to progress to truncated forms with increasing age in mammals (Truscott, 2010). In these earlier studies, the truncated proteins were found in nondividing cells, whereas the proteins described in our study were found in dividing cells. Characterization of some of the truncated proteins in mammals suggests that both enzymatic and nonenzymatic cleavage occurs. Whether similar modes of fragmented protein production can be invoked for LARPs remains to be determined.

2.3.3 **How Are LARPs Retained?**

The full-length LARPs that we were able to verify visually can be divided into those that reside in the plasma membrane (e.g., Pma1, Mrh1, Sur7) and those that are part of large cytoplasmic structures (e.g., Hsp26 and Thr1). It is likely that the mechanism of retention in mother cells is different between these two groups.

Hsp26 and Thr1 have a strong tendency to stay in the mother cell, but occasionally, part or all of the LARP structure moved into the daughter cell (Movies S4 and S5). This behavior is similar to proteins in various inclusion bodies and aggregates that form as the result of protein mis-folding in yeast cells (Escusa-Toret et al., 2013; Kaganovich et al., 2008; Liu et al., 2011; Spokoini et al., 2012). Each of these entities has a strong bias to remain in the mother cell, and several mechanisms have been proposed to explain their asymmetry (Denoth Lippuner et al., 2014; Nyström and Liu, 2014). However, how they are retained in the mother remains somewhat contentious and it appears that there are protein-specific distinctions between the various structures and their fate in the cell (Liu et al., 2010, 2011; Spokoini et al., 2012; Zhou et al., 2011). Hsp104 is associated with several of these structures and thought to facilitate disaggregation of the proteins. Interestingly, in this context, Hsp26 is hypothesized to arrive to aggregates before Hsp104 to prepare some aggregated proteins for “reactivation” by Hsp104 (26, 27). Consistent with this hypothesis, Hsp26 foci were invariably associated with Hsp104 foci; however, Hsp104 foci were not always associated with Hsp26 (Fig 2.9). Thus, the long-lived

retention of Hsp26 in mother cells may reflect its association with particular aggregates in cells.

As is the case for Hsp26-GFP foci, Thr1-GFP filaments are not obviously present in all mother cells. Dozens of metabolic enzymes have been discovered to form filaments, although most form filaments only under specific growth conditions, such as nutrient depletion (Narayanaswamy et al., 2009; Noree et al., 2010; O'Connell et al., 2012). As is the case with Hsp26, more analysis will be needed to discover how Thr1 filaments are retained in the mother cell, but it seems likely that the narrowing at the bud neck may contribute to retention in the mother cell (Caudron and Barral, 2009).

In contrast to the cytoplasmic proteins, the plasma membrane LARPs are present in every cell and remain within the mother. Integral plasma membrane proteins that are preferentially retained in mother cells have been previously identified (Eldakak et al., 2010; Khmelinskii et al., 2012). The mechanism underlying this asymmetry remains unclear. Previously it had been suggested that septins at the bud neck serve as a diffusion barrier to the plasma membrane protein between the mother and daughter (Faty et al., 2002). We tested this idea and found no evidence that septins played a role in retaining Mrh1 in the mother cell (Fig. 2.10), consistent with earlier findings for another integral plasma membrane protein (Eldakak et al., 2010). Instead, the asymmetry in budding yeast may be explained in part by the rather slow diffusion of these proteins in the plasma membrane (Greenberg and Axelrod, 1993). However, the plasma membrane LARPs do not appear to be completely immobile in the mother cell membrane. Careful examination of the time-lapse microscopy of Mrh1 and Pma1 fluorescent proteins reveals that the fluorescent signal of these fusion proteins is temporarily diminished near the site of budding on the mother cell as the daughter cell emerges. Mrh1 and Pma1 fusion proteins subsequently return to the bud site following cytokinesis (Movies S1 and S2).

The presence of the fragmented LARPs in the mother cell are perhaps the most enigmatic to explain. Although there are limitations to quantify peptide abundance in mass spectrometry data (Nahnsen et al., 2013), we can still estimate that the original fragmented 13C-labeled peptides represent ~10−2 to 10−4 of the molar equivalents of a given protein. Given these estimates, there is still a significant bias that these fragmented

peptides are retained in the mother. Assuming an infinitely long-lived protein was partitioned equally between the mother and daughter cells, and newly synthesized protein in the mother replaced the amount given to the daughter, then after 18 cell divisions the heavy-isotope form would be represented in the mother cell at (1/2)18, or ∼10−6 relative to the light-isotope form. At present we can only speculate as to where these fragmented proteins reside in the mother cell.

2.3.4 **Consequences of LARPs.**

Alterations in protein homeostasis are considered to be a major contributor to aging phenotypes, in particular the appearance and accumulation of aggregated proteins (Balch et al., 2008). We speculate that changes in LARPs as a yeast mother cell matures may contribute to imbalances in protein homeostasis. For example, the truncated proteins produced by the fragmented LARPs have the potential to interfere with normal cellular functions (Herskowitz, 1987). Such interference may act directly on the protein homeostasis machinery (e.g., proteasome or chaperones), or indirectly by disrupting other cellular processes, which in turn elicit a response by the protein homeostasis machinery. Furthermore, accumulation of some LARPs with successive cell divisions (e.g., Mrh1, Sur7) may result in an effective increase in dosage of protein in older cells. Such an accumulation not only has the potential to affect protein homeostasis, but may also change the phenotypic profile of the mother cell with age without impacting protein homeostasis (e.g., imbalances in metabolism, cell signaling, and so forth). Finally, accumulation of posttranslational modifications on LARPs may also alter protein activity in older cells (e.g., Mrh1, Pma1, Sur7) (Fig. 2.7). Taking these possibilities together, we hypothesize that LARPs may be an underlying cause of the aging process of yeast mother cells and, given the number of proteins and means by which they can change, may contribute to the complexity of age-associated phenotypes.

Finally, we speculate that LARPs are also present in metazoan cells that repeatedly divide asymmetrically (e.g., adult stem cells). There is good evidence that some stem cells have an age-associated decline, including those in muscle, the germline, hematopoietic/immune systems, epithelium, and neurons (Jones and Rando, 2011;

Montecino-Rodriguez et al., 2013; Ortells and Keyes, 2014; Signer and Morrison, 2013). Although the mechanisms underlying these age-associated changes remains a rich area of research, in Drosophila stem cells of the germline and larval neuroblasts, damaged proteins are retained as they go through repeated asymmetric cell divisions (Bufalino et al., 2013). This retention parallels the situation in mother cells of *S. cerevisiae* (Aguilaniu et al., 2003) and is consistent with the behavior or LARPs.

2.4 METHODS

Plasmids and Strains. Plasmids used in this study are presented in Table 2.2 and have been previously described, with the exception of pKTmCherry, which is derived from pKT127 (Sheff and Thorn, 2004), where eGFP was precisely replaced by mCherry.

Strains used in this study are presented in Table 2.2. Standard *S. cerevisiae* methods were used to generate PCR-mediated mutations, zygotes, sporulation, tetrad analysis, and selection of strains with relevant markers (Amberg et al., 2005). UCC5406, which was used for the heavy isotope labeling, is derived from MEP-containing strains UCC5179 and UCC5181 (Lindstrom and Gottschling, 2009), in which *LYS1* and *ARG4* were deleted to prevent arginine and lysine biosynthesis in cells (Gruhler et al., 2005). RITE-tagged strains were created by using BY4741 and BY4742 as parental strains (Brachmann et al., 1998). Into one parent, cre-EBD78 was introduced into the *CYC1* locus by integrating MluI linearized pSS146 (Verzijlbergen et al., 2010). Into the other parent, the gene of interest was fused to the RITE cassette as described using pKV015 as a template (Verzijlbergen et al., 2010). The two strains were then mated and the resulting diploid was used for analysis.

Media and Growth Conditions. Unless otherwise indicated, cells were grown at 30° in YEPD, Ymin, or YC media (Amberg et al., 2005; van Leeuwen and Gottschling, 2002). Stable isotope labeling by amino acids (SILAC) used [13C6]L-arginine and [13C6]L-lysine (Cambridge Isotope Laboratories), and was based on a previous protocol (Gruhler et al., 2005), with modifications described below. For some fluorescence-based microscopy, YEPD was treated with 30 mg/mL activated charcoal (C-3345; Sigma-Aldrich) for 20 min to reduce autofluorescence.

Pulse-Chase Labeling and Isolation of Proteins in Aged Mother Cells. UCC5406 was grown overnight to saturation in YEPD. Cells were resuspended in heavy medium (Ymin supplemented with 0.1 mg/mL L-histidine, L-tryptophan, and uracil to support growth of auxotrophic mutations, and 0.1 mg/mL [13C6]L-arginine–HCl and [13C6]L-lysine–HCl) at a starting density of ∼4 × 104 cells/mL and grown for 24 h to a density of ∼5 × 106 cells/mL. Cells were labeled with biotin as previously described (69), and grown for an additional 2 h in fresh heavy medium. Cells were then resuspended at 2 × 104 cells/mL in light medium [YEPD supplemented with 0.1 mL/mL L-arginine–HCl and L-lysine–HCl (not heavy-isotope labeled) (Sigma-Aldrich), 200 μg/mL hygromycin (Roche) and 100 μg/mL ampicillin (Sigma-Aldich) (to discourage fungal and bacterial contamination of aging culture) and 1 μM 17β-Estradiol (Sigma-Aldrich) to engage the MEP]. Cells were aged for 24 h, completing ∼18 cell divisions. Original cells were purified with streptavidin-magnetic beads (Hughes and Gottschling, 2012). Total proteins extracts were made by glass bead beating in Sample Buffer [2% (wt/vol) SDS, 10% (vol/vol) glycerol, 60 mM Tris·Cl pH 6.8, 5% (vol/vol) β-mercaptoethanol, Protease Inhibitors (PMSF, Leupeptin, Pepstatin, TPCK)]. The proteins were separated on an 8–16% (wt/vol) SDS/PAGE gradient gel (Bio-Rad Laboratories). The gel was then sliced in 27 fragments, ranging from an estimated molecular weight of >200 kDa to 8 kDa.

Gel Slice Digestion. Individual gel slices in 1.5-mL tubes (Eppendorf) were subjected to consecutive 15-min washes with water, 50% (vol/vol) acetonitrile, 100% acetonitrile, 100 mM ammonium bicarbonate, and 50% acetonitrile in 50 mM ammonium bicarbonate. After removing the final wash solution, the gel slices were dried thoroughly by vacuum centrifugation. The gel slices were then cooled on ice and an ice-cold solution of 12.5-ng/μL sequencing grade trypsin (Promega) in 50 mM ammonium bicarbonate was added to the gel slices and incubated on ice for 1 h. The trypsin solution was discarded and replaced with 50 mM ammonium bicarbonate and incubated overnight at 37°. Following digestion, the supernatants were collected and the gel slices were washed with 0.1% formic acid followed by washing with 0.1% formic acid in 50% (vol/vol) acetonitrile (30 min each wash). The original digestion supernatant and the washes for a single sample were combined into a single tube and dried by vacuum centrifugation. The digestion products

were desalted using Ziptips (EMD Millipore) per the manufacturer's instructions and dried by vacuum centrifugation.

Mass Spectrometry. Dried peptide mixtures were resuspended in 5 µL of 0.1% formic acid and analyzed by LC/ESI MS/MS with a nano2D LC (Eksigent Technologies) coupled to an LTQ-OrbiTrap mass spectrometer (Thermo Electron) using a "vented" instrument configuration, as described previously (Licklider et al., 2002) and a solvent system consisting of 0.1% formic acid in water (A) and 0.1% formic acid in 100% acetonitrile (B). In-line de-salting was accomplished using an IntegraFrit trap column (100 µm × 25 mm; New Objective) packed with reverse-phase Magic C18AQ (5 µm 200 Å resin; Michrom BioResources) followed by peptide separations on a PicoFrit column (75 µm × 200 mm; New Objective) packed with reverse-phase Magic C18AQ (5-µm 100 Å resin; Michrom BioResources) directly mounted on the electrospray ion source. A 90-min nonlinear gradient was used starting at 5% B. The percentage of acetonitrile was increased to 7% B over 2 min, then 35% B over 90 min. The acetonitrile percentage was increased to 50% B over 1 min then held at 50% B for 9 min followed by ramping to 95% B over 1 min, held at 95% B for 5 min, then decreased to 5% B over 1 min. A flow rate of 400 nL/min was used for chromatographic separations and the MS capillary temperature was set to 200 °C. A spray voltage of 2,250 V was applied to the electrospray tip and the LTQ-OrbiTrap instrument was operated in the data-dependent mode, switching automatically between MS survey scans in the OrbiTrap (AGC target value 1,000,000, resolution 60,000, and ion time 500 ms) with MS/MS spectra acquisition in the linear ion trap (AGC target value of 10,000 and ion time 100 ms). The five most intense ions from the Fourier-transform full scan were selected in the linear ion trap for fragmentation by collision-induced dissociation with normalized collision energy of 35%. Selected ions were dynamically excluded for 45 s. The MS data have been deposited to the ProteomeXchange Consortium (Vizcaíno et al., 2014) via the PRIDE partner repository with the dataset identifier PXD001251.

Peptide Identification and Quantification Acquired LC-MS/MS spectra for all gel fractions were searched against all translated ORFs from the *S. cerevisiae* S288C reference assembly (yeastgenome.org). The X! Tandem search engine (Craig et al.) was

used with a custom scoring function (MacLean et al., 2006) and parameters appropriate for SILAC labeled spectra acquired on the LTQ Orbitrap, which included trypsin cleavage, up to two missed cleavage sites, monoisotopic masses, and ±2-Da precursor mass tolerance. Variable modification of 6.02013 Da was allowed on arginine and lysine residues to accommodate dual SILAC labels, and variable modification of 15.994915 Da on methionine was allowed to accommodate a common oxidation artifact. PeptideProphet (Keller et al., 2002) was used to evaluate the likelihood of each peptide assignment.

To assess relative abundance of light- and heavy-labeled species of a given peptide, quantitation was performed with the Q3 algorithm (Faca et al., 2006) for only those peptides assigned with high confidence (PeptideProphet probability ≥ 0.9, corresponding to a false-discovery rate < 1%), and falling within 20 ppm of the measured precursor mass. Briefly, Q3 reconstructs elution curves in a 25-ppm window around major isotopes of the light and heavy peptide species in a range of precursor scans surrounding each identified MS/MS spectrum. The areas and extents of each curve are recorded, and the ratio of each pair of areas indicates the relative amounts of the SILAC labels incorporated at the two time points. Peptides species with zero area were set to a background value to avoid infinite or extreme ratios.

Custom Python scripts were developed to filter results and identify proteins of interest. We focused on proteins that had at least one peptide fragment within any single gel slice that was identified by both a heavy- and light-labeled species, and had a median 13C/12C ratio of ≥ 0.1 for all observed events. Variation in observed ratios was estimated by a bootstrapped median calculation, measuring the SD of medians repeatedly calculated from a randomly selected subset of the observations over 1,000 loops (Efron and Tibshirani, 1993). A summary figure was generated for each protein of interest where the median ratio of all peptides was plotted against the gel slice (molecular weight) in which they were found (Dataset S3). These figures were analyzed manually to identify proteins that varied in the abundance of heavy-label depending on where they migrated by SDS/PAGE.

Microscopy. Unless otherwise stated, all microscopy was performed on one of two fully automated wide-field microscopes: (*i*) a Nikon Eclipse Ti equipped with a 60×/1.40

objective or (*ii*) a Leica DMI-6000b equipped with a 63×/1.40 objective. Image processing and quantification was performed with Fiji, a distribution of ImageJ software (Schindelin et al., 2012).

Time-lapse microscopy of RITE-tagged strains on pads. Cells were grown overnight in YC-Ura + 200 µg/mL hygromycin to select for cells that have not undergone spontaneous recombination and retain the GFP fusion. Cells were diluted into fresh YEPD and allowed to grow for 2 h in the presence of 1 µM 17β-Estradiol to initiate recombination of RITE tag. After 2 h, cells were placed onto YC agar pads (Tran et al., 2004). Eleven *z*-stack (0.6-µm steps) images in GFP, RFP, and DIC channels were taken every 30 min for 12 h. A minimum of 20 original mother cells were examined in all experiments.

Comparing young versus old mother cell fluorescence. Cells were grown overnight to saturation and then diluted into fresh media and allowed to grow in log phase for 16 h. Cells were biotinylated, aged for 24 h, purified live with streptavidin-magnetic beads as previously described (Hughes and Gottschling, 2012), and allowed to recover for 2 h in fresh YEPD. Purified cells were mixed with young cells from a log culture. Cells were stained with calcofluor white (Fluorescence Brightener 28; Sigma-Aldrich) to visualize budscars. Mean fluorescence intensity at the plasma membrane was compared between young and old mother cells within a single image.

Deltavision microscopy for Sur7 Lsp1 colocalization. Cells were observed by high-resolution 3D deconvolution microscopy using an inverted Olympus IX71 microscope (Olympus 100×/1.40 Plan S Apo oil objective). Cells were placed on YC agar pads for imaging. The *z*-stacks were captured at 0.2-µm intervals using Deltavision SoftWorx software (Applied Precision). After deconvolution of the image stacks, 3D projections were made using Volocity (Perkin-Elmer).

Immunoblots. Lysates for all samples were prepared by standard NaOH/SDS lysis (Kushnirov, 2000) and analyzed as previously described (Hughes and Gottschling, 2012), with a few exceptions. Sample concentrations were measured by BCA assay (Thermo Fisher Scientific). Twenty micrograms of protein was loaded per lane and run on 10% (wt/vol) polyacrylamide gels. Primary antibodies were as follows: α-PMA1 (ab4645,

Abcam), α-GFP (#11814460001, Roche), and α-PGK1 (#459250, Life Technologies). Secondary antibody was α-Mouse (#715–035-150, Jackson ImmunoResearch).

2.5 Contributions and Acknowledgments

Much of this work was performed in collaboration with Christina Leverich, specifically microscopy experiments. Christina performed final versions of microscopy experiments used in figures. Kiersten Henderson performed experiment presented in Figure 2.10. Matt Fittzgibbon performed spectral analysis of mass-spectrometry profiles. Phil Gafken generated mass-spectrometry profiles. Zara Nelson performed heavy-isotope labeled aging experiment. Jessica Hsu first noted an age-associated accumulation of several plasma membrane LARPs, specifically Mrh1. Edward Marsh performed characterization of LARPs that was not included here. I would also like to thank all members of the Gottschling Lab for various contributions and support.

2.6 TABLES AND FIGURES

Table 2.1. List of prospective full-length LARPs

Confirmed as LARP^{L}	Unable to confirm as LARP*	RITE tag not successfully created†
Mrh1	Gcv3	Bgl2
Pma1	Lap4	Exg1
Sur7	Met6	Met3
Thr1	Sam2	Met5
Hsp26	Ynl134C	Met10
		Met17
		Pho5
		Pho11
		Por1
		Ser3
		Snq2

RITE-C-terminal-tagged versions of the 21 putative full-length LARPs were attempted and examined as described in the text. The proteins where then placed into three categories: ^{L} – Original proteins appeared both long-lived and asymmetrically retained in the original mother cell, * - Proteins were either not obviously long-lived or asymmetrically retained, † - RITE tagging either caused mislocalization of the protein, was not easily visualized, or was not attempted.

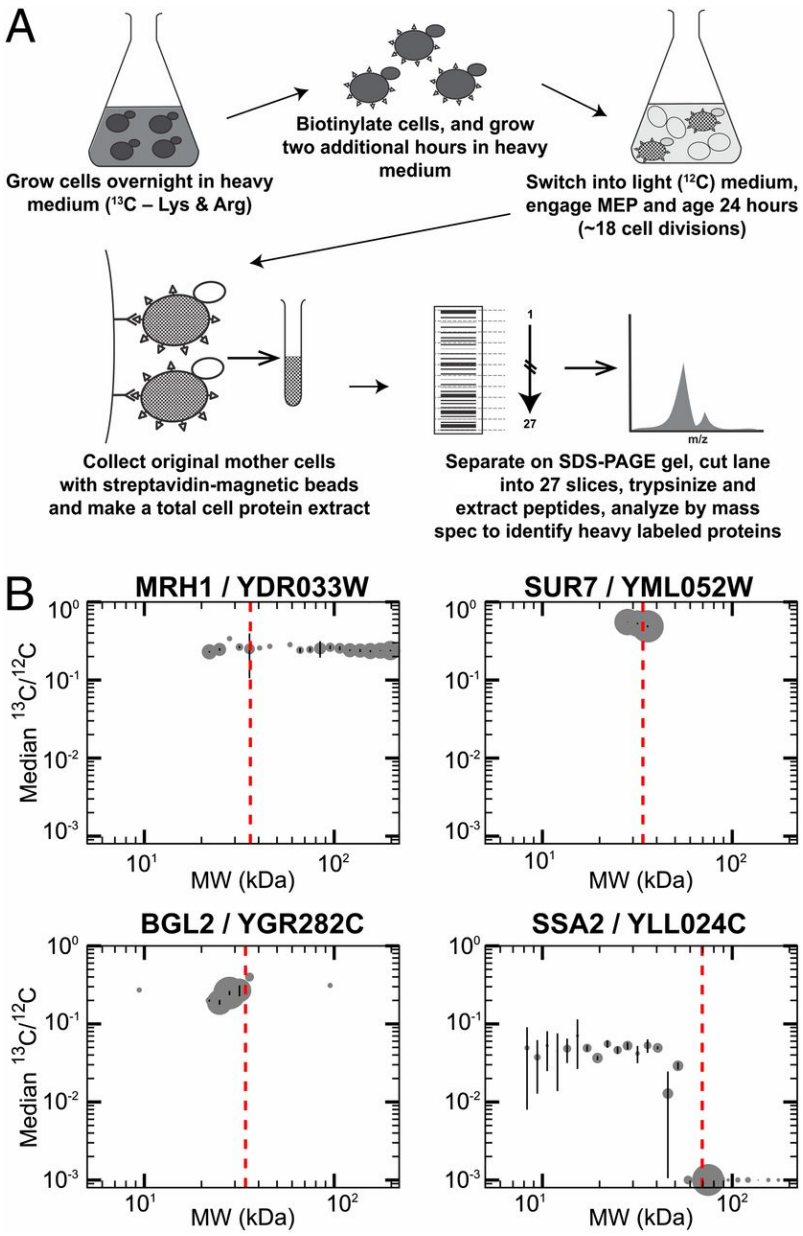

Figure 2.1. Heavy-isotope pulse-chase to identify long-lived proteins present in aged cells.

(A) Schematic representation of experimental design to identify long-lived proteins in aged mother cells (details in Material and Methods). (B) Representative plots of the $^{13}C/^{12}C$ ratio for peptides in given gel slices that correspond to specific proteins. X-axis is approximate MW of peptide (estimated from gel slice); Y-axis is median ratio $^{13}C/^{12}C$ for all peptides mapped to that protein in a gel slice; size of dots reflect the relative number of peptide observations in that slice; error bars are standard deviation of the medians calculated from 1000 bootstrapped samples; the expected MW of the full-length unmodified protein is plotted as a vertical dashed red line. Mrh1 is an integral membrane protein that appears across many gel slices, each with a similar ratio. Sur7, an integral membrane eisosome component, appears only in gel slices corresponding to its expected size with a high abundance of heavy label. Bgl2, a cell wall component, shows enrichment for heavy label. The full-length version of Ssa2, a small heat-shock protein, is primarily

newly synthesized (very low $^{13}C/^{12}C$), whereas the original ^{13}C label is predominantly in low MW gel slices that correspond to fragmented Ssa2 protein.

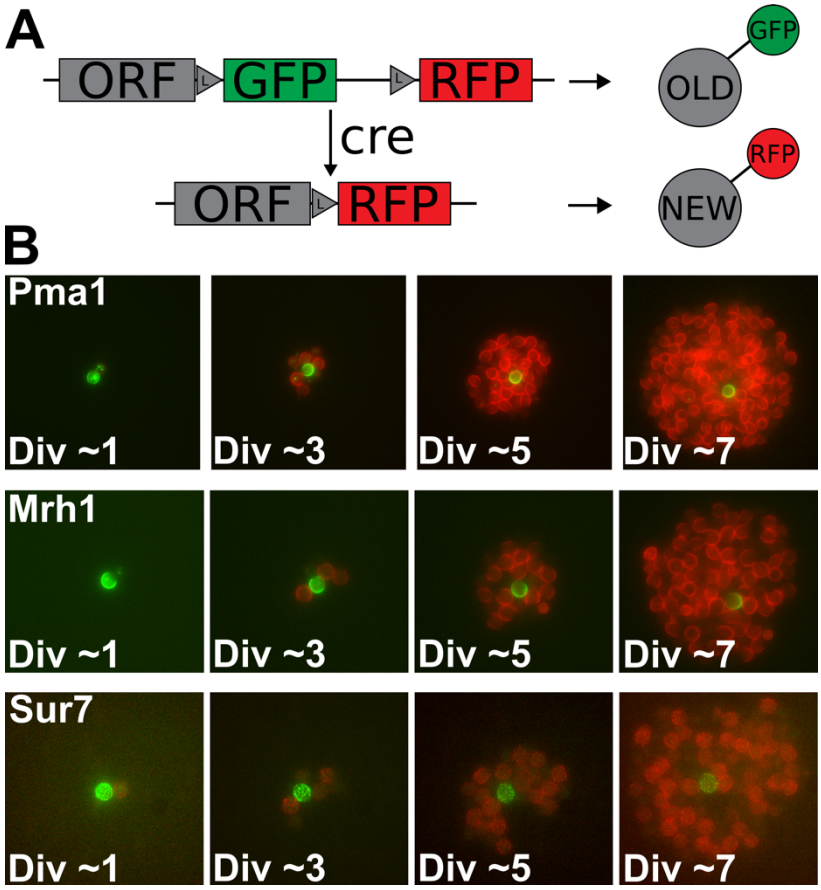

Figure 2.2. Full-length LARPs associated with the plasma membrane are retained in the mother cell throughout successive cell divisions.

(A) Schematic representation of the RITE-tag system. The RITE-tag cassette places GFP in frame with a gene's open reading frame (ORF) of interest. Upon exposure to estradiol, a *cre*-mediated recombination event removes the GFP tag and fuses the ORF to RFP. (B) Each series of panels show time-lapse images of micro-colonies formed from single mother cells of *PMA1-RITE*, *MRH1-RITE*, and *SUR7-RITE*. *Cre* activity was induced prior to the first image; any newly synthesized protein was labeled with RFP and the pre-existing protein was labeled with GFP. The approximate number of divisions the mother cell went through is indicated in the panels. Figure 2.3 contains the unmerged channels of these images. Complete time-lapse series from which these images were taken are in Movies S1-S3.

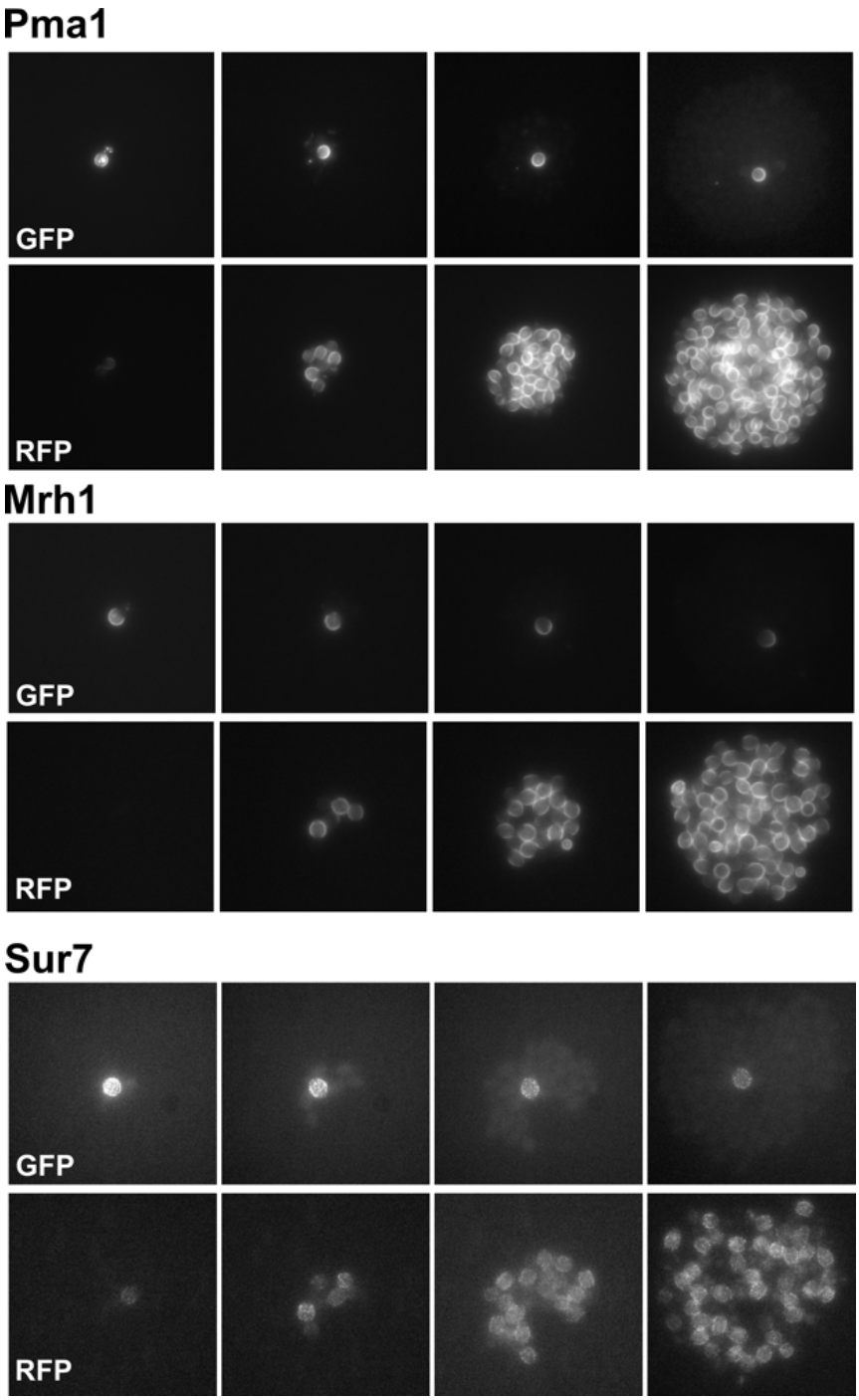

Figure 2.3. PMA1, MRH1, and SUR7 RITE-tag timelapse images with separated channels.

Images from Figure 2B presented with GFP and RFP channels as separate grayscale images. PMA1-RITE (Upper), MRH1-RITE (Middle) and SUR7-RITE (Lower).

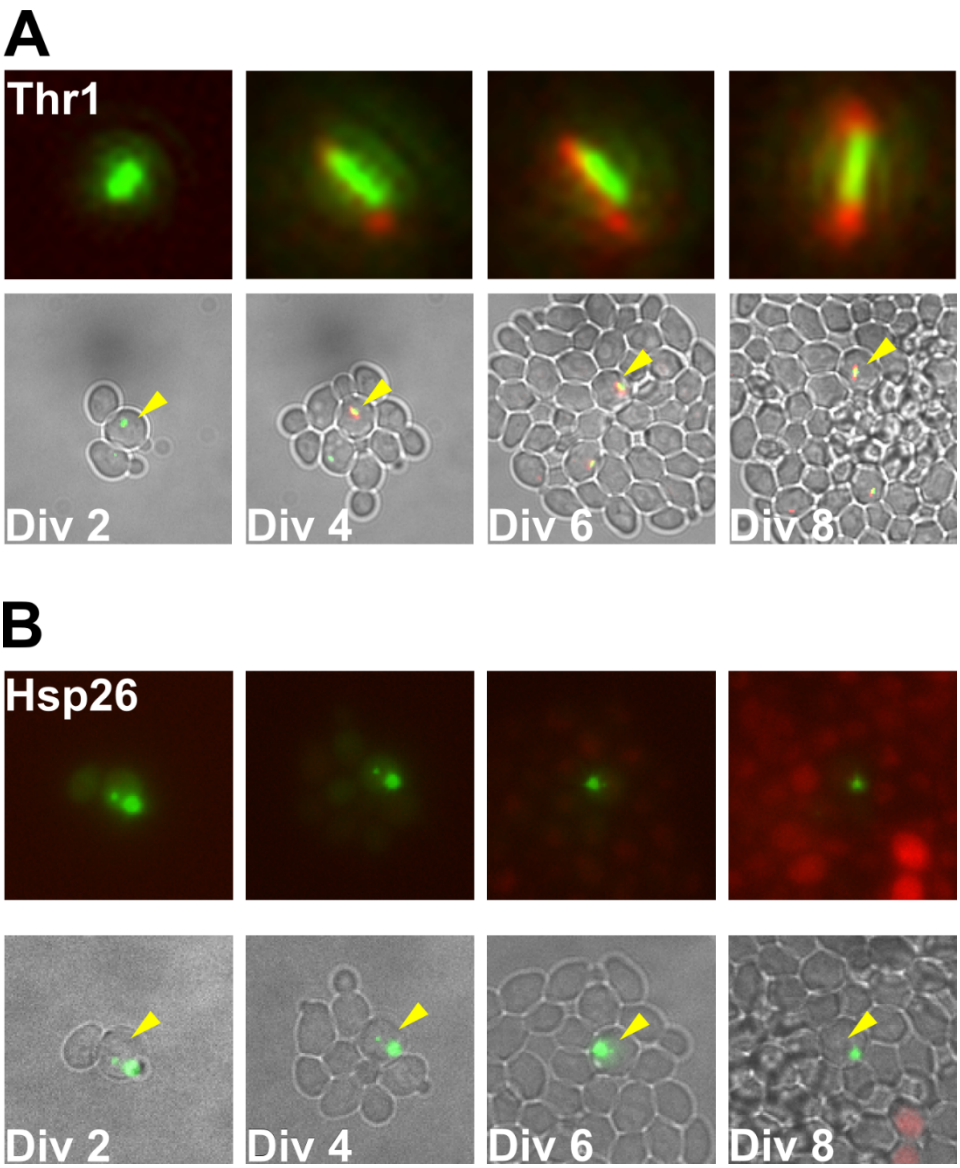

Figure 2.4. Full-length LARPs that form cytoplasmic foci remain in the mother cell throughout successive cell divisions.

(A) *THR1-RITE* cells were induced and imaged as described in Figure 2. The approximate number of cell divisions the original mother cell (denoted with arrowhead) has undergone is indicated. After the first cell division, the original Thr1-GFP containing focus remained in the mother cell. Although original protein was present in foci throughout the course of the experiment, newly synthesized Thr1-RFP appeared to be added adjacent to existing foci (enlarged in top panels). (B) *HSP26-RITE* cells were induced and imaged as described in (A). The Hsp26-GFP focus stayed within the original mother cell. As the colony became nutrient limited, several cells in the micro-colony induced *HSP26-RFP*. These images were taken from Movies S4 and S5.

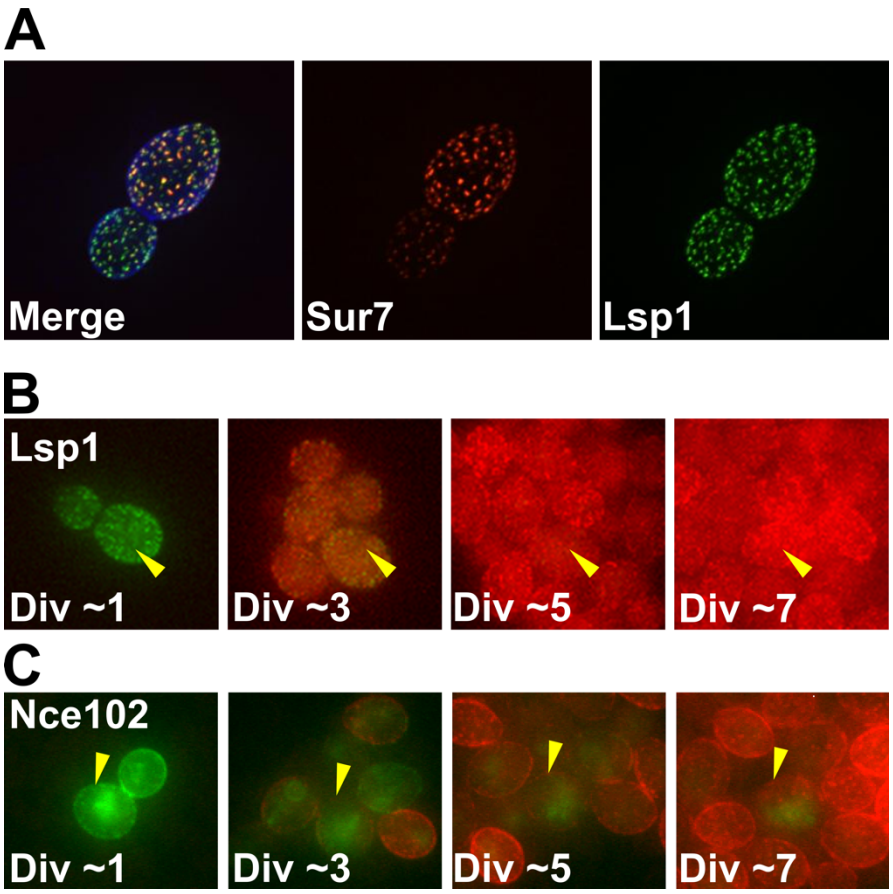

Figure 2.5. Not all components of the eisosome are LARPs

(A) Images of Sur7-mCherry and Lsp1-GFP, two components of the eisosome, which co-localized at puncta in young mother cells. Lsp1 appeared in daughters before Sur7, consistent with previous reports(Walther et al., 2006). Calcofluor staining in the merged image outlines cell walls in blue. (B) *LSP1-RITE* cells were imaged over several cell divisions, as in Figure 2. Original Lsp1-GFP protein was distributed to both mother and daughter cells, but was replaced with newly synthesized protein (RFP labeled) within a few cell divisions. (C) *NCE102-RITE* cells imaged as in B. Original Nce102-GFP at the plasma membrane was replaced with newly synthesized protein within a few cell divisions. A faint cytoplasmic haze of GFP remained in the mother cell, but it was not located at the plasma membrane. Figure 2.6 contains the unmerged channels of these images. These images were taken from Movies S7 and S8.

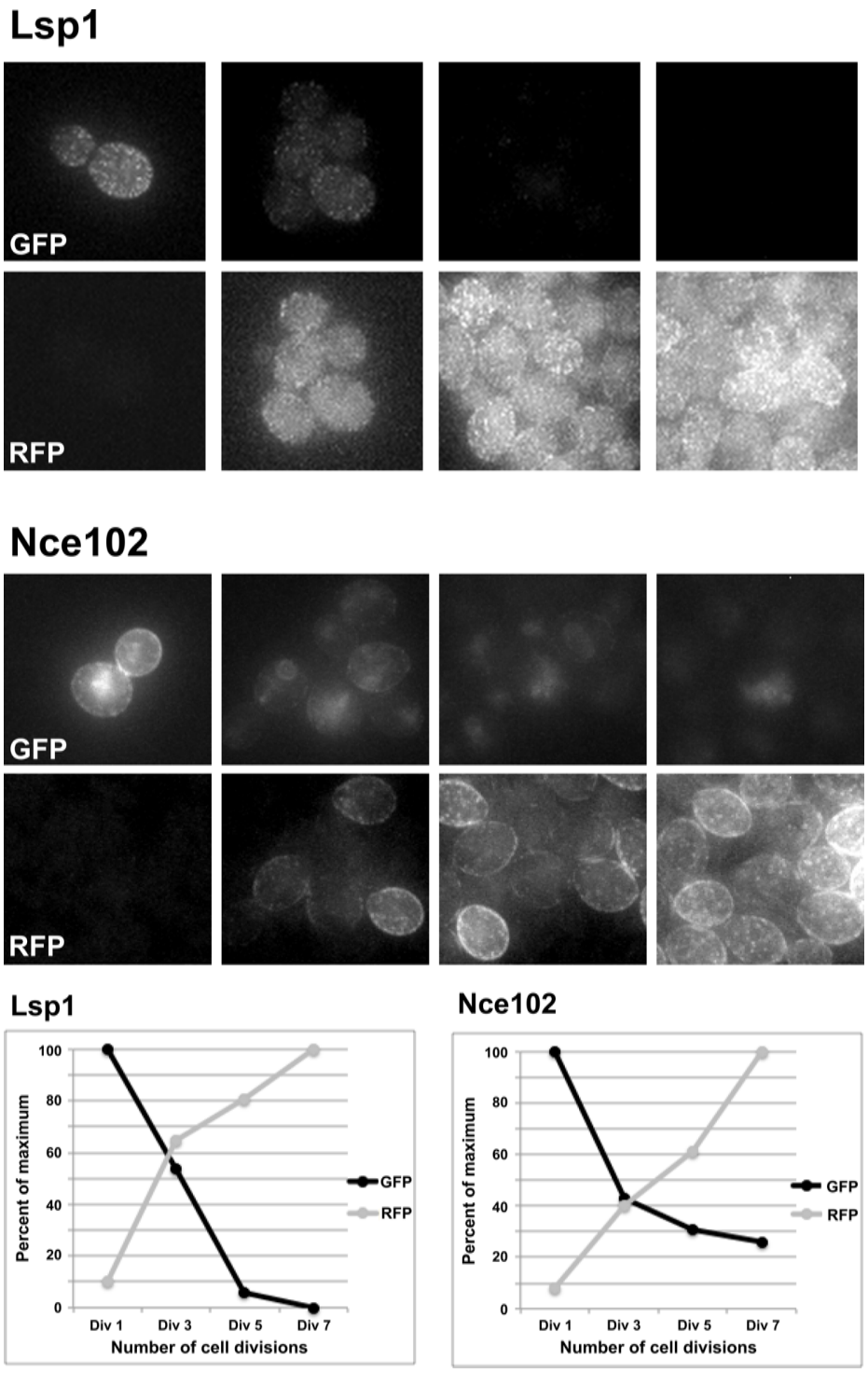

Figure 2.6 LSP1 and Nce102 RITE-tag timelapse images with separated channels.

Images from Figures 4B and 4C presented with GFP and RFP channels as separate grayscale images. LSP1-RITE (Upper) and Nce102 (Lower). Quantification of fluorescence at the plasma membrane is graphically displayed in the bottom panels.

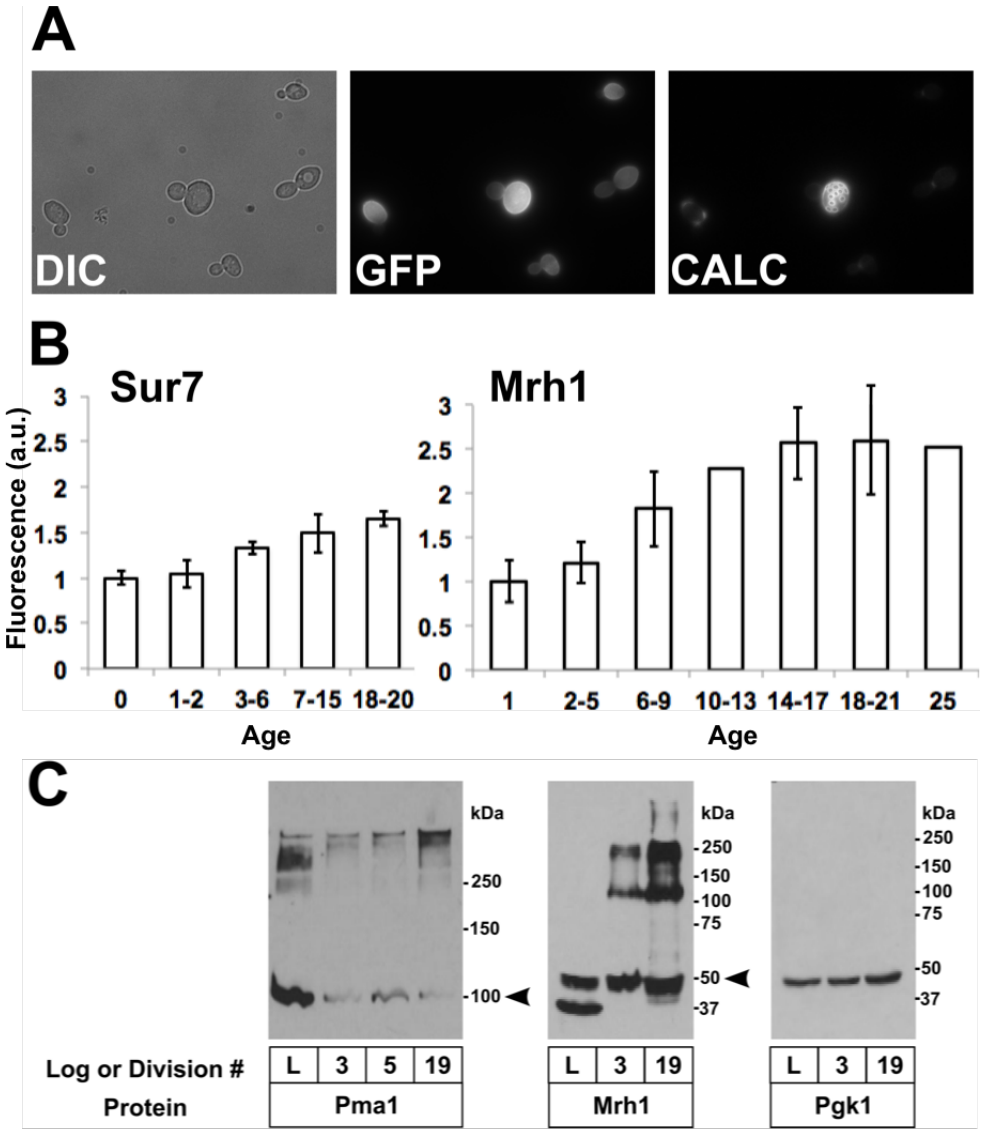

Figure 2.7. LARP proteins are altered with increasing age

(A) A representative image of Mrh1-GFP cells of various ages (newborn to >20 cell divisions old) mixed together. Panels left to right show bright field image of cells, Mrh1-GFP levels, and number of budscars (age), respectively. (B) Quantification of Mrh1-GFP and Sur7-GFP levels in aging cells. Using images as shown in A, the average Mrh1-GFP and Sur7-GFP fluorescence intensity at the plasma membrane is plotted as a function of age (arbitrary units normalized to age 0, N=100 cells for Mrh1-GFP, N=39 for Sur7-GFP). (C) Western blot analysis showed altered migration of LARP proteins during aging. Samples from young and aged cells (Mrh1-GFP and Pma1-GFP), were analyzed with anti-GFP antibody by western blot. For both Mrh1 and Pma1, protein had slower mobility relative to the expected migration (arrow head) with with increasing age. PGK1, which was not identified as a LARP, did not show this age-associated shift.

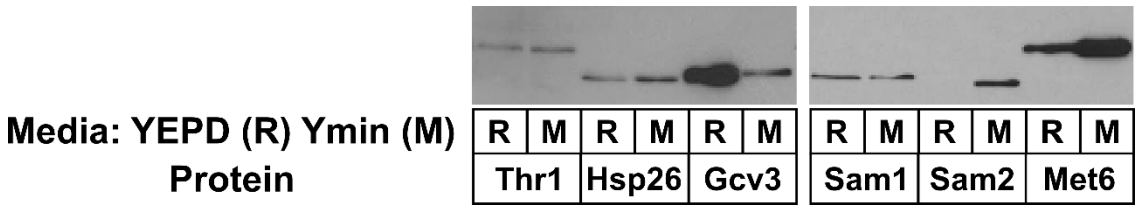

Figure 2.8. Comparison of putative LARP levels under SILAC labeling conditions.

RITE-tagged strains were grown overnight in either YEPD (R) or Ymin+his+leu (M) to mid-log phase cell density. Equivalent amounts of total whole cell protein were probed with anti-GFP antibody on western blots. All strains were heterozygous *MET15/met15*Δ. Met6 and Sam2 were more highly expressed in minimal media, and Hsp26 only slightly more expressed. Sam1 and Thr1 appeared to have no difference in expression, and Gcv3 had a decrease in expression in minimal media. Even loading was determined by poncceau staining (not shown).

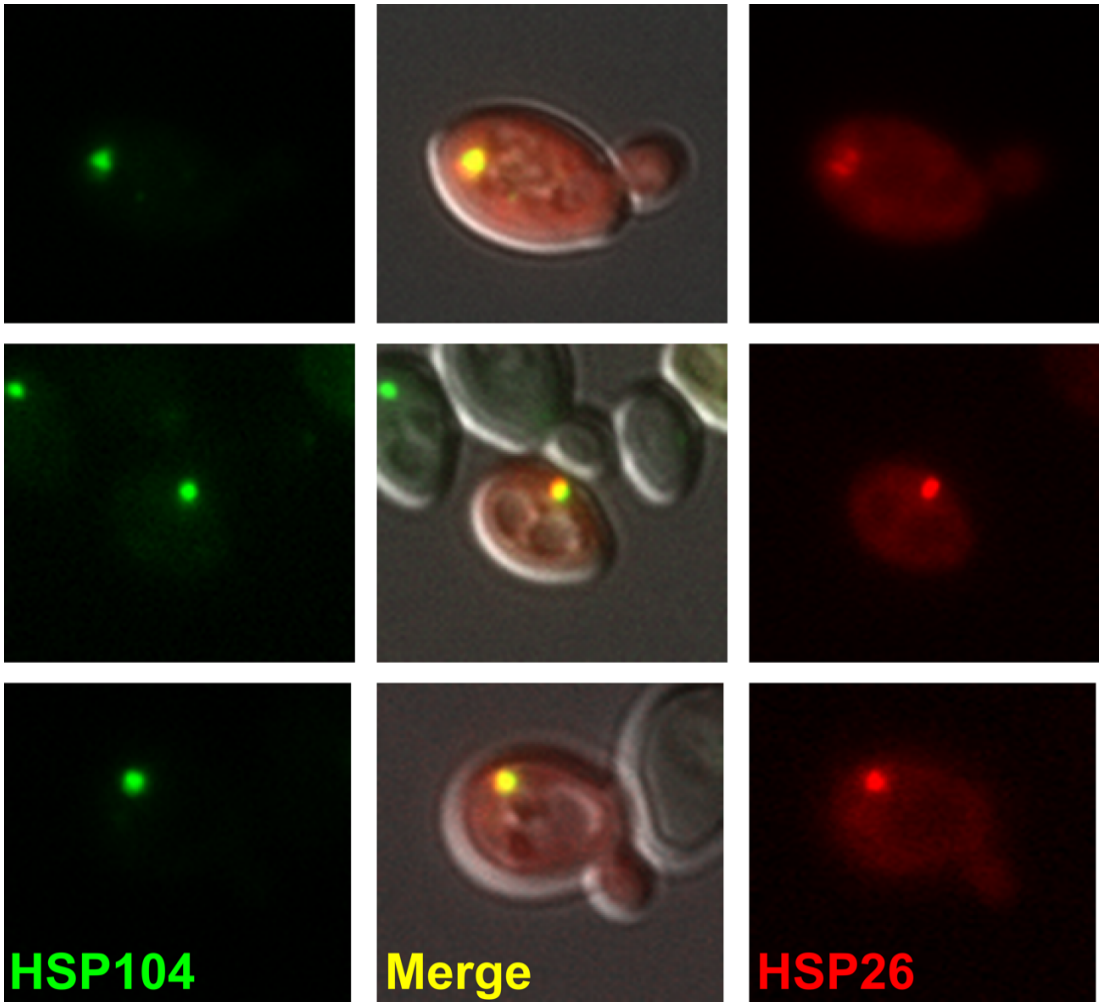

Figure 2.9. Hsp26 foci are coincident with Hsp104 foci.

Cells from a strain containing Hsp104-GFP and Hsp26-mCherry are shown. Hsp26-mCherry foci were visible in ~10% of cells, whereas Hsp104-GFP foci were visible in >50% of cells. However, all Hsp26-mCherry foci overlapped with an Hsp104-GFP focus.

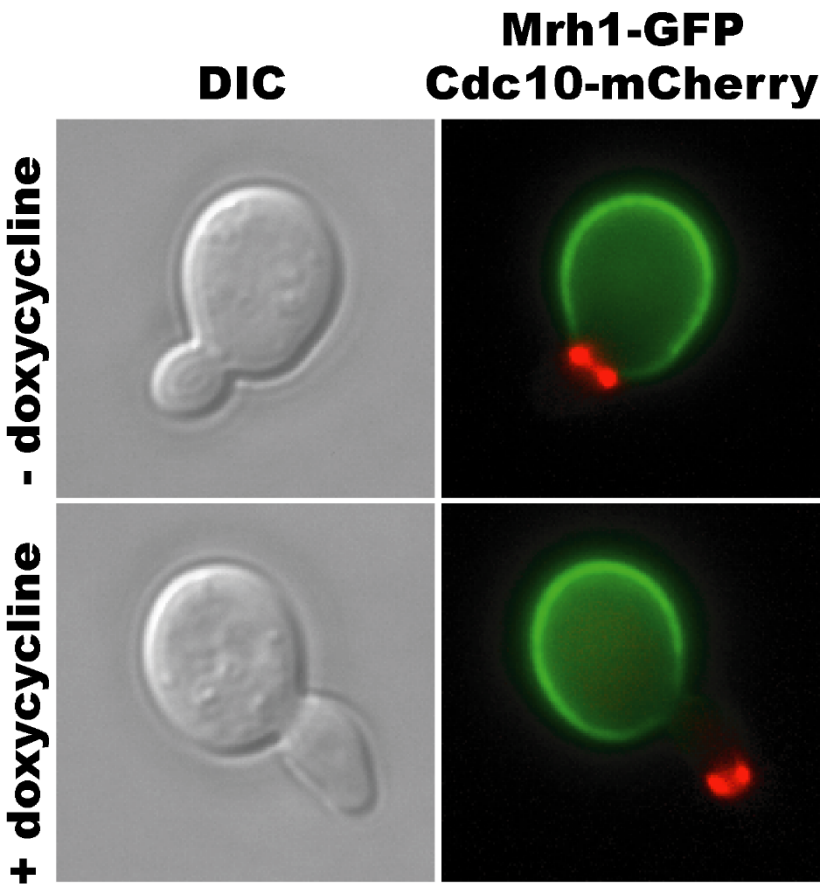

Figure 2.10. Plasma Membrane LARP asymmetry is not mediated by the septin ring.

Mrh1-GFP asymmetry between mother cells and buds was evaluated upon septin ring disruption by repressing *$TetO_7$-CDC12* (Mnaimneh et al., 2004) transcription by treating cells with 20 µg/ml of doxycycline for 5 hours. Cells also expressed Cdc10-mCherry to septin morphology to be followed. Bud elongation and Cdc10-mCherry mislocalization to the bud tip occurred upon *CDC12* repression and indicate septin ring disruption(Bouquin et al., 2000; Hartwell, 1971).

Table 2.2. Strains and plasmids used

Plasmid or strain	Genotype or descriptions	Source or reference
Plasmids		
pKV015	*V5-loxP-HA-GFP-HphMX-loxP-T7-mRFP* used to fuse RITE tag to gene of interest	(1)
pSS146	pINT-*URA3-*$P_{GPD/TDH3}$*-cre-EBD78*, *Mlu*I linearized fragment used to integrate *cre-EBD78* into $CYC1_{term}$ locus	(1)
pKT127	pFA6a-*link-yEGFP-KanMX* used to fuse GFP to gene of interest	(2)
pKT128	pFA6a-*link-yEGFP-SpHIS5* used to fuse GFP to gene of interest	(2)
pKTmCherry	*mCherry-KanMX* used to fuse mCherry to gene of interest	Gift of Adam Waite
Yeast Strains		
BY4741	*MAT***a** *his3Δ1 leu2Δ0 met15Δ0 ura3Δ0*	(3)
BY4742	*MATα his3Δ1 leu2Δ0 lys2Δ0 ura3Δ0*	(3)
UCC4044	*MAT***a**/α *his3Δ1/his3Δ1 leu2Δ0/leu2Δ0 ura3Δ0/ura3Δ0 met15Δ0/+ lys2Δ0/+ LAP4-V5-loxP-HA-GFP-HphMX-loxP-T7-mRFP/LAP4* $CYC1_{term}$*:URA3-*$P_{GPD/TDH3}$*-cre-EBD78:*$CYC1_{term}$*/+*	This study
UCC4181	*MAT***a**/α *his3Δ1/his3Δ1 leu2Δ0/leu2Δ0 ura3Δ0/ura3Δ0 met15Δ0/+ lys2Δ0/+ MRH1-V5-loxP-HA-GFP-HphMX-loxP-T7-mRFP/MRH1* $CYC1_{term}$*:URA3-*$P_{GPD/TDH3}$*-cre-EBD78:*$CYC1_{term}$*/+*	This study
UCC4190	*MAT***a**/α *his3Δ1/his3Δ1 leu2Δ0/leu2Δ0 ura3Δ0/ura3Δ0 met15Δ0/+ lys2Δ0/+* w/ *PMA1-V5-loxP-HA-GFP-HphMX-loxP-T7-mRFP/PMA1* $CYC1_{term}$*:URA3-*$P_{GPD/TDH3}$*-cre-EBD78:*$CYC1_{term}$*/+*	This study
UCC4243	*MAT***a**/α *his3Δ1/his3Δ1 leu2Δ0/leu2Δ0 ura3Δ0/ura3Δ0 met15Δ0/+ lys2Δ0/+ MET6-V5-loxP-HA-GFP-HphMX-loxP-T7-mRFP/MET6* $CYC1_{term}$*:URA3-*$P_{GPD/TDH3}$*-cre-EBD78:*$CYC1_{term}$*/+*	This study
UCC4277	*MAT***a**/α *his3Δ1/his3Δ1 leu2Δ0/leu2Δ0 ura3Δ0/ura3Δ0 met15Δ0/+ lys2Δ0/+ YNL134C-V5-loxP-HA-GFP-HphMX-loxP-T7-mRFP/YNL134C* $CYC1_{term}$*:URA3-*$P_{GPD/TDH3}$*-cre-EBD78:*$CYC1_{term}$*/+*	This study

UCC4395	*MAT***a**/α *his3Δ1/hisΔ1 leu2Δ0/leu2Δ0 ura3Δ0/ura3Δ0 lys2Δ0/+ trp1Δ63/+ hoΔ:: P_{SCW11}-cre-EBD78-NatMX/hoΔ:: P_{SCW11}-cre-EBD78-NatMX loxP-CDC20-*Intron-*loxP-HphMX/loxP-CDC20-*Intron-*loxP-HphMX loxP-UBC9-loxP-LEU2/loxP-UBC9-loxP-LEU2 LSP1-mCherry-KanMX/LSP1-mCherry-KanMX SUR7-GFP-SpHIS5/SUR7-GFP-SpHIS5*	This study
UCC4925	*MAT***a**/α *his3Δ1/his3Δ1 leu2Δ0/leu2Δ0 ura3Δ0/ura3Δ0 lys2Δ0/+ trp1Δ63/+ hoΔ::SCW11pr-cre-EBD78-NatMX/hoΔ:: P_{SCW11}-cre-EBD78-NatMX loxP-CDC20-*Intron-*loxP-HphMX/loxP-CDC20-*Intron-*loxP-HphMX loxP-UBC9-loxP-LEU2/loxP-UBC9-loxP-LEU2*	(70)
UCC5406	*MAT***a**/α *ade2Δ::hisG/ade2Δ::hisG his3Δ1/his3Δ1 leu2Δ0/leu2Δ0 met15Δ::ADE2/+ ura3Δ0/ura3Δ0 trp1Δ63/trpΔD63 hoΔ::P_{SCW11}-cre-EBD78-NatMX/hoΔ:: P_{SCW11}-cre-EBD78-NatMX loxP-UBC9-loxP-LEU2/loxP-UBC9-loxP-LEU2 loxP-CDC20-*Intron-*loxP-HphMX/loxP-CDC20-*Intron-*loxP-HphMX arg4Δ0::KanMX/arg4Δ0::KanMX lys1Δ0::KanMX/lys1Δ0::KanMX*	This study
UCC6884	*MAT***a** *his3Δ1 leu2Δ0 met15Δ0 ura3Δ0 $CYC1_{term}$:URA3-$P_{GPD/TDH3}$-cre-EBD78:$CYC1_{term}$*	This study
UCC6886	*MAT***α** *his3Δ1 leu2Δ0 lys2Δ0 ura3Δ0 $CYC1_{term}$:URA3-$P_{GPD/TDH3}$-cre-EBD78:$CYC1_{term}$*	This study
UCC8773	*MAT***a** *his3Δ1 leu2Δ0 ura3Δ0 lys2Δ0 hoΔ:: P_{SCW11}-cre-EBD78-NatMX loxP-CDC20-*Intron-*loxP-HphMX loxP-UBC9-loxP-LEU2*	(70)
UCC8774	*MAT*α *his3D1 leu2D0 ura3D0 trp1D63 hoD:: P_{SCW11}-cre-EBD78-NatMX loxP-CDC20-*Intron-*loxP-HphMX loxP-UBC9-loxP-LEU2*	(70)
UCC10141	*MAT***a**/α *his3Δ1/his3Δ1 leu2Δ0/leu2Δ0 ura3Δ0/ura3Δ0 lys2Δ0/+ trp1Δ63/+ hoΔ:: P_{SCW11}-cre-EBD78-NatMX/hoΔ:: P_{SCW11}-cre-EBD78-NatMX loxP-CDC20-*Intron-*loxP-HphMX/loxP-CDC20-*Intron-*loxP-HphMX loxP-UBC9-loxP-LEU2/loxP-UBC9-loxP-LEU2 MRH1-GFP-KanMX/MRH1-GFP-KanMX*	This study
UCC11298	*MAT***a**/α *his3Δ1/his3Δ1 leu2Δ0/leu2Δ0 ura3Δ0/ura3Δ0 lys2Δ0/+ trp1Δ63/+ hoΔ:: P_{SCW11}-cre-EBD78-NatMX/hoΔ:: P_{SCW11}-cre-EBD78-NatMX loxP-CDC20-*Intron-*loxP-HphMX/loxP-CDC20-*Intron-*loxP-HphMX loxP-UBC9-loxP-LEU2/loxP-UBC9-loxP-LEU2 SUR7-GFP-SpHIS5/SUR7*	This study
UCC12510	*MAT***a**/α *his3Δ1/his3Δ1 leu2Δ0/leu2Δ0 ura3Δ0/ura3Δ0 met15Δ0/+*	This study

	lys2Δ0/+ HSP26-V5-loxP-HA-GFP-HphMX-loxP-T7-mRFP/HSP26 CYC1$_{term}$:URA3-P$_{GPD/TDH3}$-cre-EBD78:CYC1$_{term}$/+	
UCC12520	*MAT***a**/α *his3Δ1/his3Δ1 leu2Δ0/leu2Δ0 ura3Δ0/ura3Δ*0 met15Δ0/+ lys2Δ0/+ *THR1-V5-loxP-HA-GFP-HphMX-loxP-T7-mRFP/THR1 CYC1$_{term}$:URA3-P$_{GPD/TDH3}$-cre-EBD78:CYC1$_{term}$/+*	This study
UCC12526	*MAT***a**/α *his3Δ1/his3Δ1 leu2Δ0/leu2Δ0 ura3Δ0/ura3Δ0 met15Δ0/+ lys2Δ0/+ SAM2-V5-loxP-HA-GFP-HphMX-loxP-T7-mRFP/SAM2 CYC1$_{term}$:URA3-P$_{GPD/TDH3}$-cre-EBD78:CYC1$_{term}$/+*	This study
UCC12543	*MAT***a**/α *his3Δ1/his3Δ1 leu2Δ0/leu2Δ0 ura3Δ0/ura3Δ0 met15Δ0/+ lys2Δ0/+ NCE102-V5-loxP-HA-GFP-HphMX-loxP-T7-mRFP/NCE102 CYC1$_{term}$:URA3-P$_{GPD/TDH3}$-cre-EBD78:CYC1$_{term}$/+*	This study
UCC12561	*MAT***a**/α *his3Δ1/his3Δ1 leu2Δ0/leu2Δ0 ura3Δ0/ura3Δ0 met15Δ0/+ lys2Δ0/+ GCV3-V5-loxP-HA-GFP-HphMX-loxP-T7-mRFP/GCV3 CYC1$_{term}$:URA3-P$_{GPD/TDH3}$-cre-EBD78:CYC1$_{term}$/+*	This study
UCC12592	*MAT***a**/α *his3Δ1/hisΔ1 leu2Δ0/leu2Δ0 ura3Δ0/ura3Δ0 lys2Δ0/+ trp1Δ63/+ hoΔ:: P$_{SCW11}$-cre-EBD78-NatMX/hoΔ:: P$_{SCW11}$-cre-EBD78-NatMX loxP-CDC20-*Intron*-loxP-HphMX/loxP-CDC20-*Intron*-loxP-HphMX loxP-UBC9-loxP-LEU2/loxP-UBC9-loxP-LEU2 HSP26-mCherry-KanMX/HSP26 HSP104-GFP-SpHIS5/HSP104*	This study

Chapter 3. A NOVEL ASSAY TO MEASURE THE REPLICATIVE LIFESPAN OF BUDDING YEAST

3.1 INTRODUCTION

Age is the greatest risk factor for death worldwide (Harman, 1991; Kirkwood, 2008; World Health Organization, 2010). During the aging process, cellular functions begin to degrade, eventually leading to the death of the organism. Genome-wide screens in nematodes and flies have identified several mutants and genes that modulate lifespan (Hamilton et al., 2005; Pletcher et al., 2002). However, due to the complexity of these multicellular organisms, the cellular and molecular mechanisms of how these mutations affect lifespan have not been elucidated. Budding yeast, *Saccharomyces cerevisiae,* provides an excellent model system for studying the cellular processes of aging because it is a well-characterized unicellular organism that ages by mechanisms similar to higher eukaryotes (Kaeberlein, 2010; Kaeberlein et al., 2007; Steinkraus et al., 2008). Replicative lifespan, defined by the finite number of daughter cells a single mother cell can produce, is affected by many factors that are known to alter lifespan in metazoans (Kaeberlein et al., 1999, 2005a; Mortimer and Johnston, 1959; Tissenbaum and Guarente, 2002). Despite the abundance of genetic and molecular tools available, a genome-wide approach to study aging in yeast has remained virtually impossible or extremely laborious because of the limitations of the assay for replicative lifespan (Kaeberlein and Kennedy, 2005).

Currently, the most-widely adopted method to measure replicative lifespan is micromanipulation. This assay requires manual intervention after every cell division to separate mother cells from the daughter cells until a mother cell ceases to divide (Steffen et al., 2009). Because this process is prohibitively time consuming and tedious, very few attempts have been made to screen the genome for effectors of lifespan in an unbiased way (Kaeberlein and Kennedy, 2005; McCormick et al., 2015). In the past year, McCormick et al. published their list of 238 modulators of lifespan found after using a cursory screen of the yeast deletion collection. However, this study was extremely time consuming, requiring nearly 900 days of hands-on person-hours to complete (calculation

based upon 4700 strains in the collection, 5 cells per strain, 5 WT cells included as paired control, average of 30 divisions per lifespan, and 1 minute micromanipulation required per division). It is unrealistic that a similar approach can be used to screen other large strain collections or to test the environmental requirements of each genotype and its effect on lifespan.

Recently, there have been several attempts to develop microfluidic devices capable of retaining aging mother cells while washing away daughter cells, automatically preventing their accumulation and crowding of the aging cells (Fehrmann et al., 2013; Jo et al., 2015; Lee et al., 2012; Xie et al., 2012). While there have been several devices reported capable of this task, there remain several caveats to their practicality. Firstly, these devices are currently relatively low throughput, only able to assay a few strains/conditions per experiment. Secondly, they require access to several technologies not easily accessible to every lab (clean room facilities and extended use of automated microscopes)(Huberts et al., 2013). Thirdly, all of these devices rely on several physical properties of mother cells, some of which may bias the devices to only measure/retain cells that age in a certain way or with specific physical properties (Lee et al., 2012; Liu et al., 2015). And while there is no doubt that microfluidics will one day revolutionize aging studies in budding yeast, their current applications is not quite ready for unbiased genome-wide screens for effectors of lifespan.

Over the last few years, there have also been several attempts to develop purification strategies and/or genetic systems to facilitate aging studies in budding yeast (Sinclair et al., 1998). There are various systems used to purify aging cells from a population, most using magnetic beads attached to the original and oldest cells in the population (Sinclair and Guarente, 1997; Smeal et al., 1996). These, and similar, approaches have allowed numerous labs to obtain populations of old cells and make observations of various biochemical and physical properties in these cells (Lin et al., 2001; Molin et al., 2011). However, the effectiveness of such strategies as an assay for lifespan is limited by i) the limited purity and yield of old cells during these purifications and ii) the ability to culture cells for their full lifespan without crowding from daughter cells.

Several labs have also developed strategies to fluorescently identify the original and aged cells in the population. This identification can be achieved by labeling young cells with a permanent fluorescent stain that remains associated with these cells throughout their lifespan(McFaline-Figueroa et al., 2011). There are also several strategies to fluorescently stain the budscars that accumulate in a yeast cell wall after each division – cells that stain brighter tend to be the older cells in the population(Chen and Contreras, 2007). Again, these strategies have proved extremely useful to identify relatively aged cells in a population and quantify various phenotypes either by microscopy or flow cytometry. However, these approaches have been limited to studying cells in the middle of their lifespan because of the same limitations that prohibit culturing a population of cells for the entirety of their lifespan.

A genetic system developed to overcome the issue of daughter cells crowding out aging mother cells is the Mother Enrichment Program (MEP)(Lindstrom and Gottschling, 2009). This system, by genetically inhibiting the growth of daughter cells, allows the culturing of a significant number of aging cells to their full replicative lifespan. Using this system, Lindstrom and Gottschling were able to distinguish long- and short-lived strains by monitoring original cell viability as cells aged. However, the assay presented by Lindstrom and Gottschling was still relatively time-consuming, using a low-throughput colony assay to monitor cell viability. Furthermore, the system is sensitive to mutations that arise and allow daughter cells to escape the MEP and remain viable. While lifespan assays with this system and others remain too tedious, costly, or nonspecific for high-throughput screening they have produced several useful techniques to study aging cells.

In order to facilitate genome-wide approaches to identify the determinants of lifespan, I combined several existing technologies in a novel assay for measuring replicative lifespan of yeast cells. This method was designed both to be accurate and amenable to high-throughput screening.

3.2 RESULTS

3.2.1 **Permanent fluorescent labeling of original cells.**

In order to use a flow cytometer to monitor the viability of original/aging cells in a mixed culture I needed two things. Firstly, I needed a way to easily and quickly identify the original mother cells. This identification was accomplished by crosslinking a fluorescent molecule, rhodamine, to the cell walls of a population of cells (Fig 3.1A). Because the cell wall is retained by a cell throughout its entire lifespan, and because daughter cells synthesize their cell wall *de novo,* the presence of rhodamine served as an easily identifiable marker of original cells (Ballou, 1982; Smeal et al., 1996). If a population of labeled cells were used to start an aging culture, the original-aged cells could be identified after many generations (Fig 3.1B). Furthermore, once identified these fluorescently-labeled-original cells show the expected replicative age based upon the time since labeling (Fig 3.1C).

3.2.2 **Assaying cell viability with a stable fluorescent reporter.**

Secondly, I needed a stable, fluorescent, indicator of cell viability. To create such an indicator, I stained the cells with a low concentration of an N-Hydroxysuccinamide ester (NHS) derivative of Dylight680. Because NHS-Dylight680 is a relatively large, polar molecule, it is normally excluded from live cells because they are able to maintain membrane integrity(Davey et al., 2004). However, when a cell dies, its ability to maintain an intact plasma membrane is compromised and NHS-Dylight680 is able to permeate throughout the cell. The NHS group then crosslinks the Dylight680 to any primary amines on the interior of the cell, stably associating the fluorescent molecule with the dead cell. This approach results in live cells staining very dimly when exposed to these concentrations, but dead cells staining very brightly (Fig 3.2A). The difference in staining can be detected by microscopy or flow cytometry (Fig 3.2B).

3.2.3 Original cells lose viability over time.

Combining these two fluorescent signals, I then used a flow cytometer to measure cell viability of the original cells in an aging culture over time (Fig 3.3A). At time zero, where >99% of cells are 6 divisions old or younger, I saw nearly 100% viability. However, as cells aged, I saw an increasing proportion of the cells staining as inviable. This proportion roughly corresponded to the expected cell viability determined from plating assays, except at the very late timepoint (Lindstrom and Gottschling, 2009). This difference can be explained by cells that have died disappearing from the culture (discussed below).

3.2.4 Three methods to quantify flow cytometry lifespan.

In order to control for any confounding factors in our analysis, like possible differences in dead-cell stability in culture, I quantified the data in three different ways. These methods are illustrated in Fig 3.4 and described below. I used a combination of all three of these methods to determine lifespan.

i. Percentage of viable cells of all observed cells. The simplest statistic that I used was the percentage of viable cells observed. As used above and illustrated in Fig 3.4, this percentage was calculated by counting the number of viable-original cells observed compared to all original cells observed (viable or inviable). This method showed the least deviation between biological replicates but could be confounded by a number of factors. Specifically, this statistic assumes that once a cell dies, it remains in the culture indefinitely. However, it appeared that dead cells were not infinitely stable in the culture, as the total number of all original cells observed (both live and dead, per unit volume) decreased over time. Additionally, the stability of dead cells in the culture was affected by the genetic background (haploid vs. diploid cells, data not shown). It is possible that genetic or environmental effectors of this property would confound this analysis.

ii. Concentration of viable cells. The second method that I used to assay lifespan was to measure the absolute concentration of viable cells over time. While flow cytometers are not inherently able to measure concentration, I could compare the number of viable cells to a standard of known concentration added to the aging culture (Stewart and Steinkamp, 1982). Fixed-cells or microsphere beads, distinguishable from aging cells based upon

fluorescent characteristics, were used as a standard with similar results. A known amount of this standard was added to a measured volume of aging culture sampled at each timepoint, prior to any processing steps. Absolute concentration could then be calculated by measuring the ratio between viable original cells and this known standard. While this method allows tracking of the concentration of viable original cells over time, this method is confounded by a few known factors. Any differences in the ability to retain the standard vs the original cells throughout the processing steps would bias the ratio calculated. The processing of each sample required several centrifugation/pelleting steps, and slight differences in the ability to retain cells/standards during each of these steps could affect this ratio. I noticed significant difference in retention of cells/standards depending on total cell density, a variable that is not controlled across aging culture and could be affected by the genotype/condition that is being tested (data not shown). As a result, this method tended to have a higher experimental error when calculated between biological replicates.

iii. Internal control of strain with known replicative lifespan. This third method that I used to assay lifespan was to compare viability to an internal standard wild-type strain with a known replicative lifespan (Lindstrom and Gottschling, 2009). The original cells of one genotype were labeled with rhodamine and the reference strain was labeled with fluorescein, so that each genotype could be distinguished based upon its fluorescent characteristics (Fig 3.5). Reciprocal labeling was also performed, where the reference was labeled with rhodamine and the experimental strain was labeled with fluorescein. This swap was done to control for any label-specific effects on lifespan and/or data analysis. By monitoring the ratio of viable cells of each genotype over time, subtle differences in replicative lifespan could be detected. While this method was sensitive enough to detect small difference in viability between strains over time, it was also technically challenging, sometimes showing significant error between biological replicates. While all the sources of error were not identified, I suspect that small differences in label stability, initial inoculation densities of labeled strains, and retention biases through processing steps could all contribute to experimental error.

3.2.5 **Known short-lived mutants show decreased lifespan.**

In order to test the assay's ability to identify strains and/or conditions with shortened replicative lifespan, I measured the lifespan of a *sir2*Δ strain, a strain previously reported to have a reduced lifespan (Kaeberlein et al., 1999). This strain showed decreased viability of original cells observed in all time points of significant age when compared to a wild-type control strain (Fig 3.6A). Additionally, the concentration of original *sir2*Δ cells decreased faster than the wild-type strain, indicative of these cells having a shorter lifespan (Fig 3.6B). Taken together, these data suggest that the assays can detect shortened lifespan.

3.2.6 **Known long-lived mutants show increased lifespan.**

In order to test the assay's ability to detect increased lifespan, I measured the lifespan of a *ubr2*Δ strain, previously reported as long-lived (Kruegel et al., 2011). This mutant strain showed a higher percentage of viable original cells after 24 and 48 hours (Fig 3.7A). And in agreement with the other analysis, the ratio of viable mutant to wild-type cells increased over time, indicating increased lifespan (Fig 3.7B). These data show nearly a 25% increase in viability after 48-hours, similar to the previously reported lifespan effects of this mutant. Taken together, it appears that the assay are sufficiently sensitive to detect mutants with extended lifespan.

3.2.7 **No observed effects of Caloric Restriction.**

There are several implementations of Caloric Restriction (CR) that have previously been reported to extend replicative lifespan (Lin et al., 2000). I tested their effects on the cells aging in our assay. Unexpectedly, aging cells in 0.5% glucose did not extend viability compared to cells aged in 2% glucose (Fig 3.8). Multiple methods of analyzing the relative viability of the two conditions showed the same result (Fig 3.8 A and B). This result was not due to a difference in rate of division, as cells aged for the same length of time were of similar replicative age (data not shown). I was unable to test lower concentrations of glucose (reported to extend lifespan to a greater degree), as these extremely low

concentrations would be exhausted from the media prior to cells reaching significant replicative age.

I also tested the effects of proposed CR mimetics. *GPA2* encodes a component of a major nutrient-sensing pathway and its deletion is thought to mimic CR (Lin et al., 2000). *gpa2*Δ has been reported to extend lifespan to a similar degree as 0.5% glucose. However, I did not see any effect on the viability of cells aging in our assay (Fig 3.9). Again this result was independent of the method used to analyze the data (Fig 3.9 A,B) or the relative division rate of the cells. I tested several other previously reported genetic mimetics of CR (*hxk2*Δ*, sch9*Δ) and failed to detect lifespan extension in our assay (data not shown).

3.2.8 **Investigation into the lack of Caloric Restrictions effects.**

I wanted to investigate the lack of CR effects observed by our assay, so I tested several differences between our assay and the traditional micromanipulation lifespan assay.

Temperature. Temperature has a large effect on the metabolic rate of a yeast cell. In our assay cells are maintained at 30°C for the duration of their lifespan. However, during the traditional assay, cells spend significant time at room temperature (approximately 23°C) during micromanipulation. Furthermore, because daughter cells must be removed shortly after division, micromanipulation experiments are often periodically placed at 4°C, to slow the rate of cell division at night (Steffen et al., 2009). In order to test the effect of temperature on CR, I performed two experiments. In the first, I aged cells grown in either 0.5% glucose or 2% glucose at 23°C to simulate extended periods spent at room temperature that may be experienced during micromanipulation. I was unable to detect lifespan extension by CR at 23°C (Fig 3.10). In the second experiment, I periodically shifted cells between 30°C and 4°C (cells were placed at 4°C during the night, and transferred to 30°C during the day). This was done to simulate when micromanipulation plates are placed in the refrigerator to slow division rate at night. I was unable to detect any lifespan extension by *gpa2*Δ under this condition (Fig 3.11). It should be noted that cells maintained high viability even at late timepoints, due to slowed growth rate during periods at 4°C. However, *gpa2*Δ did not show altered viability at any timepoint.

Growth media. Most aging experiments are conducted in a rich media, **Y**east Extract – **P**eptone – Glucose (**D**extrose) (YPD), in which the levels of most nutrients are thought to be in great excess and are therefore not tightly controlled (Bergman, 2001). However, some of the effects of CR have been reported in a synthetic defined media (Jo et al., 2015). In order to control for batch-to-batch and source-to-source differences in YPD, I tested for the effects of CR in synthetic defined media using our assay. Again, even when cells were aged in a defined media, 0.5% glucose or CR mimetics failed to extend lifespan (Fig 3.12).

Osmotic and mechanical stress. I reasoned that a yeast cell may experience substantially different forces and/or stresses when grown on the surface of an agar plate or when shaken in a liquid culture, some of which may be required or detrimental to lifespan extension by CR (Kaeberlein et al., 2002). Therefore, in our assay, I aged cells in the presence of 1M Sorbitol, a concentration shown to alter lifespan through osmotic forces placed on aging cells(Figure 3.13)(Kaeberlein et al., 2002). While the rate at which dead cells disappeared from the culture was affected in both 0.5% and 2% glucose, as inferred from a lower percentage of viable original cells observed at later timepoints (Figure 3.13 A), the additional of 1M sorbitol did not reveal lifespan extension in .5% glucose (Figure 3.13 A,B). This experiment was not an extensive effort to replicate the forces experienced by cells on a microdissection plate, and further experiments may be needed to fully exclude this variable.

Small secreted metabolite. Recently, Mei et al. reported the absence of lifespan extension when a cell is removed from its local environment on an agar plate (Mei and Brenner, 2015). They suggest that this response is due to a small metabolite that is secreted into the environment that is required for the lifespan-extending effects of CR. If the aging cell is constantly removed from its local environment, not unlike in a well-mixed dilute liquid culture, there is no lifespan extension by CR. While the exact identity of this secreted molecule is unknown, treatment with nicotinic acid (NA) was sufficient to rescue lifespan extension under CR conditions, as NA likely facilitates the molecule's synthesis. I therefore looked for the effects of CR in our assay when cells are grown in the presence of nicotinic acid. I failed to see lifespan extension by a CR mimetic, *hxk2*Δ, even in the

presence of NA (Fig 3.14). However, I did not test other CR conditions or mimetics in the presence of NA.

3.3 DISCUSSION

3.3.1 Comparison to other lifespan assays

The goal of this project was to develop a novel and tractable assay, requiring minimal experimentalist intervention, capable of distinguishing long- and short-lived mutants and/or conditions. The assay, as described above, achieves many of these goals.

First, the assay requires much less manual intervention than the traditional lifespan assay. Populations of original cells are permanently labeled at the beginning of the experiment, eliminating the need to track mother cells throughout every cell division. Timepoints are only taken as often as necessary, dictated by the temporal resolution required in each experiment. Additionally, the MEP prevents daughter cells from dividing exponentially, so there is no need to purify mother cells at any point during the protocol. The populations of mother cells can be left in a single culture for the duration of their lifespan.

Using the MEP also allows us to look at large numbers of mother cells. Aging cultures are inoculated with $2x10^4$ original cells per milliliter of culture. And in all experiments presented here, viability was determined by at least 10^3 cells at each timepoint (usually greater than 10^4 cells). During a traditional micromanipulation experiment, 40 cells are used to determine lifespan(Steffen et al., 2009). And because there is inherent stochasticity in the absolute lifespan of a given single cell, significant error can be introduced by using low sample numbers to determine the lifespan of a population.

The assay also uses technology widely available to any laboratory. The chemistry used to permanently label mother cells is similar to that used to make fluorescent secondary antibodies, and the reagents are readily available for relatively little cost. Components of the MEP do need to be introduced into the experimental strains, but this effort can be done using standard yeast genetic techniques. And while the assay requires access to a flow cytometer to quickly assess the viability of the fluorescently labeled cells in the

population, a flow cytometer is not required constantly throughout the aging process to track specific cells.

3.3.2 The assay did not detect the effects of Caloric Restriction or mutants mimicking Caloric Restriction

While the assay was able to detect the lifespan modulating effects of mutants not thought to act through CR, there was no observed effect from several implementations of CR. While the lack of these effects could not be explained by several environmental factors that I tested, there remain several possibilities why the assay was not able to replicate the previously reported effects of CR.

Recently, the reported effects of CR on the lifespan of *S. cerevisiae* have been challenged (Huberts et al., 2014). Reporting the absence of lifespan extension under CR conditions in their microfluidic device, Huberts et al. suggest that a majority of studies using the traditional micromanipulation assay suffer from under sampling error. In a meta-analysis of aggregated lifespan assays they show no evidence of lifespan extension under CR conditions.

While Huberts et al. provide compelling evidence that there is no lifespan extension by CR under their experimental conditions, there remains a number of uncontrolled variables that could explain the lack of CR effects. First, many aging experiments have been performed in a poorly defined rich media (YPD). The levels of many metabolites could vary from batch-to-batch or lab-to-lab, with unknown effects on metabolism or lifespan. Second, it is possible that conditions are fundamentality different between growth in a liquid culture, in a microfluidic device, or on an agar plate. The availability of many nutrients could be dramatically altered in each of these environments. While these variables may not affect the growth rate or other properties of young cells, they may be sufficient to alter the aging process.

Lastly, there are a number of additional variables between lifespan/aging experiments. There are a number of strain backgrounds, auxotrophic markers, culturing conditions and other variables that could have unanticipated effects on how cells age. Aging is an extremely complicated process and it is obvious that we, as a field, do not know many of

the factors capable of determining lifespan. In order to resolve the controversy of the effects of CR and prevent others from arising, I feel there needs to be a concerted effort to control as many of these variables as possible.

3.3.3 Ability to adapt this assay for genome-wide screening

The assay, as designed, is not limited to pairwise testing of mutants. Many different genotypes can be tested in a single experiment as long as they can be distinguished by some unique identifier. While this multiplexing can be achieved by additional fluorescent labels (and combinational labeling), identifiers can be encoded in the DNA sequence of each genotype. Several genome-wide collections already exist with DNA sequence barcodes used to identify each genotype (Giaever et al., 2002; Ho et al., 2009). While discussed in more detail in the next chapter, these barcodes can allow a dramatic increase in throughput in a screen to identify genotypes that maintain viability with increased age.

3.3.4 Ability to adapt this assay to measure other characteristics of the aging process

The assay can also be made to sensitive to changes in particular aging phenotypes. Because a flow cytometer is able to rapidly quantify several fluorescent characteristics of cells at once, it can also measure any phenotype that can be characterized by a loss or gain in fluorescence. Again while discussed in much greater detail in the next chapter, this feature greatly increases the flexibility of the assay. Rather than being restricted to screening for mutants that simply maintain viability in increased age, this method can be used to identify mutants that age with particular characteristics – aged cells that do or do not express a particular gene, maintain organelle function, accumulate a particular protein, or any of a number of other phenotypes.

3.4 METHODS

Plasmids and Strains. Plasmids used in this chapter are presented in Table 3.1 and have previously been described. Strains used in this study are presented in Table 3.1. Standard

S. cerevisiae methods were used to generate PCR-mediated mutations, zygotes, sporulation, tetrad analysis and selection of strains with relevant markers(Dunham et al., 2015).

Media and Growth Conditions. Unless otherwise indicated (exceptions are explicitly discussed below) cells were grown at 30°C in YEPD.

Labeling of original cells. As described in the protocol included as Appendix A, cells were grown overnight to saturation. Cells were diluted back and grown for 16 hours to early log-phase (~.1 OD^{600}). Cells were washed at least twice in PBS to remove any molecules that would quench reaction with NHS. Cells were resuspended in 500mg/mL NHS-Rhodamine or NHS-Fluorescein (Thermo Fisher Scientific) in PBS and labeled for 15-20 minutes. Cells were then washed at least twice in PBS to remove any excess label and resusupended in growth media at approximately $2x10^4$ cells/ml. 1 μM 17β-Estradiol (Sigma-Aldrich) was added 2 hours after labeling to engage the MEP(Lindstrom and Gottschling, 2009).

Live/dead cell staining. As described in the protocol included as Appendix A, growth media was removed and cells were washed at least twice in PBS. Cells were then stained for 20 minutes in 50μg/mL NHS-Dylight680 (Thermo Fisher Scientific) in PBS. Cells were then washed in PBS and fixed in ~4% formaldehyde for 10 minutes.

Microscopy. All microscopy was performed on one of two wide-field fluorescence microscopes: (*i*) a Nikon E800 equipped with a 60×/1.40 objective or (*ii*) a Leica DMI-6000b equipped with a 63×/1.40 objective. Image processing and quantification was performed with Fiji, a distribution of ImageJ software(Schindelin et al., 2012).

Flow cytometry. Flow cytometry was performed on a Beckman Dickinson LSR II flow cytometer. Rhodamine fluorescence was measured through PE channel. Fluorescein fluorescence was measured through FITC channel. Dylight680 fluorescence was measured through APC-700 channel. Events with extremely high or low Forward and Side Scatter properties were excluded from analysis. Flow cytometry data were analyzed with the FlowJo software package.

Experimental details:

*sir2*Δ lifespan – *sir2*Δ (UCC8836) and WT (UCC5185) cells were labeled as described above, aged and samples were taken at 0, 24, 48 and 72 hours. The percentage of viable original cells and the normalized concentration of viable original cells were compared at each timepoint.

*ubr2*Δ lifespan – *ubr2*Δ (UCC11031) and WT (UCC4925) cells were labeled as described above, aged and samples were taken at 0, 24, 48 and 72 hours. The percentage of viable original cells and the normalized concentration of viable original cells were compared at each timepoint.

Lifespan in 0.5% or 2% glucose – WT cells (UCC4925) cells were labeled with rhodamine as described above. Samples were taken at timepoints listed in each experiment. The percentage of viable original cells and the normalized concentration of viable original cells were compared at each timepoint.

*Gpa2*Δ lifespan – *gpa2*Δ (UCC11029) and WT (UCC4925) cells were labeled as described above, aged and samples were taken at 0, 3, 24, and 48 hours. The percentage of viable original cells and the normalized ratio of viable original cells from each genotype were compared at each timepoint.

Temperature Variation – Experiments were performed as described above ('Lifespan in 0.5% or 2% glucose' or '*gpa2*Δ lifespan') except cells were either: i) cultured at 23°C for the duration of the aging process or ii) periodically shifted to 4°C during the aging process. Cells were kept at 30°C during the day and transferred to 4°C at night. Cells were agitated (either on a shaker or roller drum) at all temperatures.

CR in synthetic media – 'Lifespan in 0.5% or 2% glucose' was performed as described excepted for cells were maintained in YC media for all growth steps (saturated culture, log culture, aging culture).

*Gpa2*Δ lifespan in the presence of 1M sorbitol – '*gpa2*Δ lifespan' was performed as described except 1M Sorbitol was added to specified aging cultures.

*Gpa2*Δ lifespan in the presence of Nicotinic Acid – '*gpa2*Δ lifespan' was performed as described except .5mM Nicotinic Acid was added to specified aging cultures.

3.5 Contributions and Acknowledgments

Nathaniel Thayer and Dan Gottschling designed all experiments. Nathaniel Thayer performed all experiments. Kenneth Chen, Edward Marsh, Nina Yazvenko used the assay presented in this chapter to measure lifespan of various strains, however the results were not included here. I would also like to thank all members of the Gottschling Lab for various contributions and support of this project.

3.6 TABLES AND FIGURES

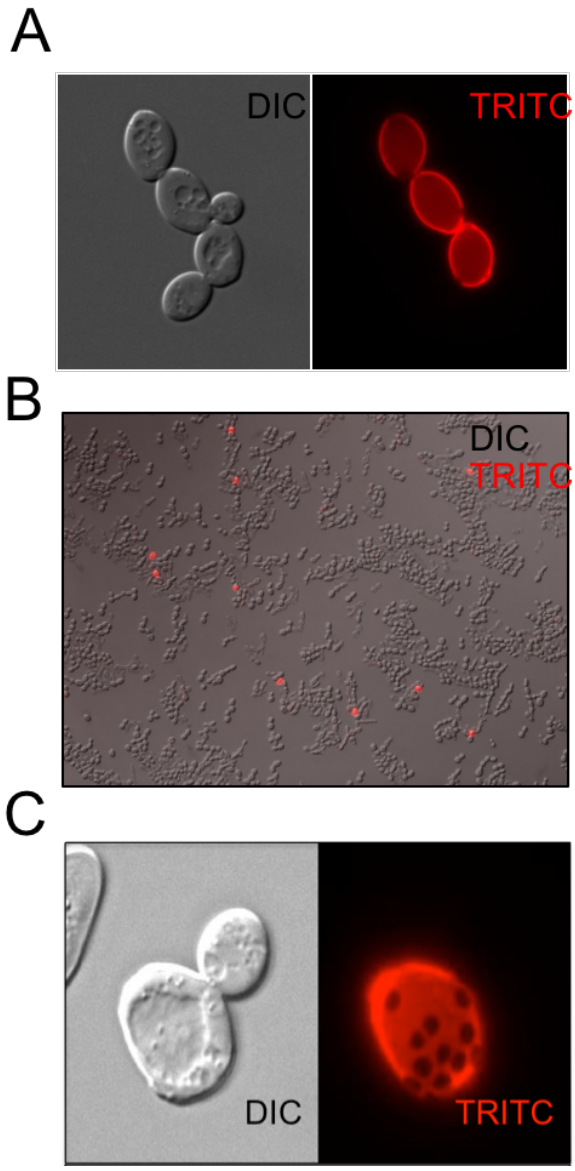

Figure 3.1. Permanent labeling of original cells.

A) Cells were labeled with NHS-Rhodamine, cross-linking the fluorophore to primary amines present in the yeast cell wall. Cells were imaged 2 hours after labeling. Daughter cells that were produced after the labeling lack fluorescence. B) A population of labeled cells was used to start an aging culture and imaged 24 hours later. The original, fluorescent cells, are easily identifiable. C) Fluorescently labeled cells are the expected replicative age. Age can be determined by budscars visualized as either voids in the rhodamine signal or calcofluor white fluorescence (calcofluor channel not shown).

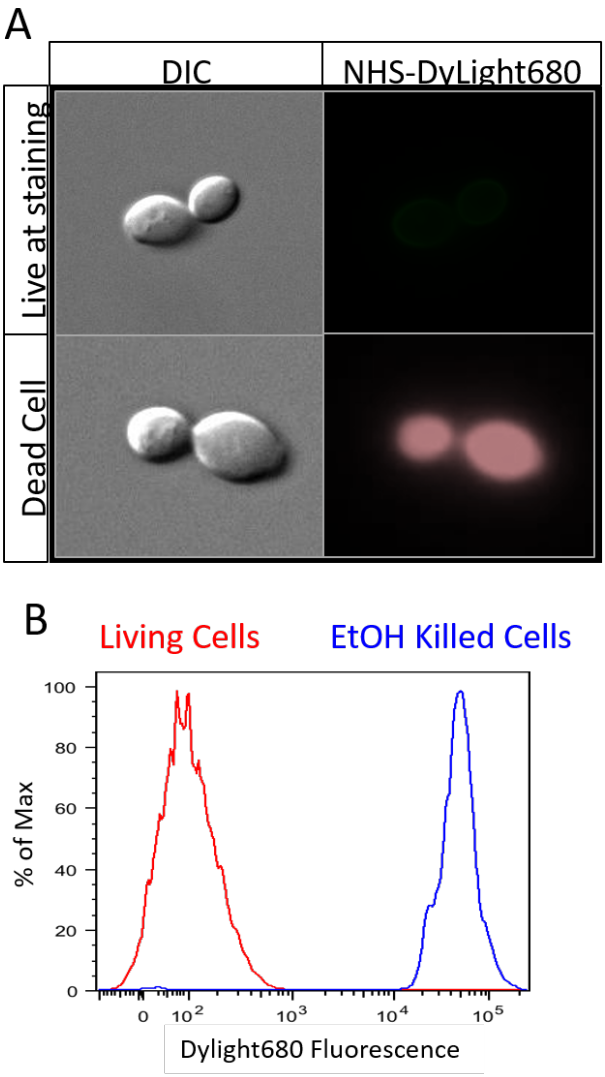

Figure 3.2. NHS-Dylight680 as a viability stain

A) Two populations of cells were stained with NHS-Dylight680, one live population and one dead (killed with 70% EtOH). These two populations show vastly different Dylight680 staining intensity. B) These two populations are easily distinguishable by flow cytometry. Dead cells show >2 orders of magnitude increases in fluorescence.

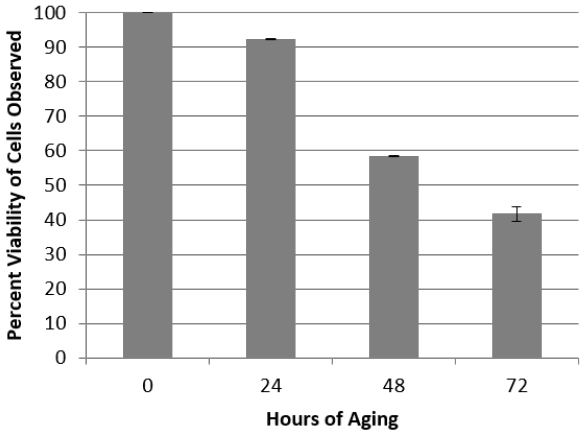

Figure 3.3. Original cells lose viability of time

A population of diploid cells was aged for 72 hours and the fraction of original cells that remained viable was monitored by flow cytometry. The percentage of viable cells, except at later timepoints, roughly matches that expected based upon the known lifespan of this strain. The percentage is likely higher than expected at later timepoints because dead cells may disappear from the culture (discussed in section 3.2.4).

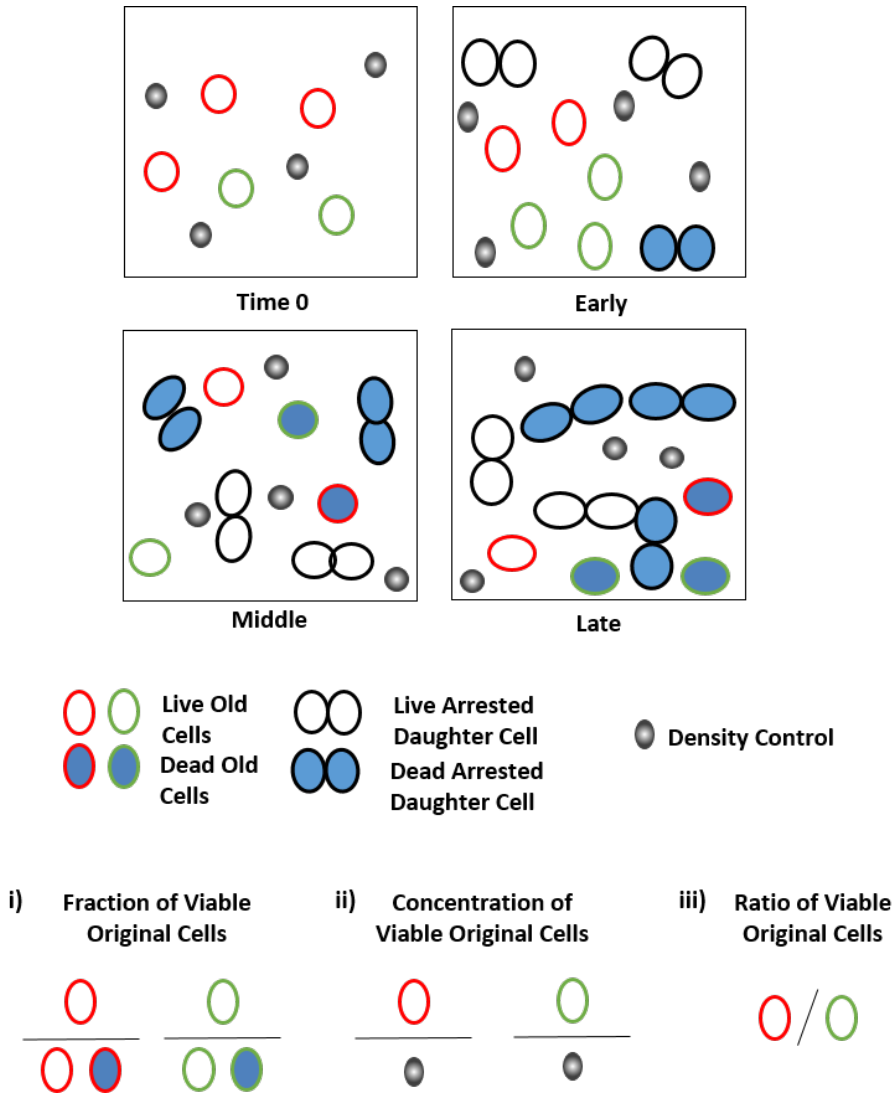

Figure 3.4. Methods of analyzing lifespan assay cultures

i) Calculate the fraction of old cells still viable at each timepoint. This calculation can be done for any labeled population of cells. ii) Calculate the relative density of viable original cells against a standard of known density. This calculation can be done for any labeled population of cells. iii) Calculate the ratio of viable cells from one population versus another population. This approach requires the two populations be uniquely labeled and aged within the same culture.

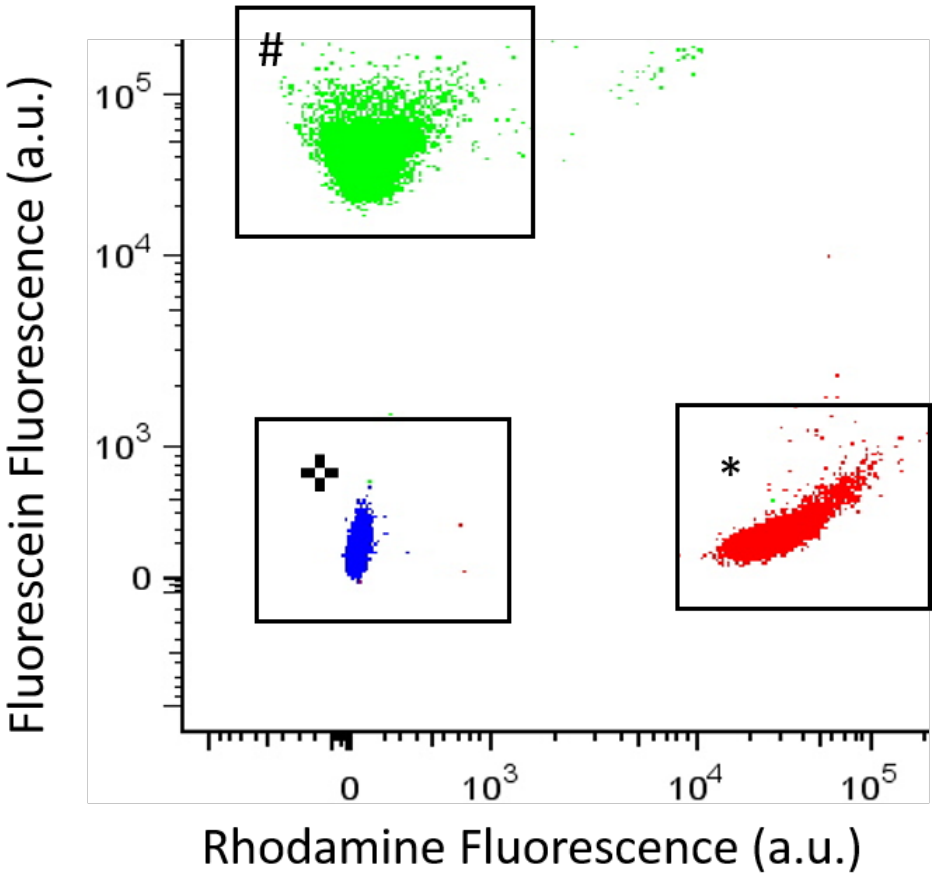

Figure 3.5. Differential labeling to identify populations of cells.

Populations of cells were either labeled with NHS-Rhodamine (marked by *), NHS-Fluorescein (marked by #). Using flow cytometry, these populations are easily distinguishable from both each other and unlabeled cells (marked by ✣).

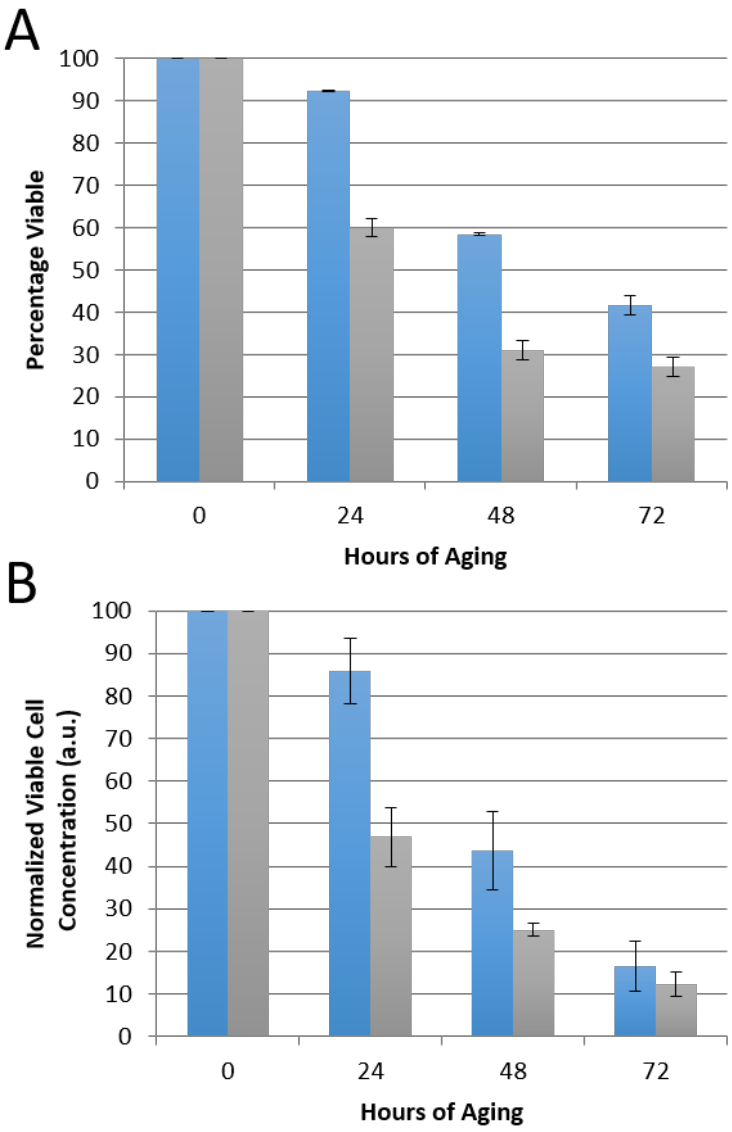

Figure 3.6. sir2Δ appears short-lived by this lifespan assay

A) The percentage of viable sir2Δ (gray bars) and WT (blue bars) cells were monitored over time. sir2Δ cells show decreased viability at several aged timepoints compared to WT. B) The concentration of viable sir2Δ cells decreases faster than that of WT, indicative of a short-lived strain.

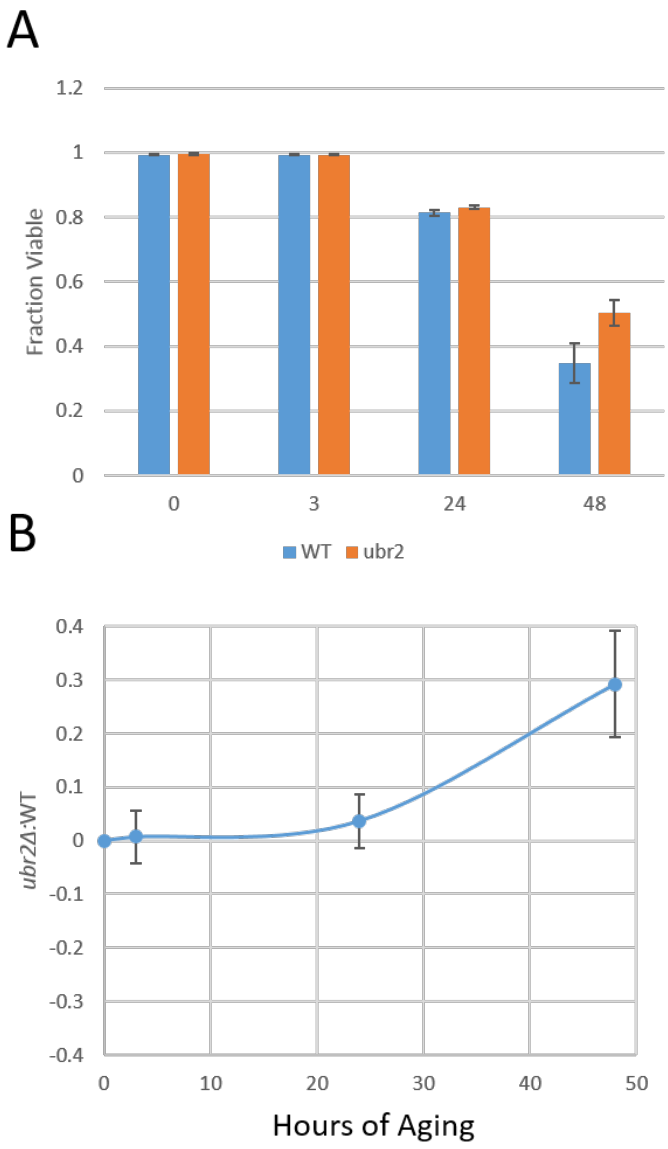

Figure 3.7. ubr2Δ appears long-lived by this lifespan assay

A) The fraction of viable ubr2Δ and WT cells were monitored over time. ubr2Δ cells show increased viability at several aged timepoints compared to WT. B) The ratio of viable ubr2Δ cells to viable WT increases as the cells age, indicating that the ubr2Δ strain is longer-lived that WT.

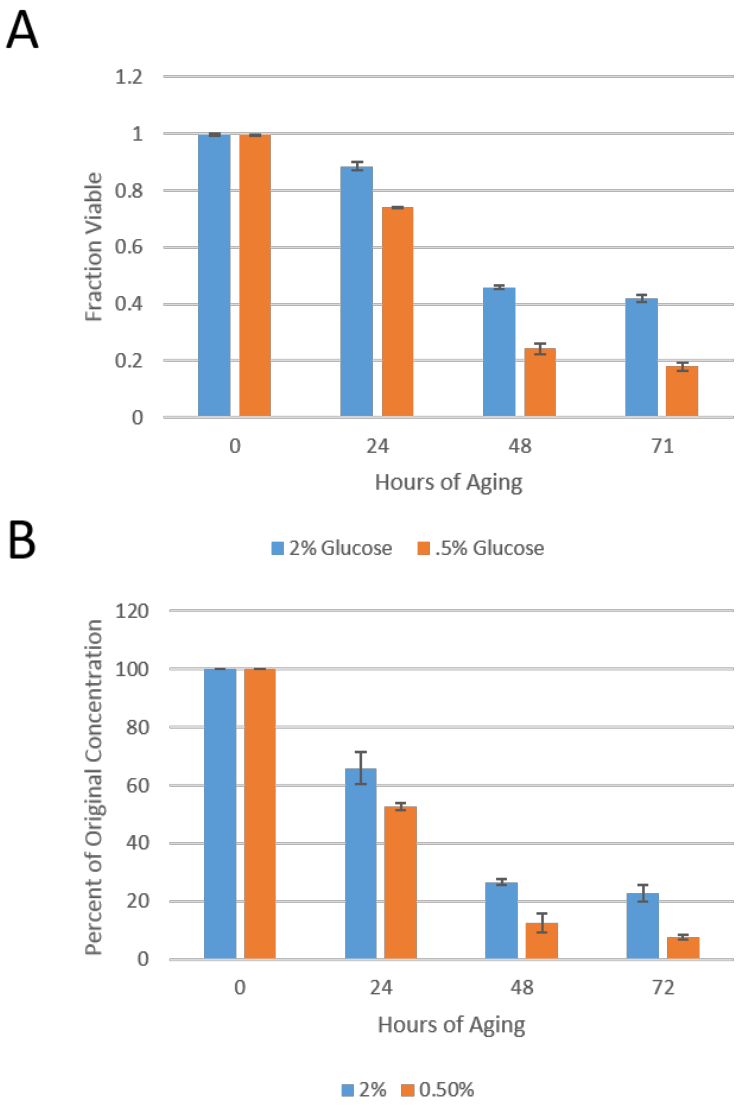

Figure 3.8. No detectable effects of 0.5% glucose

A) The fraction of viable cells grown in .5% glucose and 2% glucose were monitored over time. Unexpectedly, the cells grown in .5% glucose did not show increased viability compared to those grown in 2% glucose. B) Surprisingly, the concentration of viable cells in in 0.5% glucose decreases more rapidly than cells aged in 2% glucose.

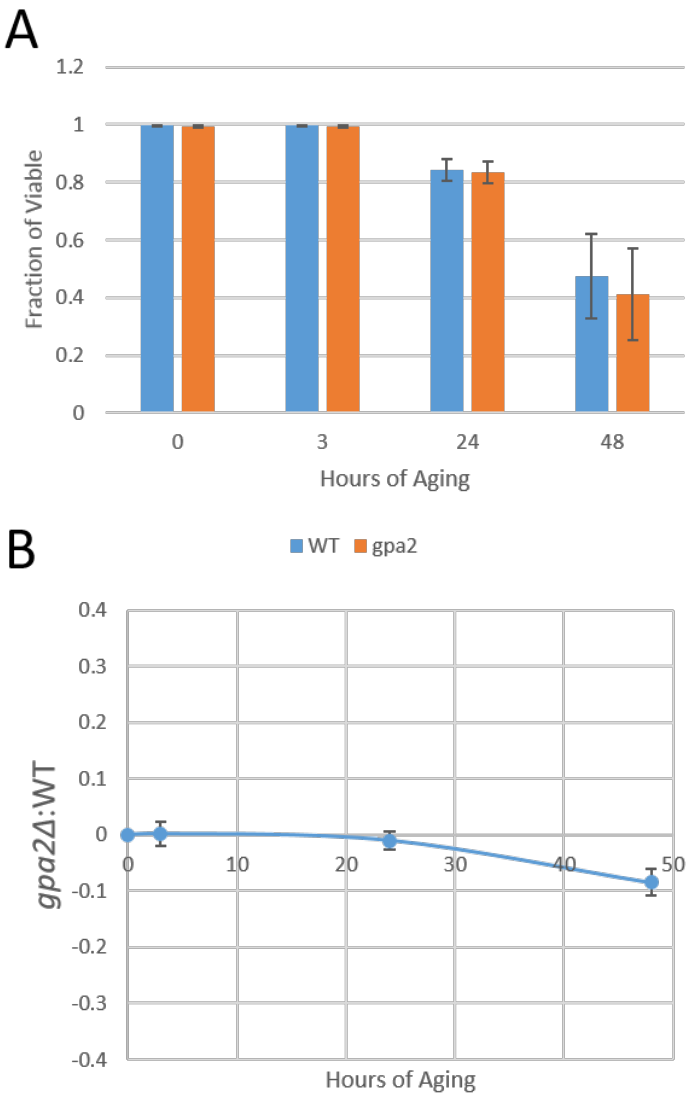

Figure 3.9. No detectable effects of the CR mimetic, gpa2Δ

A) The fraction of viable *gpa2*Δ and WT cells were monitored over time. *gpa2*Δ cells do not show increased viability at aged timepoints compared to WT.B) The ratio of viable *gpa2*Δ cells to viable WT does not increase as the populations age, suggesting that this mutant is not long-lived.

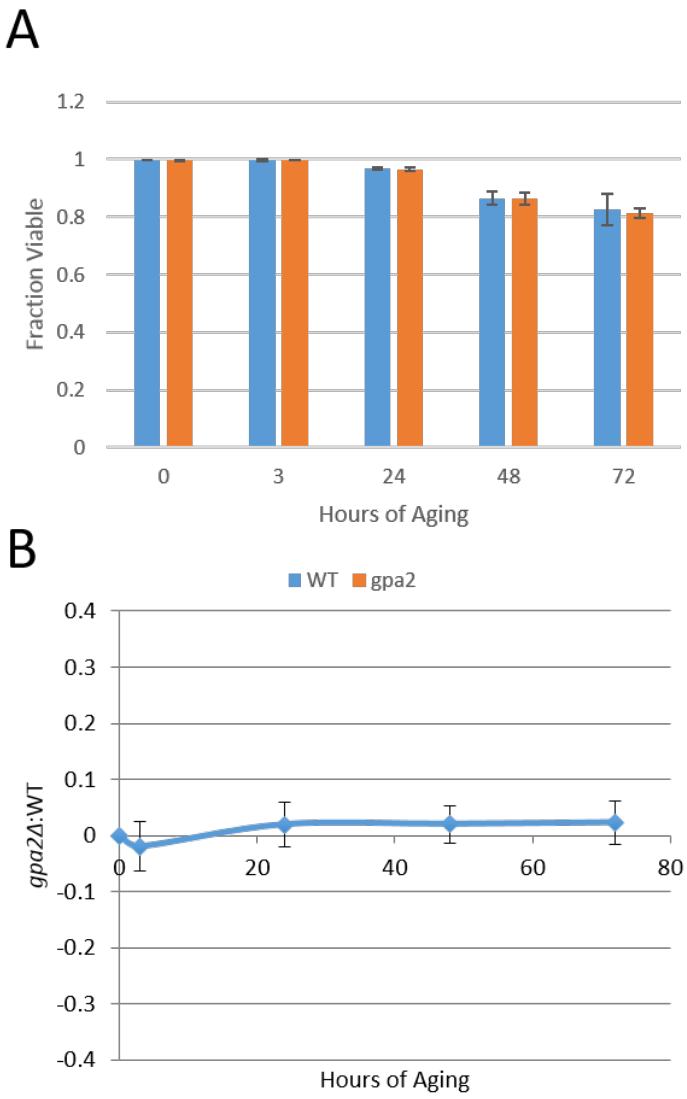

Figure 3.10. No detectable CR effects when cells are periodically shifted to 4°C.

*gpa2*Δ and WT cells were aged at 30°C during the day and shifted to 4°C at night to simulate placing a microdissection plate in the refrigerator overnight. This procedure resulted in no significant difference in viability (A) or change in the ratio of viable *gpa2*Δ:WT cells at any timepoint (B).

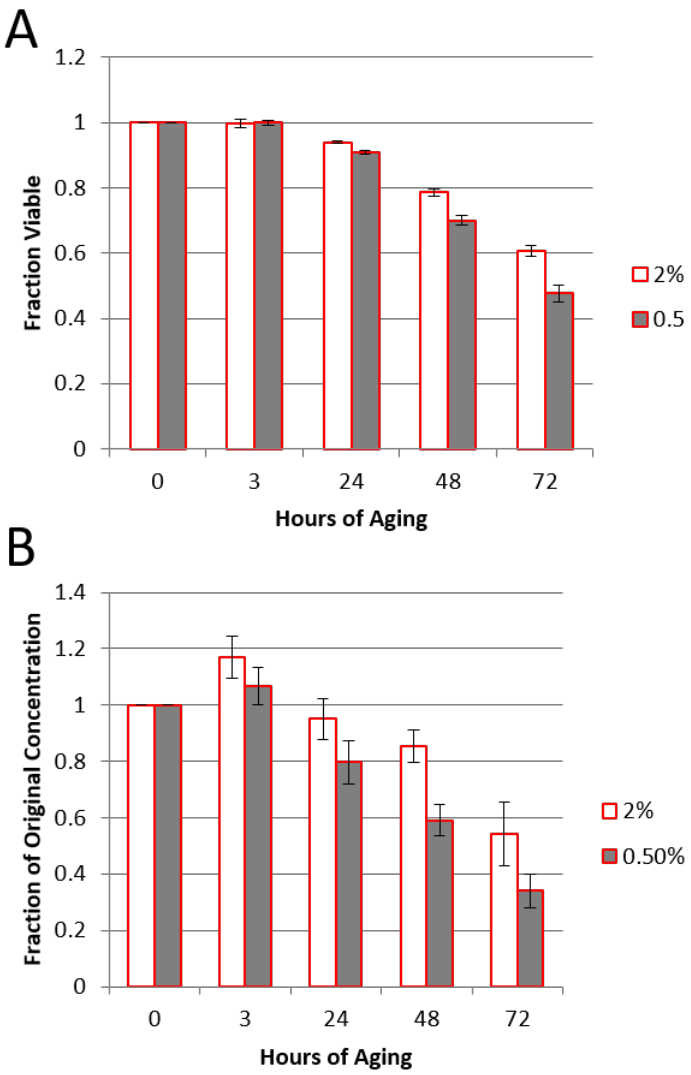

Figure 3.11. No detectable CR effects when cells are aged at room temperature.

Cells were aged in YP-2% Glucose or YP-.5% Glucose at room temperature to simulate the extended time cells experience room temperature during micromanipulation steps. A) This procedure did not result in cells aged in YP-0.5% Glucose having increased viability at any timepoint taken. B) The concentration of cells aged in YP-0.5% Glucose did not decrease slower than cells aged in YP-2% Glucose.

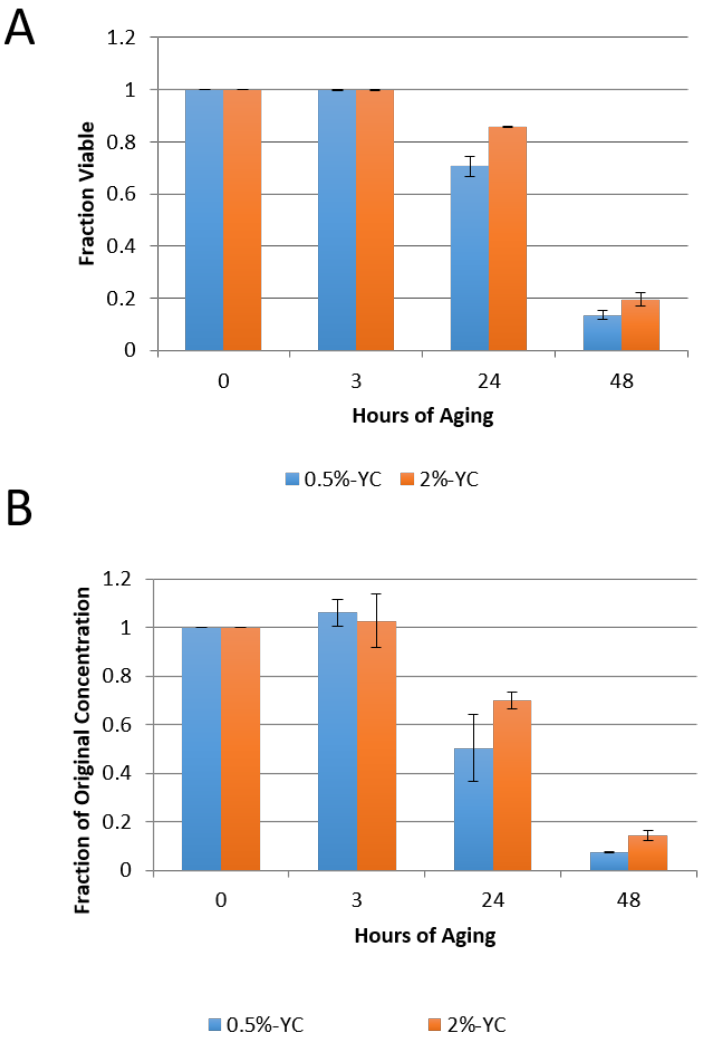

Figure 3.12. No detectable CR effects when cells are aged in synthetic media.

A) The fraction of viable cells grown in YC-0.5% glucose and YC-2% glucose were monitored over time. Cells aged in the 2% media did not appear long-lived. B) The concentration of viable cells aged in YC-0.5% glucose does not decrease more slowly than those aged in YC-2% glucose.

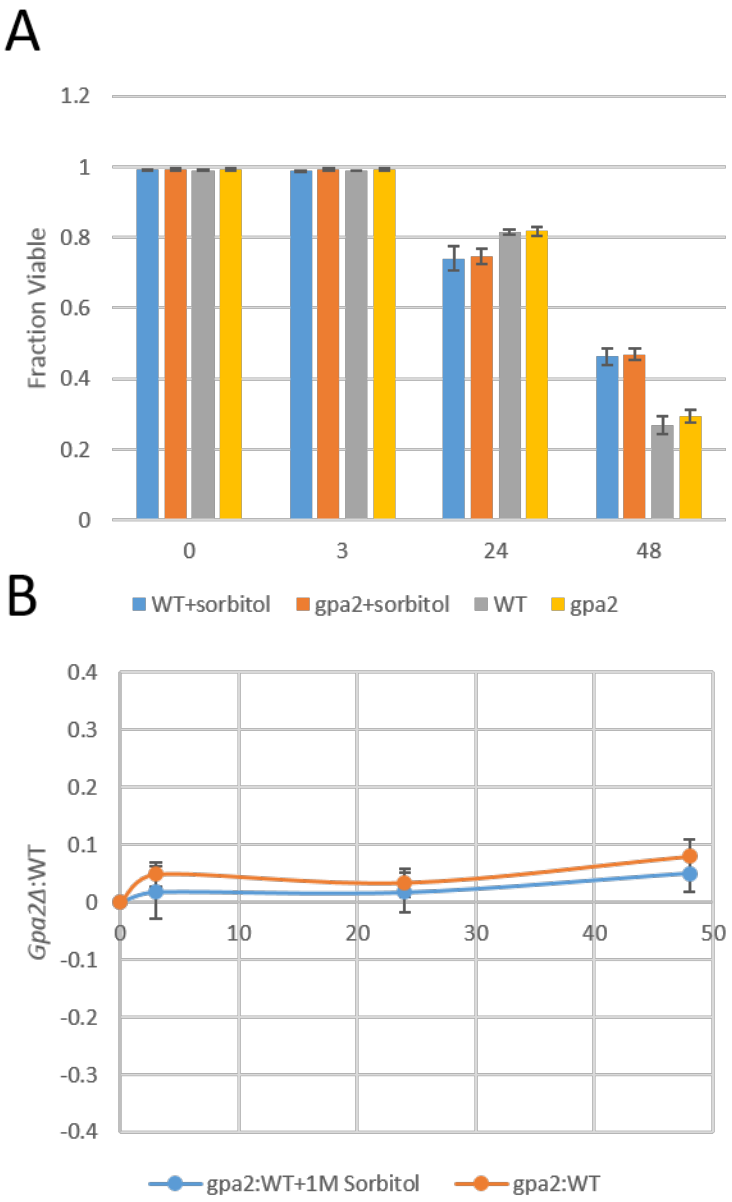

Figure 3.13. No detectable CR effects in the presence of 1M Sorbitol.

The fraction of viable of *gpa2*Δ and WT cells aged in the presence of 1M sorbitol was monitored over time. *gpa2*Δ cells do not show increased viability at aged timepoints compared to WT. B) The ratio of viable *gpa2*Δ cells to viable WT does not increase as the populations age in the presence of 1M sorbitol, suggesting that this mutant is not long-lived under these conditions.

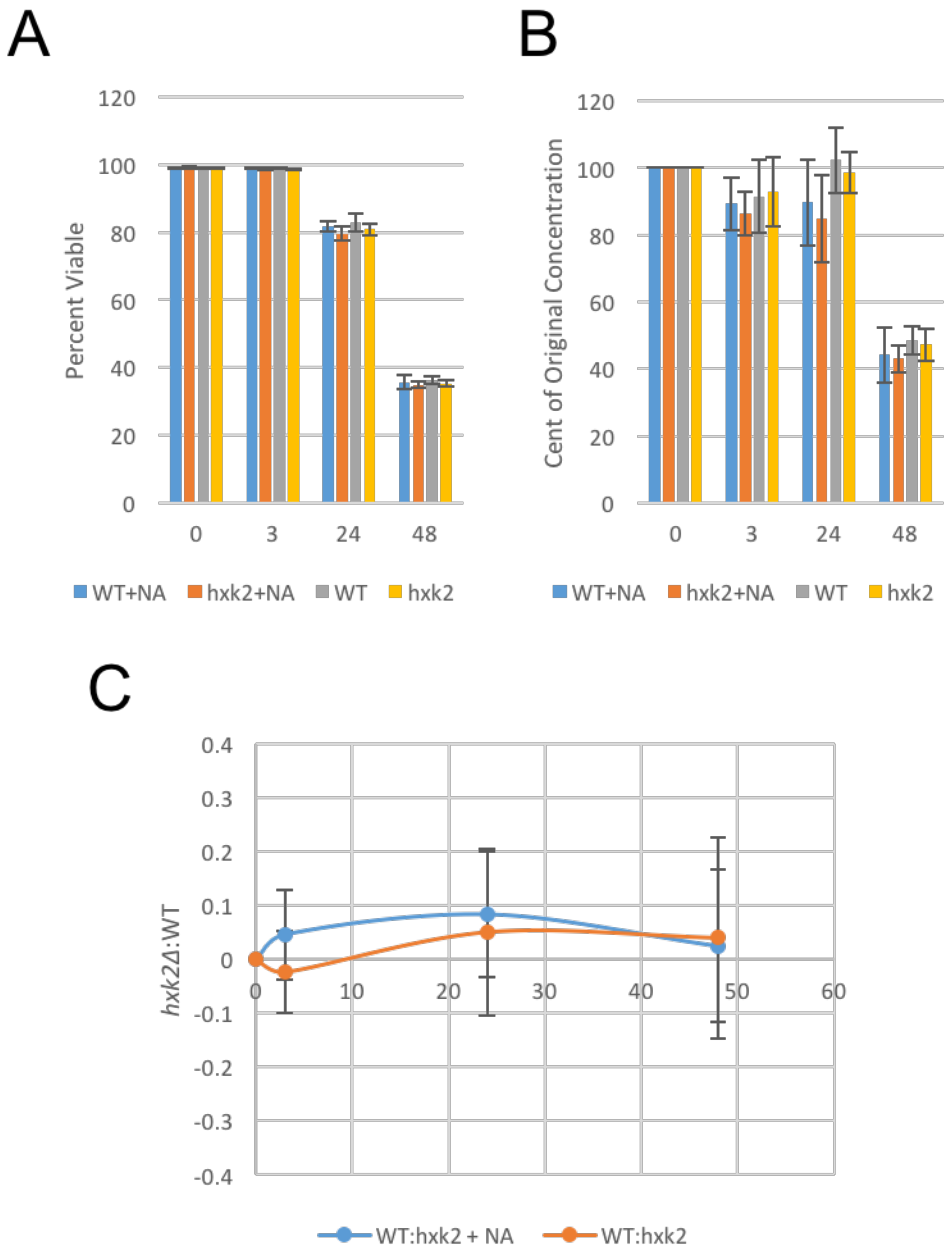

Figure 3.14. No detectable CR effects in the presence of nicotinic acid.

A) The fraction of viable *hxk2*Δ and WT cells aged in the presence of nicotinic acid was monitored over time. *hxk2*Δ cells do not show increased viability at aged timepoints compared to WT. B) The concentration of viable hxk2Δ does not decrease more slowly than that of WT in presence of 1mM nicotinic acid. C) The ratio of viable hxk2Δ cells to viable WT does not increase as the populations age in the presence nicotinic acid, suggesting that this mutant is not long-lived under these conditions.

Table 3.1. Strains and plasmids used

Plasmid or strain	Genotype or descriptions	Source or reference
Plasmids		
pRS400	Used to delete genes with *KanMX* cassette	(Brachmann et al., 1998)
pRS306	Used to delete genes with *URA3* cassette	(Brachmann et al., 1998)
Yeast Strains		
UCC4925	*MAT***a**/α *his3Δ1/his3Δ1 leu2Δ0/leu2Δ0 ura3Δ0/ura3Δ0 lys2Δ0/+ trp1Δ63/+ hoΔ::SCW11pr-cre-EBD78-NatMX/hoΔ:: P_{SCW11}-cre-EBD78-NatMX loxP-CDC20*-Intron-*loxP-HphMX/loxP-CDC20*-Intron-*loxP-HphMX loxP-UBC9-loxP-LEU2/loxP-UBC9-loxP-LEU2*	(Lindstrom and Gottschling, 2009)
UCC5185	*MAT***a**/α *ade2::hisG/ade2::histG his3Δ1/his3Δ1 leu2Δ0/leu2Δ0 ura3Δ0/ura3Δ0 lys2Δ0/+ trp1Δ63/ trp1Δ63 met15Δ::ADE2/+ hoΔ::SCW11pr-cre-EBD78-NatMX/hoΔ:: P_{SCW11}-cre-EBD78-NatMX loxP-CDC20*-Intron-*loxP-HphMX/loxP-CDC20*-Intron-*loxP-HphMX loxP-UBC9-loxP-LEU2/loxP-UBC9-loxP-LEU2*	(Lindstrom and Gottschling, 2009)
UCC8836	UCC5185 + *sir2Δ::KanMX/ sir2Δ::KanMX*	This study
UCC11031	UCC4925 + *ubr2Δ::URA3/ ubr2Δ::URA3*	Jessica Hsu – Gottschling Lab
UCC11029	UCC4925 + *gpa2Δ::URA3/ gpa2Δ::URA3*	Jessica Hsu – Gottschling Lab
UCC529	UCC5185 + *hxk2Δ::KanMX/ hxk2Δ::KanMX*	Michelle DuBois – Gottschling Lab

Chapter 4. GENOME-WIDE SCREEN FOR GENETIC SUPPRESSORS OF AN AGE-ASSOCIATED LOSS OF MITOCHONDRIAL MEMBRANE POTENTIAL

4.1 INTRODUCTION

As an organism ages, there is a characteristic decline in viability, reported as a lifespan or survival curve. These curves have been well defined for many organisms and most curves show similar traits, although with altered timescales. Underlying the decline in viability is a breakdown of many systems required to sustain life; these failures can be termed 'aging phenotypes'. While there are a number of noted aging phenotypes on the tissue and organism level (decline in cognitive function, heart and other organ failure, reduced tissue elasticity, etc.), there are far fewer processes on the cellular level that are known to be affected by age.

One cellular aging phenotype observed in many organisms is an age-associated decline in mitochondrial function. Age-associated mitochondrial phenotypes have been reported in yeast, worms, flies, and mammals (reviewed in ref. (Seo et al., 2010). Decreases in mitochondrial number, altered mitochondrial structure, and dysfunctional mitochondrial respiration have all been reported as a function of age. Furthermore, mutations in specific mitochondrial components can lead to early onset of the aging process and can limit lifespan (Edgar and Trifunovic, 2009).

In budding yeast, mitochondrial aging phenotypes can be characterized by a loss of mitochondrial membrane potential ($\Delta\psi^{mito}$) and altered mitochondrial morphology (Hughes and Gottschling, 2012; Scheckhuber et al., 2007). $\Delta\psi^{mito}$ is used by the mitochondria for generation of ATP, import of mitochondrial proteins, and active metabolite transport with the cytosol, and it is an important measure of mitochondrial health (Chen, 1988). In 2012, Hughes and Gottschling reported that this aging phenotype is important in determining the lifespan of a yeast cell – mutations that suppressed the age-associated loss of $\Delta\psi^{mito}$ also extended lifespan.

In addition to strongly correlating $\Delta\psi^{mito}$ with lifespan, Hughes and Gottschling also showed that this aging phenotype is preceded by another age-associated phenomenon, a loss of vacuole acidity. Mutations that suppressed or delayed the loss of vacuole acidity also delayed the onset of mitochondrial dysfunction. Additionally, chemically induced loss of vacuole acidity was sufficient to cause mitochondrial dysfunction in young cells. This work established an important aging cascade, initiated by an early loss of vacuole acidity, leading to mitochondrial dysfunction, ultimately determining lifespan. However, there remains a number of unanswered questions:

What are all of the factors responsible for regulating vacuole acidity? There are a number of processes known to regulate vacuole function (Li and Kane, 2009). Hughes and Gottschling reported that an overexpression of two components of the vacuolar proton pump is sufficient to maintain vacuole acidity. Nutrient-sensing pathways are known to regulate activity of this same proton pump (Kane and Smardon, 2003). However, the full extent of factors capable of altering vacuole acidity is not known, especially with age.

Why does loss of vacuole acidity lead to mitochondrial dysfunction? Hughes and Gottschling suggested that mitochondrial function is altered, at least in part, by an inability to store nutrients in the vacuole after loss of acidity (Fig 4.1). Overexpression of a vacuole nutrient transporter, *AVT1,* prevented mitochondrial dysfunction even after loss of vacuole acidity. It is suggested that *AVT1* overexpression increases transport of several metabolites into vacuoles with lower acidity. However, there is still no established mechanism for why a loss of vacuole acidity leads to mitochondrial dysfunction. *AVT1* is responsible for transporting several nutrients and/or the effect on the mitochondria could have been indirect (Russnak et al., 2001; Tone et al., 2015).

Are there factors that can protect the mitochondria and block this aging cascade? It would be interesting to identify factors that are able to protect the mitochondria from other events that occur during the aging process. Not only would such factors help establish a mechanistic link between these two processes, they would also suggest possible interventions to prevent this aging cascade from limiting lifespan through mitochondrial dysfunction.

In order to elucidate the mechanism by which the phenotypes are interconnected and to find additional genetic regulators of these aging processes, I carried out a genome-wide screen to identify genetic suppressors of the age-associated loss of mitochondrial membrane potential.

4.2 RESULTS

4.2.1 Age-associated loss of mitochondrial membrane potential can be monitored by flow cytometry.

Firstly, in order to perform a genome-wide screen, I needed to monitor $\Delta\psi^{mito}$ using a technology that is amenable to high-throughput screening. While microscopy techniques can accurately measure DiOC6(3) staining as a reporter of $\Delta\psi^{mito}$, this technique is limited in its throughput (Pringle et al., 1989). Using techniques outlined in Chapter III of this dissertation, I was able to adapt flow cytometry and Fluorescence-Activated Cell Sorting (FACS) to measure DiOC6(3) staining, specifically in aged cells. Briefly, the cell walls of a population of cells were permanently labeled with a fluorescent molecule, rhodamine. Because any cells produced after the labeling process are devoid of fluorescent signal, this fluorescent signature was used to identify the original, aged, cells in a flow cytometer. This method could then be used to monitor other fluorescent characteristics of these aged cells, like DiOC6(3) staining intensity (Fig 4.2A). This technique was sensitive enough to detect the age-associated decline in DiOC6(3) staining intensity, indicative of the previously characterized loss of mitochondrial membrane potential (Fig 4.2B)(Hughes and Gottschling, 2012).

4.2.2 A genome-wide screen to identify genetic regulators of the age-associated loss of mitochondrial membrane potential.

To identify genetic regulators of the aging phenotype, I screened the yeast deletion collection for deletion mutants that are able to maintain DIOC6(3) staining in aged cells (Outlined in Fig 4.3). In order to culture cells to any significant age, mutants were first crossed into a genetic background containing the Mother Enrichment Program (MEP) machinery (Lindstrom and Gottschling, 2009). Due to technical complications,

approximately 60% of the yeast deletion collection was successfully combined with the MEP (this complication is addressed in greater detail in the discussion section of this chapter). These strains were then combined and mixed into several pools containing approximately 400 different deletion mutant strains each. Pools were restricted to 400 strains to prevent statistical bottlenecks due to technical limitations imposed by the lifetime of DiOC6(3) stain and the number of cells that could be isolated by FACS. These cells were then rhodamine labeled and aged for approximately 9-10 cell divisions, long enough for wildtype cells to begin to lose membrane potential and DiOC6(3) staining. The top 15% of DIOC6(3) staining original cells were then isolated by FACS. The 15% cutoff was chosen to allow identification of several genotypes from each pool. It is possible that a higher threshold would have been more stringent, but may have failed to identify multiple suppressors from a single pool. Illumina sequencing was then used to identify the genotypes enriched in this population (details of the sequencing process described below).

4.2.3 Barcode sequencing strategy for highly multiplexed samples.

In order to sequence multiple isolated populations simultaneously, I used a '2D Multiplexing' strategy (Outlined in Fig 4.4)(Smith et al., 2010). Briefly, an indexing tag was included in each of the primers used to amplify the unique barcodes present in each deletion strain. These indexed primers could then be paired to give a unique sequence barcode combination to each library – resulting from each pool for strains examined. This strategy allowed multiplexing of many samples into a single lane of Illumina sequencing, greatly reducing sequencing costs. The primers used in this study are listed in Table 4.1.

4.2.4 Barcode analysis to identify enriched genotypes.

To identify genotypes that were enriched in the top 15% of DiOC6(3)-staining original cells, I used Illumina sequencing read counts as a measure of abundance (Smith et al., 2009a). I compared read frequency in the top '15% Population' to the frequency from an unsorted population. To be considered for further analyses, I required that a barcode have at least 50 total reads from either population. This constraint helped reduce noise from spurious barcode counts due to sequencing errors or lowly abundant strains. Additionally,

I required that a genotype show consistent enrichment across biological and technical replicates (described in materials and methods). The 79 genotypes that met these criteria are listed in Table 4.2.

4.2.5 Prioritized list of strains to follow-up with secondary screening.

Because 79 strains were too many to independently verify during secondary screening, I created a prioritized list for secondary analysis based upon annotated functions, cellular location, and previously observed phenotypes. I focused my analysis to genes that met one of the following criteria: i) genes with known localization or interactions with the mitochondria; ii) genes with roles in pathways known to be affected during the aging process; iii) genes with asymmetric distribution between mother and daughter cells. The 18 genes chosen for further analysis are listed in Table 4.3 with their annotated functions.

4.2.6 Several mutants show increased, non-specific DiOC6(3) staining.

In order to verify the effects of the mutants identified by the screen and find the mutants that were able to suppress the loss of $\Delta\psi^{mito}$ in significantly aged cells, the 18 mutants chosen for further analysis were aged for 24 hours and scored for DiOC6(3) staining intensity and mitochondrial structure by microscopy. During this analysis, it appeared that some mutants altered DiOC6(3) staining dynamics, possibly without altering mitochondrial membrane potential. Several mutants showed bright, but diffuse staining unlikely to represent increased $\Delta\psi^{mito}$ (Fig 4.4).

4.2.7 preCox4-NeonGreen as an independent measure of mitochondrial membrane potential in aging cells.

To specifically test each mutant's effects on mitochondrial membrane potential, our lab developed a novel membrane potential reporter. This tool takes advantage of the fact that import of some proteins into the mitochondrial matrix is a $\Delta\psi^{mito}$-dependent process (Hartl et al., 1989). Our tool fuses the mitochondrial targeting sequence of Cox4 (preCox4) to a bright fluorescent protein, NeonGreen (Shaner et al., 2013; Veatch et al., 2009). The preCox4 sequence targets NeonGreen to be imported into the mitochondria in a $\Delta\psi^{mito}$-

dependent manner. In cells that lack membrane potential, this construct fails to be imported into the mitochondrial matrix (Fig 4.6A). Protein that fails to be imported is subject to cellular degradation in the cytoplasm, leading to a loss of total fluorescence that can be detected by flow cytometry (Fig 4.6B).

Additionally, our construct contains the IAA17 degron from an auxin inducible degron system (Nishimura et al., 2009). While this domain was originally designed to be used with the auxin-sensitive degradation machinery, we find that the presence of this degron leads to a greater signal difference between $\Delta\psi^{mito}$ + and $\Delta\psi^{mito}$ - cells even in the absence of the exogenous degradation machinery. This difference is by some unknown mechanism, as the IAA17 degron is not thought to be recognized by the native cellular protein degradation system.

4.2.8 Environmental conditions alter dynamics of the age-associated loss of mitochondrial membrane potential.

During characterization of the new reporter and further testing of the DiOC6(3) system, I discovered that the age-associated loss of $\Delta\psi^{mito}$ is dependent on the environment that the cells are aged in. I found that cells aged in different batches of media showed different mitochondrial phenotypes (Fig 4.7). There were no intended differences between the two tested batches of media. Cells aged in “Batch 1” showed normal loss of $\Delta\psi^{mito}$ and mitochondrial form, however the same cells aged in “Batch 2” maintained $\Delta\psi^{mito}$ and mitochondrial structure into late age.

Aging experiments are typically performed in a rich media called ‘YPD’ – named for its three components Yeast Extract, Peptone, and Dextrose. Nutrients required for growth are thought be in vast excess, so the exact nutrient composition is not tightly controlled (Bergman, 2001). It is possible that a number of nutrient levels could vary from batch to batch, any of which could alter mitochondrial aging dynamics. In order to identify some nutrients that vary in concentration between “Batch 1” and “Batch 2”, we subjected both batches to mass-spectrometry metabolite analysis. This analysis could detect approximately 200 different metabolites, most of which were at similar concentrations in both batches of media (Fig 4.8A). However, we identified 12 nutrients that were at least

2-fold more abundant in either batch of media (Fig 4.8B). The nutrient that varied the most between the two batches was pyruvate, 18-fold higher in “Batch 2”. This result was of particular interest because *mpc1*Δ*,* a deletion of a component of the mitochondrial pyruvate carrier, was identified during the genetic screen. It should be noted that the mass-spec analysis was only sensitive to certain nutrients. A number of unmeasured nutrients could vary between batches of media, any of which could be responsible for sensitizing and/or protecting the mitochondria during the aging process.

4.2.9 Several mutants alter preCox4-NeonGreen signal in cells aged in synthetic media.

To avoid batch-to-batch differences in media composition, I continued the characterization of the age-associated loss of $\Delta\psi^{mito}$ in a synthetic defined medium (SC). While cells grown in this media are known to have significantly different metabolism relative to those grown in rich media, wild-type cells aged in SC still show an age-associated loss of $\Delta\psi^{mito}$ and mitochondrial structure (Fig 4.9A). I tested the 18 mutants identified in the primary screen for their effects on $\Delta\psi^{mito}$ in cells aged in this synthetic medium. I identified four mutants that show preCox4-NeonGreen import into mitochondria in cells of significant replicative age under these conditions: *mpc1*Δ, *vms1*Δ, *kin4*Δ, and *tpm1*Δ. Again, cells grown and aged in this synthetic medium are known to have altered metabolism relative to those grown in rich media, so it may not be surprising that only 4 of the 18 mutants still suppressed the aged-associated $\Delta\psi^{mito}$ when aged in synthetic medium.

4.2.10 Chemical inhibition of the mitochondrial pyruvate carrier also alters loss of $\Delta\psi^{mito}$ in some aged cells.

MPC1 encodes a major component of the mitochondrial pyruvate carrier and is required for normal transport of pyruvate into the mitochondria (Bricker et al., 2012; Herzig et al., 2012). UK5099 is a known potent inhibitor of this transporter complex (Halestrap, 1975). Treatment of cells with μM concentrations of UK5099 during the aging process delays loss of $\Delta\psi^{mito}$, indicated by a substantial proportion of cells maintaining the ability to import preCox4-NeonGreen in late age (Fig 4.10). The effects of UK5099 treatment are similar

to those of the *mpc1*Δ mutant, suggesting the suppression in the mutant is due specifically to the loss of pyruvate carrier activity. However, treatment with UK5099 appears to slow the division rate of aging cells, as cells aged for 24 hours tended to have divided fewer times than those aged in the absence of the drug. This result suggests that this concentration of the drug may not exactly mimic *mpc1*Δ, and may explain why the loss of $\Delta\psi^{mito}$ is not rescued to the same extent as in the deletion strain.

4.2.11 Exogenous environmental pyruvate alters mitochondrial phenotypes in a small population of cells.

Because both the mitochondrial pyruvate carrier activity and environmental pyruvate levels were implicated during my characterization of the age-associated loss of $\Delta\psi^{mito}$, I tested the effects of exogenous pyruvate added to the growth media. A small percentage of cells aged in SC + 1mM pyruvate showed altered $\Delta\psi^{mito}$ in old cells (Fig 4.11, pyruvate is not normally found in SC media). This concentration of pyruvate is similar to that estimated to be found in 'Batch 2' of YPD – the media that did not cause an age-associated loss of $\Delta\psi^{mito}$. Because simply adding 1mM pyruvate was not sufficient to rescue in $\Delta\psi^{mito}$ in a majority of old cells, argue that the effects from aging cells in different batches of rich media cannot be fully explained by simply varying pyruvate levels.

4.2.12 Vacuole acidity is altered in several mutants that suppress mitochondrial membrane potential loss.

Loss of vacuole acidity was previously reported to precede the loss of $\Delta\psi^{mito}$ (Hughes and Gottschling, 2012). Mutants known to prevent or delay loss of vacuole acidity also delayed loss of $\Delta\psi^{mito}$. To find if the mutants identified by the screen are acting by a similar mechanism, or acting directly on the mitochondria, I tested their effects on vacuole acidity in cells of several different ages. Vacuole acidity can be measured by quinacrine staining, a fluorescent dye that accumulates in acidic compartments (Weisman et al., 1987). Wildtype cells show bright quinacrine staining in the vacuole in young cells, but this staining well is diminished after 2 or 3 cell divisions (Fig 4.12 A and B). *mpc1*Δ shows a small population of cells that retain quinacrine staining after 2-3 divisions (Fig 4.12 A and

B). Staining in this mutant appears to be more variable than WT in older cells. *vms1*Δ shows a subtle increase in quinacrine staining, mostly detectable in cells 1-2 divisions old (Fig 4.12 A and B). The staining in older *vms1*Δ cells appeared very similar to WT after several cell divisions. *kin4*Δ shows the most dramatic increase in quinacrine staining (Fig 4.12 A and B). However, a fraction of *kin4*Δ cells show decreased staining, even less than WT. A small fraction of *tpm1*Δ cells show increased staining, although a majority of the population show less staining than WT cells at most ages (Fig 4.12 A and B). Also, very few young *tpm1*Δ cells were observed, possibly indicating a decreased presence in the population compared to other genotypes. It appears that the four mutants tested do alter vacuole acidity, although some only in a subset of cells. Because vacuole acidity measurements are performed in relatively young cells, it is difficult to say if these subsets (of cells with increased vacuole acidity) are the populations that is surviving for 24 hours with increased $\Delta\psi^{mito}$.

4.3 DISCUSSION

4.3.1 **Mutants identified during primary screen.**

The primary screen identified many mutants that appeared to have increased DiOC6(3) staining in cells that have aged for 12 hours. For technical reasons, only a subset of these were chosen for further analysis. It is possible that some of the unverified strains from the primary screen do suppress the age-associated loss of $\Delta\psi^{mito}$.

The primary screen identified several genes involved with, and responding to, DNA damage. The explanation for this observation may be trivial, as several of these genes are reported to be slow growing, possibly indicating that these strains were younger than the rest of the population at the time of sampling (Giaever et al., 2002). However, there are several known links between mitochondrial and nuclear responses. Nuclear stresses are known to up-regulate mitochondrial biogenesis, perhaps sufficient to protect mitochondrial function from normal age-associated dysfunction (Haynes and Ron, 2010).

The primary screen also identified several genes with known roles in the peroxisome (*pex2*Δ*, pex8*Δ*, pex15*Δ)(Sacksteder and Gould, 2000). While I was unable to confirm

their effects, it is possible this apparent coordinate response was due to the altered environmental conditions used during the secondary screen (these mutants did not suppress age-associated mitochondrial phenotypes in synthetic media). The peroxisome is required for various metabolic reactions, some of which may or may not be active during growth in either environmental condition(Schlüter et al., 2010). It is possible that altering peroxisome biogenesis alters the age associated loss of $\Delta\psi^{mito}$ in certain environments or certain metabolic states of the cell.

4.3.2 Multiple reporters of $\Delta\psi^{mito}$

This study used two different reporters of $\Delta\psi^{mito}$, DIOC6(3) and preCox4-NeonGreen. While both show $\Delta\psi^{mito}$-dependent changes in total fluorescence, DiOC6(3) was seen (and previously known) to stain other cellular structures under certain conditions(Salvioli et al., 1997). I feel that repeating the screen using preCox4-NeonGreen as the primary measure of $\Delta\psi^{mito}$ would be extremely valuable. While I did not have the technology available during the design of the primary screen, robotic techniques for crossing reporter constructs into large strain collections are becoming increasingly available. Using preCox4-NeonGreen, or possibly a combination of two reporters, will greatly reduce the false positives of the primary screen.

preCox4-NeonGreen is similar to several other published reporters of $\Delta\psi^{mito}$, relying on the $\Delta\psi^{mito}$-dependent import of mitochondrial targeted fluorescent proteins. However, preCox4-NeonGreen does have the useful property of showing a $\Delta\psi^{mito}$-dependent change in fluorescence, not shared by all other similar reporters (preCox4-mCherry). The recently published MitoLoc is a two-component tool to simultaneously measure $\Delta\psi^{mito}$ and mitochondrial mass of the cells (Vowinckel et al., 2015). Similarly, MitoLoc relies on the $\Delta\psi^{mito}$-dependent import of a fluorescent protein into the mitochondrial matrix of cells. However, MitoLoc also uses a second reporter that is imported into the mitochondria in an $\Delta\psi^{mito}$-independent manner. Measuring the ratio of mitochondrial localized fraction of these two reporters provides an accurate measure of $\Delta\psi^{mito}$ that has been corrected for the mitochondrial mass present in the cell. Using a tool similar to MitoLoc could further improve the accuracy of this screening protocol.

4.3.3 Environmental dependence on phenotype and phenotype suppression.

During characterization of several mutants identified by the screen, it became apparent that subtle changes to the environment have the potential to alter normal aging processes. Some of these environmental variables were identified by mass-spec metabolite analysis; however, we did not have the capability to measure every component. In order to avoid any unknown variables, I continued my characterization in a defined synthetic medium. This medium was different than that used for the primary screen. While cells aged in this defined medium still showed an age-associated loss of $\Delta\psi^{mito}$, there are a number of known differences between cells grown in these two media types (Hahn-Hägerdal et al., 2005; Hjortmo et al., 2008). It is possible that several of the mutants identified in the primary screen are only able to suppress the phenotype under those specific media conditions. This constraint may explain why only a small number of mutants from the primary screen could be verified during subsequent analysis. Further, the potential effects from subtle variations in the environment suggest the need to establish a defined environment in which aging experiments are conducted. Using a defined medium will also allow screening for effects due to altering the levels of specific nutrients.

4.3.4 Mitochondrial Pyruvate Carrier and its effects on aging phenotypes.

MPC1 encodes the major subunit of the mitochondrial pyruvate carrier, required for transport of pyruvate into mitochondria (Bricker et al., 2012; Herzig et al., 2012). This activity is not ordinarily required for growth, partially because oxidative phosphorylation of pyruvate is not required for energy production during normal growth in the presence of glucose (Timón-Gómez et al., 2013). The transporter is not thought to be extremely active under these conditions. However, it is required for the production of branched-chain amino acids, a downstream metabolite of pyruvate in mitochondria (Herzig et al., 2012). So somewhat surprisingly, the deletion of *MPC1* (or chemical inhibition of the entire transporter) suppresses the age-associated loss of $\Delta\psi^{mito}$, even in conditions where it is not thought to be active. This result suggests that the metabolism of cells could be changing as a cell ages, despite constant environmental conditions.

While more work is needed to establish a mechanism for the effects of *mpc1*Δ*,* it appears that this mutant somehow alters the normal age-associated loss of vacuole acidity. It was somewhat surprising that this mitochondrial localized protein was altering an event in another organelle. However, pyruvate metabolism is a major contributor to the overall metabolism of a cell (Pronk et al., 1996). Major changes in a cell's ability to metabolize pyruvate may alter the cells overall metabolism, altering the normal aging process.

4.3.5 Altered protein quality control may alter mitochondrial aging phenotypes

VMS1 encodes a component of the CDC48 complex, a major regulator of protein quality control pathways (Heo et al., 2010; Tran et al., 2011). *VMS1* is involved in quality control pathways at the endoplasmic reticulum (ERAD), but also has specific roles at the mitochondria. In 2010, Heo et al. reported cells lacking *VMS1* show progressive loss of mitochondrial function and hypersensitivity to mitochondrial stressors. It is therefore surprising that I identified *vms1*Δ*,* a mutation previously associated with mitochondrial dysfunction, as a suppressor of the age-associated loss of $\Delta\psi^{mito}$. It is possible that the lack of normal mitochondrial quality control pathways provides a stress that initiates a response pathway, somehow protecting mitochondria from normal aging processes. Similarly, mitochondrial stress response pathways (UPR^{mito}) have previously been implicated in modulating aging pathways in metazoans (Haynes and Ron, 2010).

*vms1*Δ showed very subtle effects on quinacrine staining. Quinacrine is a somewhat binary reporter of vacuole acidity, with a narrow range of sensitivity. The subtle effects of *vms1*Δ on quinacrine staining may reflect a significant change in vacuole acidity, sufficient to alter $\Delta\psi^{mito}$. However, additional experiments are required to further study the effects of *vms1*Δ on both vacuole acidity and the age-associated loss of $\Delta\psi^{mito}$.

4.3.6 Tropomyosin is required for normal mitochondrial inheritance

TPM1 encodes the major isoform of tropomyosin (Liu and Bretscher, 1989). Mutants lacking *TPM1* show destabilized actin cables altering many different cellular processes. However, *tpm1*Δ is known to alter mitochondrial distribution, morphology, and inheritance to the bud (McFaline-Figueroa et al., 2011). Mitochondria with higher $\Delta\psi^{mito}$ are normally

preferentially inherited by the daughter cell. While the exact mechanism by which *tpm1*Δ alters the age-associated loss of $\Delta\psi^{mito}$ remains uncharacterized, it is possible that mother cells lacking tropomyosin retain mitochondria with higher membrane potential during each division and maintain $\Delta\psi^{mito}$ into later age.

*tpm1*Δ also appeared to alter the distribution of age in the culture, with young cells appearing a lot less frequently than in WT cultures. This may be due to a global loss of many polarized processes in the *tpm1*Δ mutant. In the absence of functioning actin cables, the ability to direct inheritance of many factors to the budding daughter cell may be impaired. Ultimately, this may inhibit the ability to produce a viable daughter cell.

4.3.7 **A mitotic kinase alters aging phenotypes.**

KIN4 encodes a protein kinase that is thought to delay mitotic exit in cells that have misaligned spindle poles (D'Aquino et al., 2005; Pereira and Schiebel, 2005). It was chosen for further characterization after the primary screen because it asymmetrically localizes to the mother cell. However, it has no known effects on mitochondria. Again, future work is needed to establish a mechanism by which *kin4*Δ alters this aging phenotype, but it may indicate the importance of nuclear-mitochondrial signaling regulating mitochondrial function during the aging process.

*kin4*Δ also appears to robustly alter vacuole acidity. A significant fraction of mutant cells show increased staining both in young cells and cells that are several divisions old. Again the connection between this mitotic kinase and vacuolar function is unclear. However, vacuole acidity is regulated by several processes sensitive to metabolic state and cell cycle dynamics. Altered signaling during mitotic exit could potentially change the regulation of these processes, in turn altering vacuole acidity.

4.3.8 **Adaptability of screening protocol to study other aging phenotypes.**

The screening protocol outlined in this study was designed to be extremely adaptable and extendable to studying other age-associated phenotypes. With minimal modifications, this technique could be used to study any aging phenotype that can be characterized by a loss/gain in fluorescence. There are several organelle-function-sensitive stains that show

altered staining in young vs. old cells (Gottschling Lab – unpublished data). Additionally, there are several genes that are known to change expression level with age, any of which could be used as a reporter of characteristic aging pathways (Janssens et al., 2015). Further applications of this screening protocol to study the aging process will be discussed in greater detail in the Chapter V.

4.4 METHODS

Plasmids and Strains. Plasmids used in this chapter are presented in Table 4.4 and have previously been described, with the exception of 'pGPD-precox4-IAA17-neon-xsome I'. This plasmid was constructed by Gibson assembly of preCox4 sequence, IAA17 sequence, and NeonGreen into our chromosome I integrating vector (Gibson et al., 2009; Hughes and Gottschling, 2012; Shaner et al., 2013; Veatch et al., 2009). Strains used in this study are presented in Table 4.4. Standard *S. cerevisiae* methods were used to generate PCR-mediated mutations, zygotes, sporulation, tetrad analysis and selection of strains with relevant markers (Dunham et al., 2015). The MEP deletion collection was performed by mating the MEP entry strain (UCC8894) to the yeast deletion collection(Giaever et al., 2002). This library construction was done in collaboration with the Boone Lab at the University of Toronto. This collaboration was initiated by Derek Lindstrom (Gottschling Lab) and Franco Vizeacoumar (Boone Lab). With technical assistance from Merideth Borden, I performed a reselection of mutants containing all required MEP components was done by first growing cells on YPD+200 µg/mL Hygromycin+100µg/mL clonNAT+200 µg/mL G418, followed by selection of the positive colonies on YC-Leu. Strains that grew after both rounds of selection were used during the screen.

Primers. Primers used in this study to amplify deletion-collection barcodes are listed in table 4.1. Primers used to remake deletions during recharacterization hits from primary screen are not provided but follow standard *S. cerevisiae* methods to generate PCR-mediated mutations (Dunham et al., 2015).

Media and Growth Conditions. Unless otherwise indicated cells were grown at 30°C in YEPD. Synthetic medium experiments were performed in Synthetic Complete (SC) medium (Dunham et al., 2015).

Microscopy. All microscopy was performed on one of two wide-field fluorescence microscopes: (*i*) a Nikon E800 equipped with a 60×/1.40 objective or (*ii*) a Leica DMI-6000b equipped with a 63×/1.40 objective. Budscars were visualized by Calcofluor White staining at approximately 5µg/mL (included during final washing steps). Image processing and quantification were performed with Fiji, a distribution of ImageJ software (Schindelin et al., 2012).

DiOC6(3) staining. DiOC6(3) (Invitrogen) staining was performed according to manufacturer's directions and as previously described (Hughes and Gottschling, 2012). Briefly, cells were washed twice in buffer (10mM HEPES pH 7.6, 5% Glucose). Cells were then stained in 175nM DiOC6(3) in the same buffer for 15 minutes. Cells were then washed, and resuspended in the same buffer for imaging.

Flow cytometry. Flow cytometry was performed on a Beckman Dickinson LSR II flow cytometer. FACS isolations were performed on a Beckman Dickinson FACSAriaII. Rhodamine fluorescence was measured through the PE channel. GFP or DiOC6(3) fluorescence was measured through the FITC channel. Events with extremely high or low Forward and Side Scatter properties were excluded from analysis. Flow cytometry data were analyzed with the FlowJo software package.

Screen to identify suppressors of the age-associated loss of mitochondrial membrane potential. Approximately 400 strains from the MEP yeast deletion collection were pooled as previously described. Frozen pools of strains were used to inoculate a YPD culture and grown for 16 hours to early log phase (~.1 OD). Cells were labeled with NHS-Rhodamine (as described in Chapter III), aged for 12 hours, and stained with DiOC6(3). The top 15% of DiOC6(3) staining cells (corrected for cell size) were isolated by FACS. The population of all rhodamine-positive cells was also isolated. UPtag and DNtag barcodes from each population of stains were amplified by a unique pair of primers (Table 4.2)(Smith et al., 2010). Barcode libraries were sequenced in an Illumina HiSeq2000. Sequencing reads were demultiplexed, trimmed to barcode and best matching barcode

was identified by global sequence alignments. 1 mismatch was allowed, however allowing 2 or 3 mismatches did not significantly change analysis. Strains enriched in the “Top 15% Staining” population were identified by comparing read frequency in this population compared to that in the “all rhodamine-positive cell” population. Barcodes that had a ratio z-score > 2 were considered as enriched. Strains that were enriched for at least one tag (UPtag or DNtag) in at least one biological replicate, yet showed no significant depletion in any tag in any biological replicate, were considered for further analysis. Strains were pooled so that each strain should have been included in at least 2 aging experiments (biological replicate).

Quinacrine staining. Quinacrine (Sigma) staining was performed as previously described (Hughes and Gottschling, 2012; Weisman et al., 1987). Briefly, cells were washed twice in YPD buffered with 100mM HEPES pH 7.6. Cells were then stained in 200μM quinacrine in this buffered medium at 30°C for 10 minutes, then 5 minutes on ice. Cells were then washed and then resuspended in 100mM HEPES pH 7.6 plus 2% glucose for imaging.

4.5 Contributions and Acknowledgments

Nathaniel Thayer and Dan Gottschling designed all experiments. Meredith Borden optimized mitochondrial membrane potential reporter. Christina Leverich and John Berude assisted with strain construction. Thank you to Fred Hutchinson Cancer Research Center Shared Resources for assistance during various parts of this project – specifically the Flow Cytometry, Genomics and Scientific Imaging Cores. Thank you to Jesse Bloom and Linda Breeden for sharing sequencing lanes. Mass-spectrometry metabolite analysis was performed in collaboration with the University of Washington Mitochondria and Metabolism Center. I would also like to thank all members of the Gottschling Lab for various contributions and support of this project.

4.6 TABLES AND FIGURES

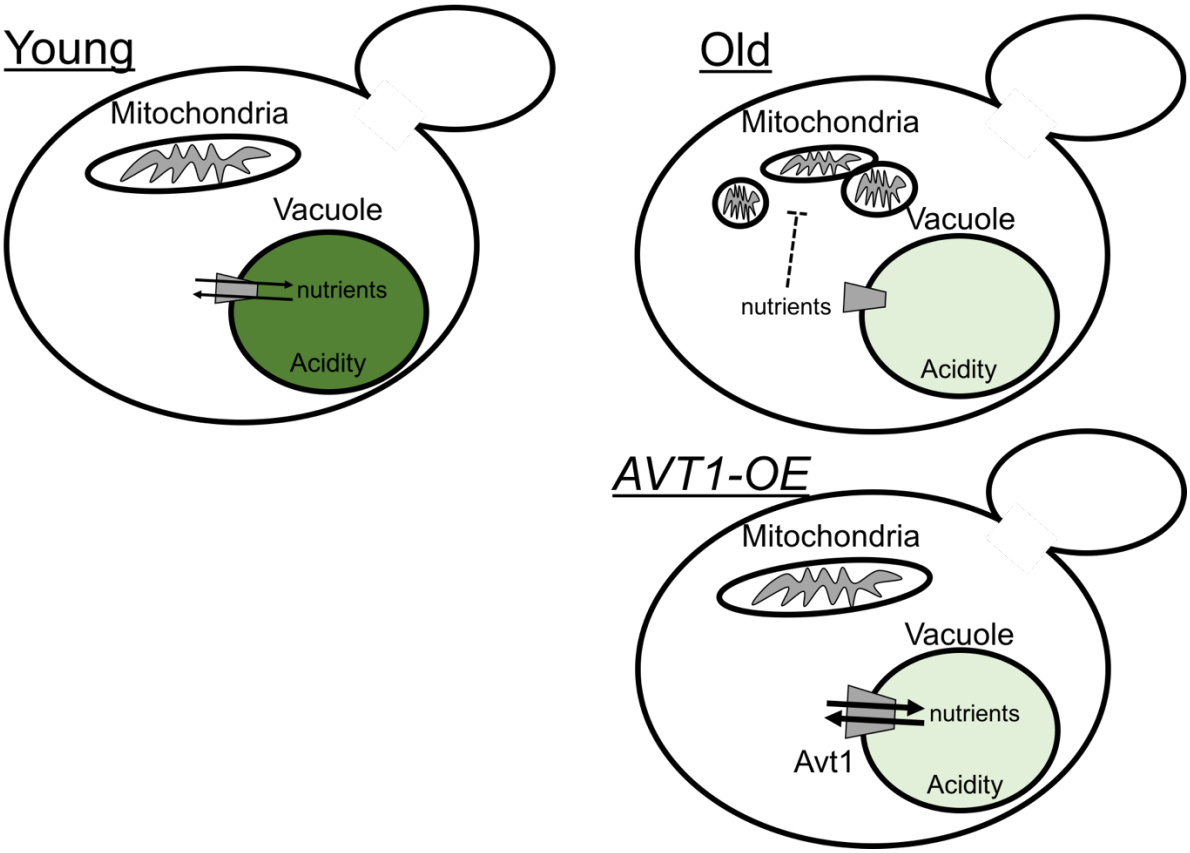

Figure 4.1. Loss of vacuole acidity leads to mitochondrial dysfunction

The overexpression of *AVT1* is suspected to suppress the age associated loss of mitochondrial function by overcoming a deficiency in nutrient storage due to decreased vacuole acidity (indicated by shading in vacuole). However, the exact mechanism by which a loss of vacuole acidity leads to mitochondrial dysfunction is still not known (Figure was adapted from Hughes and Gottschling, 2013).

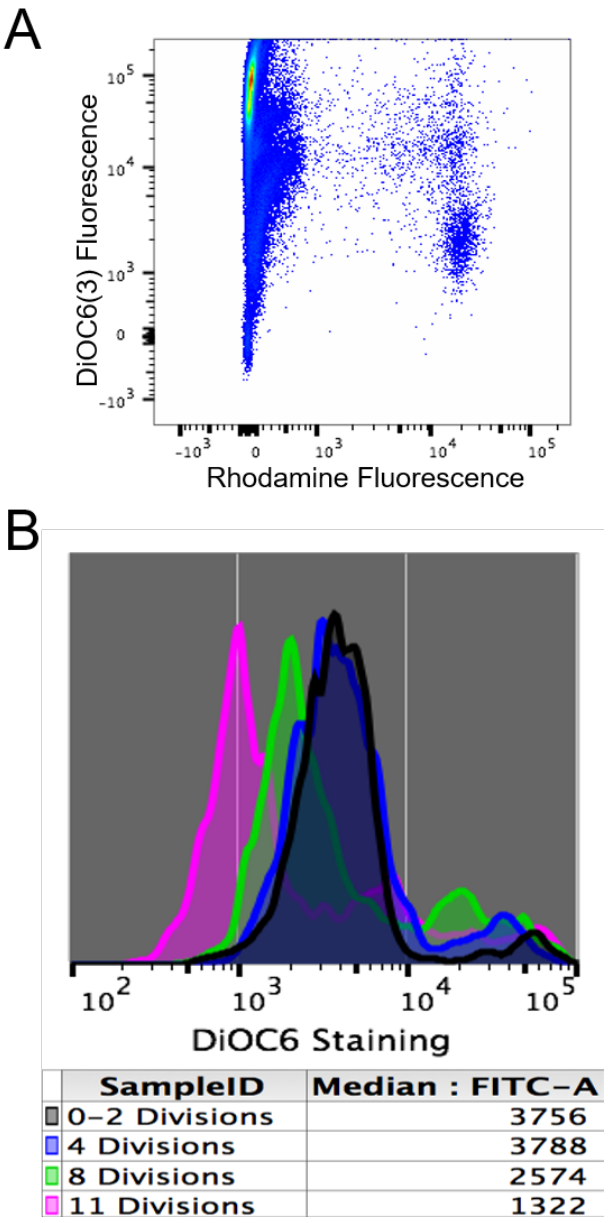

Figure 4.2. Monitoring DiOC6(3) staining intensity in aged cells in a mixed population.

A) Original cells are distinguished by rhodamine fluorescence. Daughter cells show very little fluorescence in the rhodamine channel. Other fluorescent properties can be measured in the rhodamine + original cells.

B) Timecourse of DiOC6(3) staining in young to old cells. Young cells (black) stain brightly with DiOC6(3), however as cell age there is a decrease in DiOC6(3) staining. This shows similar kinetics as described by Hughes and Gottschling.

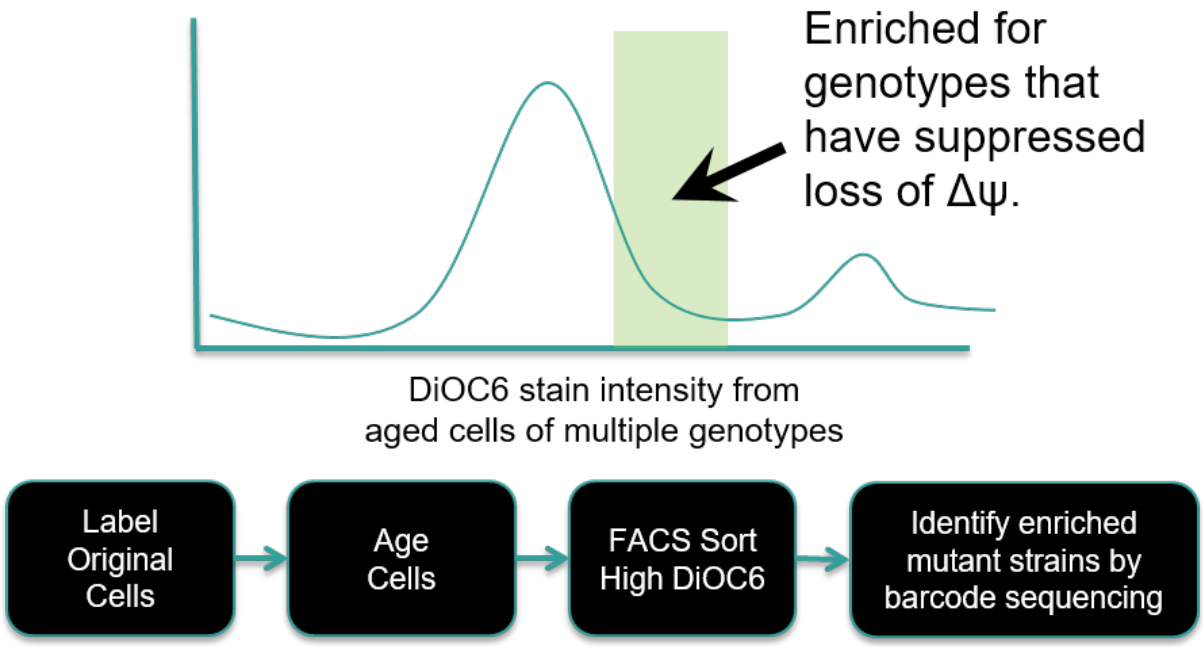

Figure 4.3. Screen strategy to identify suppressors of the age-associated loss of DiOC6(3) staining.

A population of cells is permanently labeled with rhodamine. These cells are then aged for approximately 10 divisions, long enough to see a loss in DiOC6(3) staining. The population of original cells that retain high DiOC6(3) staining is then isolated by FACS and the genotypes present in this population are then identified by barcode sequencing.

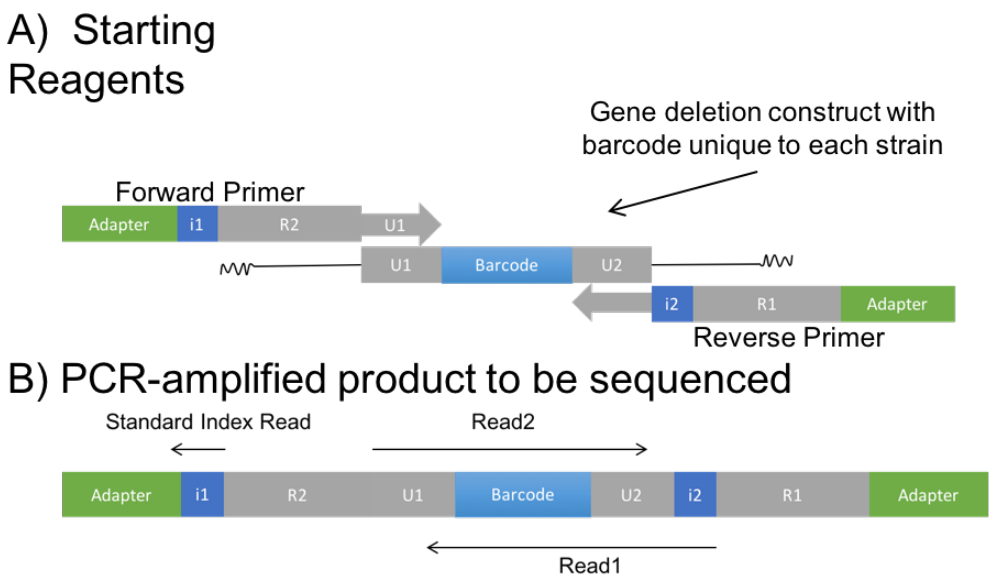

Figure 4.4. "2D-Multiplexing" strategy to amplify barcodes for yeast deletion collection.

Index sequences (e.g. i1 and i2) were included within the primers used to amplify the barcodes from deletion collection strains. After PCR amplification each fragment contains all the necessary components for sequencing in an illumina flowcell. i1 is read during the standard indexing read. i2 is read as the first basepairs from Read1. Each population/library can be amplified with a unique pair of primers, pooled, sequenced, and the origin can be determined based upon the pair of indexes. 'Adapter' is required for annealing to flow cell. 'R1' and 'R2' match sequencing primers. 'U1' and 'U2' sequences match common sequences of deletion construct.

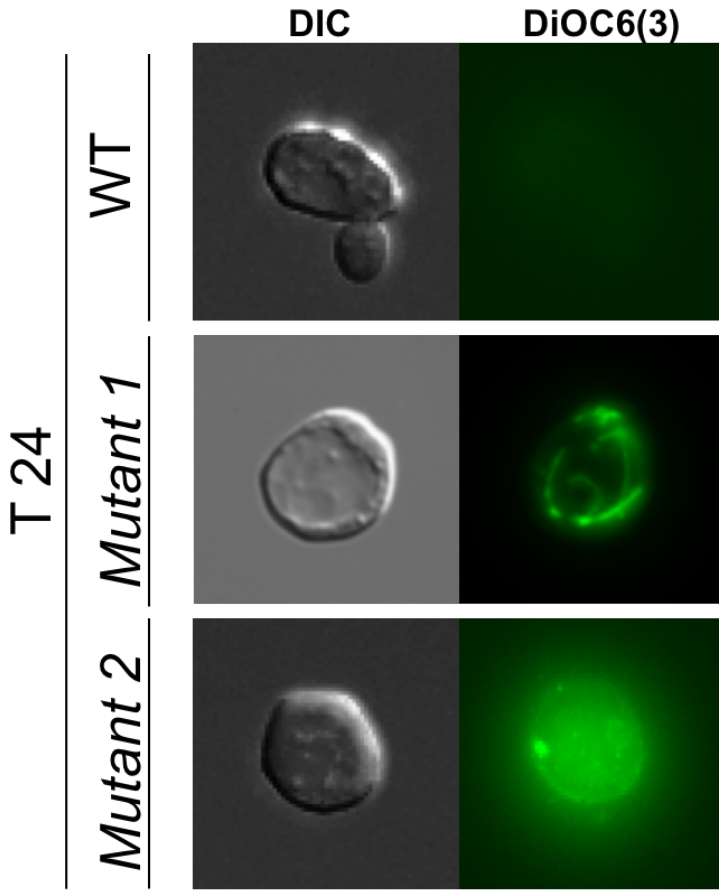

Figure 4.5. Altered DiOC6(3) staining properties in some mutants.

Some mutants showed aberrant DiOC6(3) staining. Cells were aged for 24 hours and stained with DiOC6(3). WT cells showed the expected loss of mitochondrial staining. Some mutants showed increased mitochondrial-localized staining. Some mutants (*vms1*Δ shown) showed bright, but diffuse staining that did not appear mitochondrial. These mutants likely alter Δψ across other membranes in the cell or alter dye permeability, without necessarily altering $\Delta\psi^{mito}$.

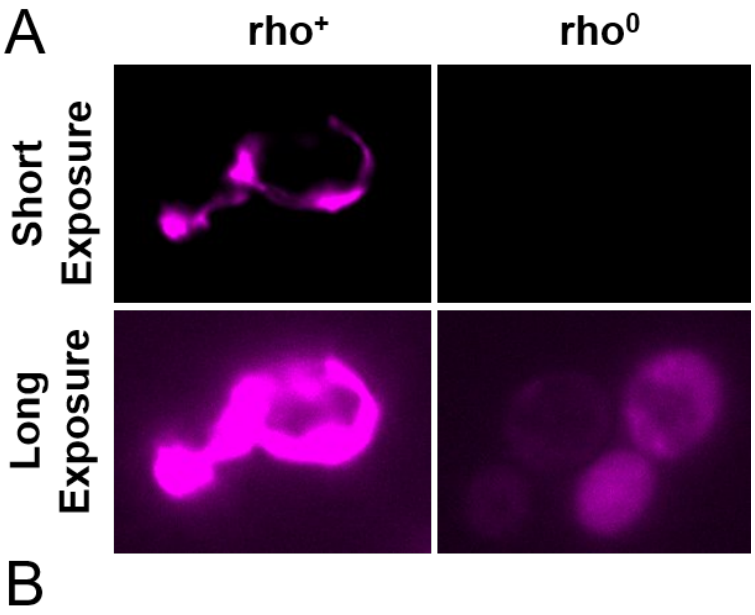

Figure 4.6. preCox4-NeonGreen is a reporter of $\Delta\psi^{mito}$.

As a secondary measure of $\Delta\psi^{mito}$ we used preCox4-NeonGreen. A) Cells that should not have $\Delta\psi^{mito}$ (rho^0) showed less mitochondrial import of this fluorescent protein than cells that have $\Delta\psi^{mito}$ (rho^+). Fluoresence of preCox4-NeonGreen has been pseudo-colored magenta. B) These results are also detectable by flow cytometry.

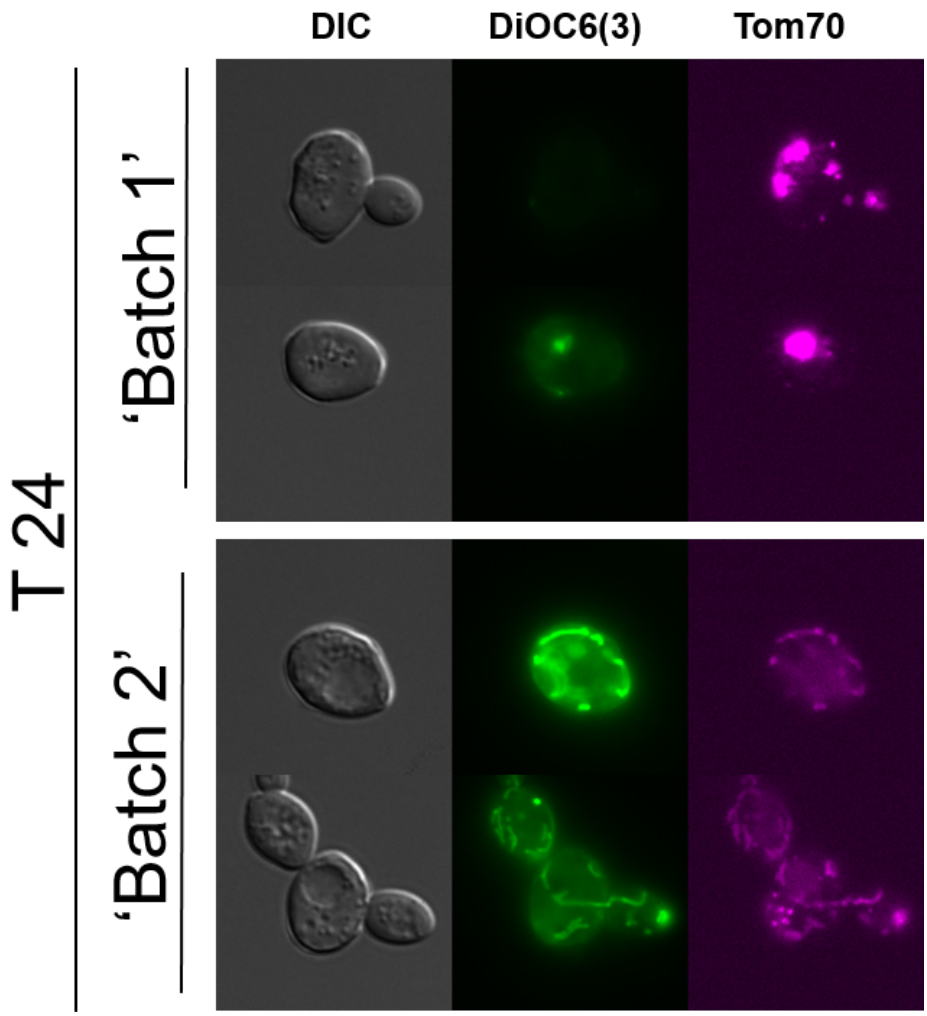

Figure 4.7. Mitochondrial phenotypes differ depending on the media.

WT cells were aged in two different batches of YPD rich media. Cells aged in "Batch 1" showed the normally age-associated loss of $\Delta\psi^{mito}$ and fragmented mitochondrial morphology. Cells aged in "Batch 2" maintained DiOC6(3) staining and tubular mitochondrial morphology. There was no intended difference in media components between these two batches of media.

A

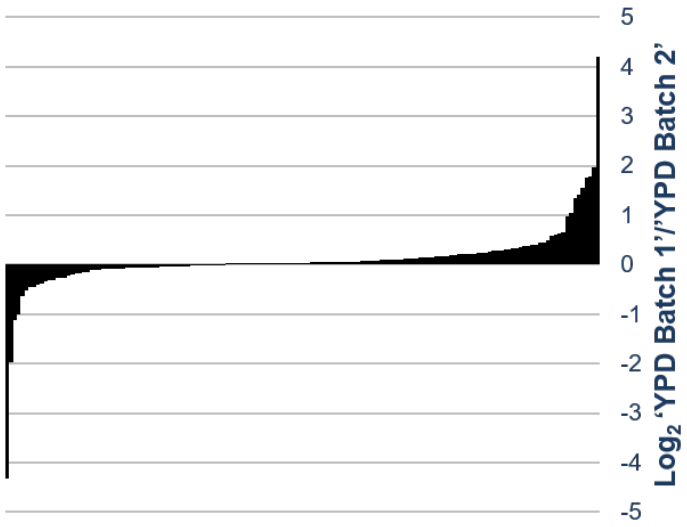

B

Measured Metabolite/Nutrient	Log2(2/1)
Pyruvate	4.20757
Glutamine	1.95884
13-HODE	1.77799
1-Methyladenosine	1.75584
3-Methyl-2-Oxovaleric Acid	1.55255
5-Hydroxytryptophan	1.42321
Oxidized glutathione	1.35219
Acetylcarnitine	1.04774
Reduced glutathione	-1.00525
Benzoic acid	-1.11112
Cysteinyl-Glycine (Cys-Gly)	-1.97556
L-Kynurenine	-4.31364

Figure 4.8. Metabolite analysis of media batches.

"Batch 1" and "Batch2" were subjected to mass-spectrometry sensitive to detecting the concentrations of approximately 200 metabolites/nutrients. A) The log2 ratio of each metabolite was plotted in a bar chart. Most measured metabolites/nutrients showed similar concentrations between the two batches of media. B) 12 metabolite/nutrients showed more than a 2-fold difference in concentrations between the media batches.

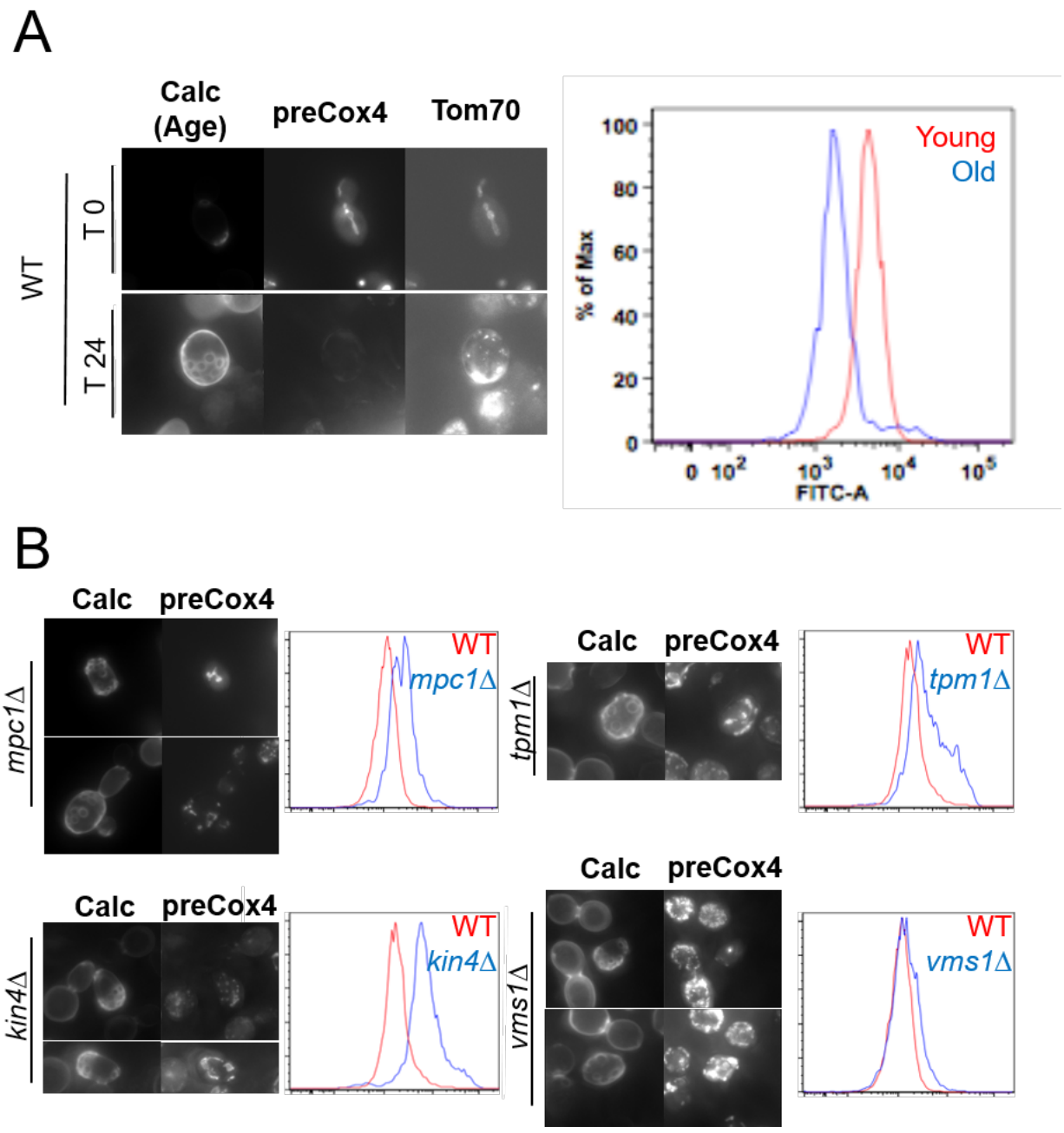

Figure 4.9. Mutants suppress inability to import preCox4-NeonGreen in aged cells

A) WT cells were aged for 24 hours and the level of preCox4-NeonGreen fluorescence was compared to young cells. WT cells showed decreased mitochondrial fluorescence of this reporter detectable by both microscopy and flow cytometry. B) preCox4-NeonGreen was detectable in mitochondria of several mutant genotypes in 24-hour-old cells. Increased mitochondrial fluorescence compared to WT was detectable by flow cytometry.

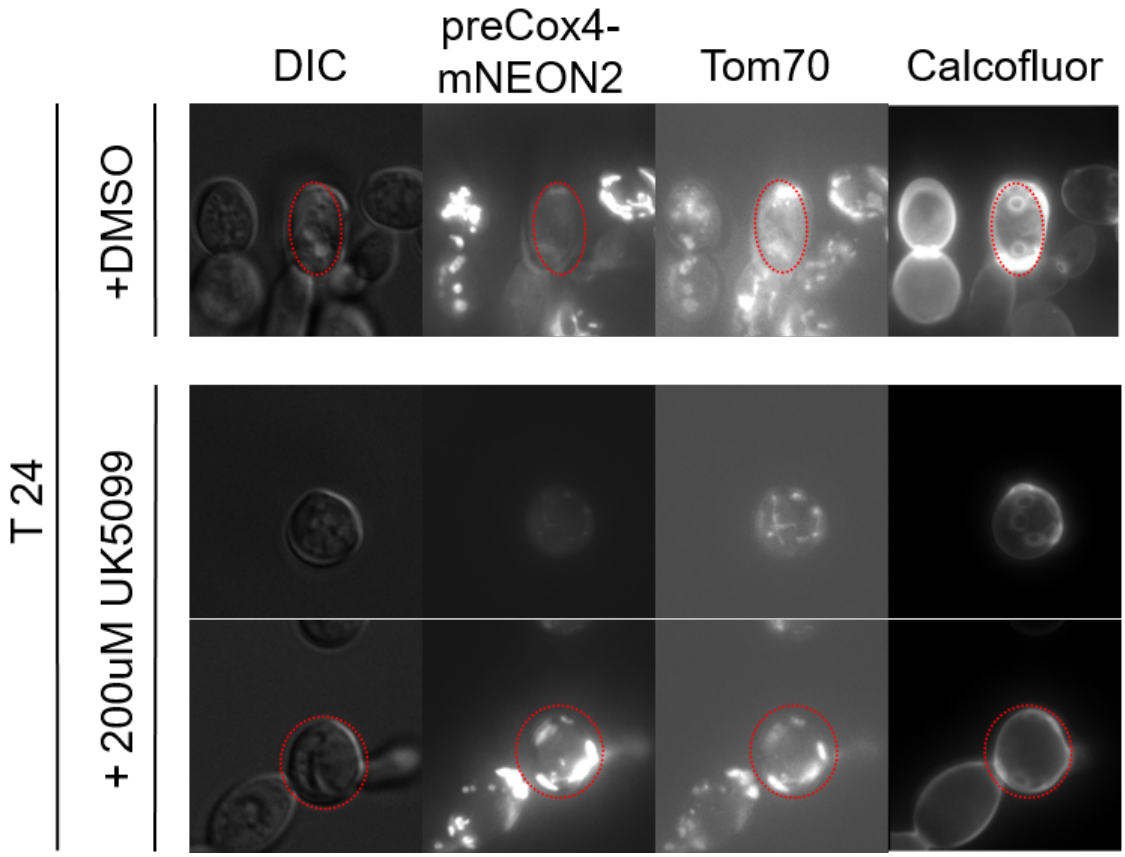

Figure 4.10. UK5099 treatment alters import of preCox4-NeonGreen in aged cells.

Wildtype cells were aged in the presence of 200uM UK5099 or DMSO control. A portion (~50%) of cells aged in presence of the drug showed tubular mitochondria structure. Some of these (25% of total population) show dim but mitochondrial localized preCox4-NeonGreen. Some (25% of total population) showed bright mitochondrial localized preCox4-NeonGreen. However, a significant portion of original cells showed reduced replicative age compared to WT, indicating a slower rate of division in the presence of the drug. Cell of interest is outlined in red if multiple cells are present in the panel.

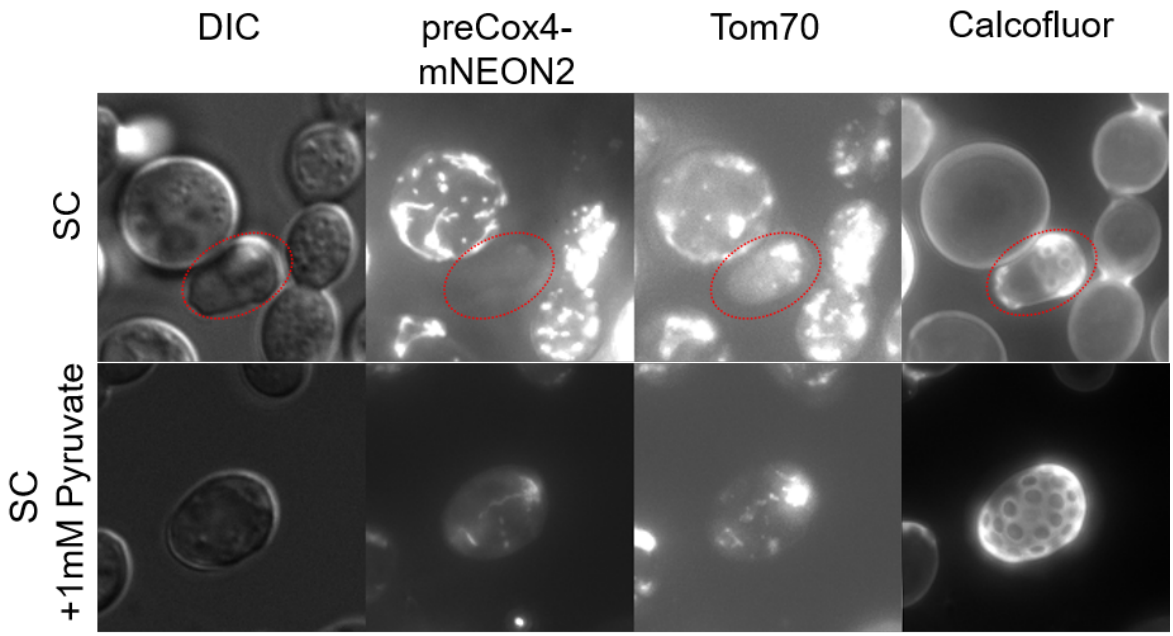

Figure 4.11. Few cells aged in the presence of 1mM pyruvate show altered mitochondrial phenotypes.

Exogenous pyruvate added to the media does not rescue mitochondrial phenotypes in a large percentage of cells. Cells aged in the presence of 1mM pyruvate show normal mitochondrial phenotypes. However a small fraction of aged cells (15-20% are as shown in figure) show some tubular mitochondrial morphology and dim but mitochondrial localized preCox4-NeonGreen

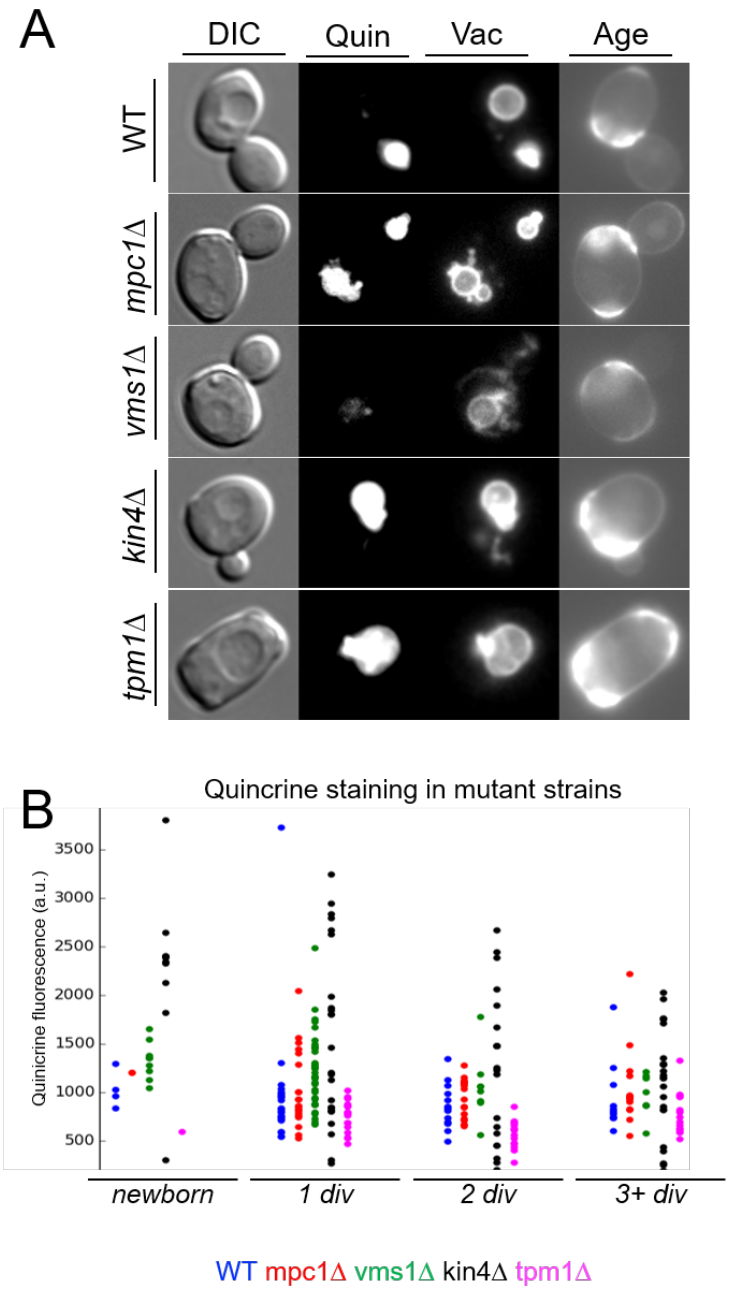

Figure 4.12. Vacuole acidity is altered in several mutants identified by screen.

A) Microscopy images of quinacrine staining, reporting vacuole acidity, of cells that are several divisions old. WT cells have lost vacuole acidity by 2-3 cell divisions, however vacuole acidity returns in developing buds. Several mutants altered showed increased quinacrine staining. Vacuoles are marked with Vph1-mCherry. B) Quantification of maximum intensity of quinacrine fluorescence found in mother cell vacuole plotted against age.

Table 4.1. Primers used to amplify barcodes with unique indexes

UP_F-Index2	CAAGCAGAAGACGGCATACGAGATacatcgGTGACTGGAGTTCAGACGTGTGCTCTTCCGATCTGA TGTCCACGAGGTCTCT
UP_F-Index5	CAAGCAGAAGACGGCATACGAGATcactgtGTGACTGGAGTTCAGACGTGTGCTCTTCCGATCTGAT GTCCACGAGGTCTCT
UP_F-Index6	CAAGCAGAAGACGGCATACGAGATattggcGTGACTGGAGTTCAGACGTGTGCTCTTCCGATCTGA TGTCCACGAGGTCTCT
UP_F-Index12	CAAGCAGAAGACGGCATACGAGATtacaagGTGACTGGAGTTCAGACGTGTGCTCTTCCGATCTGA TGTCCACGAGGTCTCT
UP_F-Index15	CAAGCAGAAGACGGCATACGAGATtctgacatGTGACTGGAGTTCAGACGTGTGCTCTTCCGATCTG ATGTCCACGAGGTCTCT
UP_F-Index19	CAAGCAGAAGACGGCATACGAGATcgtttcacGTGACTGGAGTTCAGACGTGTGCTCTTCCGATCTG ATGTCCACGAGGTCTCT
UP_F_Index7	CAAGCAGAAGACGGCATACGAGATgatctgGTGACTGGAGTTCAGACGTGTGCTCTTCCGATCTGA TGTCCACGAGGTCTCT
UP_R-Index2	AATGATACGGCGACCACCGAGATCTACACTCTTTCCCTACACGACGCTCTTCCGATCTacatcgGTC GACCTGCAGCGTACG
UP_R-Index5	AATGATACGGCGACCACCGAGATCTACACTCTTTCCCTACACGACGCTCTTCCGATCTcactgtGTC GACCTGCAGCGTACG
UP_R-Index6	AATGATACGGCGACCACCGAGATCTACACTCTTTCCCTACACGACGCTCTTCCGATCTattggcGTC GACCTGCAGCGTACG
UP_R-Index7	AATGATACGGCGACCACCGAGATCTACACTCTTTCCCTACACGACGCTCTTCCGATCTgatctgGTC GACCTGCAGCGTACG
UP_R-Index12	AATGATACGGCGACCACCGAGATCTACACTCTTTCCCTACACGACGCTCTTCCGATCTtacaagGTC GACCTGCAGCGTACG
UP_R-Index15	AATGATACGGCGACCACCGAGATCTACACTCTTTCCCTACACGACGCTCTTCCGATCTtctgacatGT CGACCTGCAGCGTACG
UP_R-Index19	AATGATACGGCGACCACCGAGATCTACACTCTTTCCCTACACGACGCTCTTCCGATCTcgtttcacGT CGACCTGCAGCGTACG
DN_F-Index2	CAAGCAGAAGACGGCATACGAGATacatcgGTGACTGGAGTTCAGACGTGTGCTCTTCCGATCTCG AGCTCGAATTCATCGAT
DN_F-Index5	CAAGCAGAAGACGGCATACGAGATcactgtGTGACTGGAGTTCAGACGTGTGCTCTTCCGATCTCG AGCTCGAATTCATCGAT
DN_F-Index6	CAAGCAGAAGACGGCATACGAGATattggcGTGACTGGAGTTCAGACGTGTGCTCTTCCGATCTCG AGCTCGAATTCATCGAT
DN_F-Index12	CAAGCAGAAGACGGCATACGAGATtacaagGTGACTGGAGTTCAGACGTGTGCTCTTCCGATCTCG AGCTCGAATTCATCGAT
DN_F-Index15	CAAGCAGAAGACGGCATACGAGATtctgacatGTGACTGGAGTTCAGACGTGTGCTCTTCCGATCTC GAGCTCGAATTCATCGAT
DN_F-Index19	CAAGCAGAAGACGGCATACGAGATcgtttcacGTGACTGGAGTTCAGACGTGTGCTCTTCCGATCTC GAGCTCGAATTCATCGAT
DN_F_Index7	CAAGCAGAAGACGGCATACGAGATgatctgGTGACTGGAGTTCAGACGTGTGCTCTTCCGATCTCG AGCTCGAATTCATCGAT
DN_R-Index2	AATGATACGGCGACCACCGAGATCTACACTCTTTCCCTACACGACGCTCTTCCGATCTacatcgCGG TGTCGGTCTCGTAG
DN_R-Index5	AATGATACGGCGACCACCGAGATCTACACTCTTTCCCTACACGACGCTCTTCCGATCTcactgtCGG TGTCGGTCTCGTAG
DN_R-Index6	AATGATACGGCGACCACCGAGATCTACACTCTTTCCCTACACGACGCTCTTCCGATCTattggcCGG TGTCGGTCTCGTAG
DN_R-Index7	AATGATACGGCGACCACCGAGATCTACACTCTTTCCCTACACGACGCTCTTCCGATCTgatctgCGG TGTCGGTCTCGTAG
DN_R-Index12	AATGATACGGCGACCACCGAGATCTACACTCTTTCCCTACACGACGCTCTTCCGATCTtacaagCG GTGTCGGTCTCGTAG
DN_R-Index15	AATGATACGGCGACCACCGAGATCTACACTCTTTCCCTACACGACGCTCTTCCGATCTtctgacatCG GTGTCGGTCTCGTAG
DN_R-Index19	AATGATACGGCGACCACCGAGATCTACACTCTTTCCCTACACGACGCTCTTCCGATCTcgtttcacCG GTGTCGGTCTCGTAG

Primers used to amplify **UP** and **DN** tags from Yeast Deletion Collection constructs. Lowercase letters are indexing sequences. All sequences are written 5’ > 3’.

Table 4.2. 79 genotypes identified by primary screen

ACE2	HOC1	PEX15	SHE3
ADE6	HSP30	PEX2	SNF6
ARN2	ICL2	PEX8	SPO21
ASM4	IKS1	PML39	STP3
BEM2	INP1	PMS1	TCD2
BER1	IOC3	PMT1	TDH3
BRE5	IRC6	POL32	TOP1
CAF40	KIN4	PSY1	TPM1
CAP2	LDB18	PTC1	UBP13
CBC2	LDB19	QRI7	UBP3
CIN1	LYS2	RDL1	VMS1
CYM1	MAG2	ROM2	YDR149C
DBF2	MPC1	RPL11B	YEL025C
DUS3	MPH1	RPL31B	YEL047C
ELG1	NKP2	RPL35B	YKL075C
FKS1	NOP12	RPN10	YKL162C
FRM2	OPI6	RTC1	YMR316C-A
FSH3	ORM1	RTT10	YOR152C
FYV1	PAC10	RTT101	YOR343C
HDA3	PBP1	SAT4	

Common gene names of the 79 genotypes identified by the primary screen. Systematic gene names are provided if no common name is available.

Table 4.3. Mutants chosen for further analysis and annotated functions

Gene	Function
SAT4	Ser/Thr protein kinase involved in salt tolerance
QRI7	Protein involved in threonylcarbamoyl adenosine biosynthesis
VMS1	Component of a Cdc48p-complex involved in protein quality control
CYM1	Lysine-specific metalloprotease of the pitrilysin family
FRD1	Soluble fumarate reductase
MPC1	Highly conserved subunit of mitochondrial pyruvate carrier
PEX8	Intraperoxisomal organizer of the peroxisomal import machinery
TDH3	Glyceraldehyde-3-phosphate dehydrogenase (GAPDH), isozyme 3
ARN2	Iron/Siderophore Transporter
TCD2	tRNA threonylcarbamoyladenosine dehydratase
YKL162C	Putative protein of unknown function – localizes to the mitochondria
YHM2	Citrate and oxoglutarate carrier protein
TPM1	Major isoform of tropomyosin
PEX15	Tail-anchored type II integral peroxisomal membrane protein
YPQ1	Putative vacuolar membrane transporter for cationic amino acids
KIN4	Serine/threonine protein kinase with asymmetrically distribued to mother cell
RDL1	Thiosulfate sulfurtransferase
ICL2	2-methylisocitrate lyase of the mitochondrial matrix

These were the genes selected for further analysis based upon known functions/localization in the mitochondria or other organelles known to be affected by age. Proteins with known asymmetric distributions between mother and daughter cells were also chosen. Source: Saccharomyces Genome Database

Table 4.4. Strains and plasmids used

Plasmid or strain	Genotype or descriptions	Source or reference
Plasmids		
pRS306 & pRS400	Used to delete genes with either URA3 or KanMX	(Brachmann et al., 1998)
pGPD-precox4-IAA17-neon-xsome I	Mitochondrial membrane potential reporter. Integrates into Chromosome I after digestion with NotI and transformation. Integration is confirmed by the presence of *URA3*	Derived from (Hughes and Gottschling, 2012)
pFA6a-link-yomRuby2-KanMX	Yeast optimized version of Ruby2. Used to tag genes with this bright-red fluorescent protein.	(Lee et al., 2013)
Yeast Strains		
UCC8894	MAT@ his3D leu2D ura3D0 met15D0 can1D::STE2pr-Sp_his5 lyp1D hoD::SCW11pr-cre-EBD78-NATMX loxP-UBC9-loxP-LEU2 loxP-CDC20-Intron-loxP-HPHMX	Derek Lindstrom – Gottschling Lab
UCC8773	MATa his3D1 leu2D0 ura3D0 lys2D0 hoD::SCW11pr-Cre-EBD78-NATMX loxP-CDC20-Intron-loxP-HPHMX loxP-UBC9-loxP-LEU2	(Hughes and Gottschling, 2012)
UCC8774	MAT@ his3D1 leu2D0 ura3D0 trp1D63 hoD::SCW11pr-Cre-EBD78-NATMX loxP-CDC20-Intron-loxP-HPHMX loxP-UBC9-loxP-LEU2	(Hughes and Gottschling, 2012)
UCC8994	MAT@ his3D1 leu2D0 ura3D0 trp1D63 hoD::SCW11pr-Cre-EBD78-NATMX loxP-CDC20-Intron-loxP-HPHMX loxP-UBC9-loxP-LEU2 Tom70-Ruby-KanMX	This study
UCC13695	MATa his3D1 leu2D0 ura3D0 lys2D0 hoD::SCW11pr-Cre-EBD78-NATMX loxP-CDC20-Intron-loxP-HPHMX loxP-UBC9-loxP-LEU2 ChrI::pGPD-precox4-neon-IAA-URA3	This study

UCC10201	MATa his3D1 leu2D0 ura3D0 lys2D0 hoD::SCW11pr-Cre-EBD78-NATMX loxP-CDC20-Intron-loxP-HPHMX loxP-UBC9-loxP-LEU2 VPH1-mCherry-KANMX	(Hughes and Gottschling, 2012)
UCC12198	UCC13695 + mpc1Δ::KanMX	This study
UCC12197	UCC13695 + vms1Δ::KanMX	This study
UCC12214	UCC13695 + tpm1Δ::KanMX	This study
UCC12217	UCC13695 + kin4Δ::KanMX	This study
UCC12304	UCC8774 + mpc1Δ::KanMX	This study
UCC12305	UCC8774 + vms1Δ::KanMX	This study
UCC12306	UCC8774 + tpm1Δ::KanMX	This study
UCC12307	UCC8774 + kin4Δ::KanMX	This study
UCC12768	UCC8773 + vms1Δ::URA3	This study
UCC12766	UCC8994 + mpc1Δ::URA3	This study
UCC12769	UCC8994 + vms1Δ::URA3	This study
UCC12308	UCC8994 + tpm1Δ::URA3	This study
UCC12309	UCC8994 + kin4Δ::URA3	This study
UCC12300	UCC10201 + mpc1Δ::URA3	This study
UCC12301	UCC10201 + vms1Δ::URA3	This study
UCC12302	UCC10201 + tpm1Δ::URA3	This study
UCC12310	UCC10201 + kin4Δ::URA3	This study

Diploids created as necessary by mating and selecting for auxotrophic/drug markers

Chapter 5. DISCUSSION

In the previous chapters of this dissertation, I presented projects designed to explore three important aspects of the aging process: asymmetry, lifespan, and phenotypes of the aging process. In this chapter, I will discuss these projects in more detail, focusing on how these projects and their findings relate to what is known about the aging process and highlight some important questions that remain unanswered.

5.1 Discussion of Long-Lived Asymmetrically Retained Proteins

5.1.1 How LARPs relate to other aging factors.

The aging of a yeast cell is an inherently asymmetric process, as the mother cell ages but produces rejuvenated, young, daughter cells (Egilmez and Jazwinski, 1989; Kennedy et al., 1994). Because of this inequality, Egilmez and Jazwinski, and others, suggested the existence of a putative aging factor that is asymmetrically distributed between these two cells (reviewed in ref. (Henderson and Gottschling, 2008)). However, the nature of the aging factor is not completely clear and researchers have suggested a number of factors to fill this role. Several of which are capable of affecting the aging process of the cells and altering lifespan.

Despite the existence of known aging factors, we thought that at least one component of the aging factor could be protein based. Proteins are an essential, abundant, and fundamental component of the architecture and biochemical activity of a cell. It is not surprising then, that we found there to be proteins that are asymmetrically retained in aging mother cells throughout their lifespan. However, this work does not rule out the importance of non-protein aging factors that are also retained in the mother cells. I suggest, that in combination with previously known aging factors and processes, LARPs influence how a cell ages (Erjavec et al., 2007; Sinclair and Guarente, 1997).

In support of this hypothesis, no known aging factor, once removed or remedied, makes a cell immortal (Defossez et al., 1999; Hughes and Gottschling, 2012; Kaeberlein et al., 2005b). Though delayed, cells still die in an age-dependent manner. I feel this observation

suggests that there is a combination of aging factors that each are responsible for a part of the asymmetry of the aging process. Some factors may be DNA, some may be dysfunctional organelles, some may be various types of accumulating damage, and some may be LARPs.

5.1.2 **There are possibly other LARPs yet to be identified.**

This project used a total mass-spec proteomics approach to identify LARPs. This method has several caveats that may have limited our ability to detect certain proteins.

First, we were limited to detect proteins that are good candidates for mass-spectrometry (de Godoy et al., 2006). Some proteins are simply not amenable to detection because of their biochemical properties. We would have missed these proteins in our analysis, independent of their LARP-like behavior. We also primarily detected abundant proteins. It is possible that there are LARPs that are not abundant enough to be detected by total proteomics methods.

Secondly, our experiment was performed under one specific growth condition. A significant number of proteins in the yeast proteome are only expressed under certain environmental conditions (DeRisi et al., 1997). It is possible that if we aged the cells in a different environment (carbon source, nitrogen source, amino acids, etc.), we would identify more proteins that behave as LARPs. It would be particularly interesting to find LARPs that are present independent of environment versus the ones that are only present under certain environmental conditions. These proteins could represent aging pathways that affect all cells and pathways that only affect cells aged in certain environments.

Additionally, it is formally possible that certain proteins could alter their behavior (independent of expression) in certain environments – behaving as LARPs in one condition but not another. Such behavior would provide additional evidence for the existence of multiple aging pathways that are dependent on the environment that the cells are aged in. Also, identifying such proteins may help identify a mechanism for establishing and maintaining LARP behavior.

5.1.3 **Fragmented LARPs**

The largest class of LARPs were those that were found as low molecular weight fragments. This category has the primary characteristic that full-length protein was mostly newly synthesized, where only the small fragments contained a significant fraction of the heavy isotope label. Unfortunately, this group was the most technically difficult category of LARPs to further characterize, and a number of questions still remain.

What makes these fragments and why are they retained? One of the most basic questions is why we detected these specific proteins and fragments. We do know that they are enriched for some of the most abundant proteins in the yeast proteome, but we do not know if this enrichment is causal (Ghaemmaghami et al., 2003). It would be interesting to see if expressing any protein, like GFP, at these levels is sufficient to drive this behavior, or whether there is something specific about the proteins identified in this study.

Where are fragmented LARPs located? As of now, we do not know if these fragmented LARPs are retained in some sort of aggregate or cellular structure that is retained in the mother cell during each cell division. Ideally, we could visualize these fragments and follow their segregation throughout several cell divisions. This approach would allow us to more accurately measure the degree of asymmetry with which these protein fragments are retained. Additionally, this strategy would allow us to possibly colocalize these fragmented LARPs with known markers of specific aggregate types and regulators of asymmetry (e.g. Hsp104)(Zhou et al., 2011).

Do LARPs exist in other organisms? We only identified this class of LARPs because we separated our proteins by molecular weight prior to trypsinization and mass-spec analysis. While this approach helped reduce the complexity of the samples provided to the mass-spectrometer, it is not common practice for all proteomics studies (Martins-de-Souza, 2014). It is possible that if our method is applied to studying aging in other organisms, similar proteins would be identified. There is no reason to think the LARPs are unique to the aging process in yeast. However, characterization in multicellular organisms may be difficult due to the need to identify and purify the “mother” cells in these systems.

5.1.4 LARPs that are localized to the cell wall.

A number of proteins identified by our analysis were previously known to be localized to the yeast cell wall (Cappellaro et al., 1998; Klebl and Tanner, 1989). We found the presence of these proteins in our dataset to be reassuring, as the cell wall is known to be both long-lived and asymmetrically retained, the two criteria for proteins we set out to identify (Ballou, 1982). The cell wall was originally not thought to be a major effector of the aging process, as early experiments showed that mutants with altered cell-wall maintenance did not exhibit altered lifespan (Egilmez and Jazwinski, 1989; Kennedy et al., 1994). However, recent reports may contradict these initial observations and show the cell wall may be capable of limiting lifespan (Kaeberlein et al., 2002; Meitinger et al., 2014; Yang et al., 2011). The cell wall plays crucial roles in a cell's ability to tolerate many stresses that a cell may encounter during its lifespan. Additionally, a cell wall must be remodeled to allow cells to grow; defective cell-wall growth is a common phenotype of the aging process (Bi and Park, 2012). For these reasons and others, the function and activity of the cell wall is important for a cell's ability to survive and continue to divide. It would be interesting to know if there are particular activities of the cell wall that are changing as a cell ages, perhaps as a consequence of accumulating and/or damaged LARPs.

Furthermore, the yeast cell wall is functionally similar to the extracellular matrix found in multicellular organisms, known to have roles in the aging process of metazoans (Kurtz and Oh, 2012). Some proteins in the metazoan extracellular matrix are also known to be extremely long-lived and experience an age-associated decline in function (Toyama and Hetzer, 2013). It is intriguing that proteins with similar characteristics in a similar structure may also contribute to the aging of dividing yeast cells.

5.1.5 LARPs that form foci.

Several of the proteins that we identified have a tendency to form foci in aging cells (Hsp26 and Thr1). However, at this point, the nature of these foci remains unclear. First, these foci could be part of a reversible higher-order structure that forms in response to cellular stress. Several such proteins have previously been identified in yeast and other organisms (Narayanaswamy et al., 2009; Noree et al., 2010; O'Connell et al., 2012).

Second, these proteins could be part of an irreversible aggregate. Aggregated proteins have long been implicated in the aging process. There are several reports studying Hsp104 associated aggregates that directly regulate replicative aging of a yeast cells (Erjavec et al., 2007, 2012; Zhou et al., 2011). Aggregated proteins were also some of the first proposed mechanisms of several age-associated neurodegenerative diseases in humans (Ross and Poirier, 2004).

One large question about LARPs that form foci is whether they are composed of active, or potentially active, protein. It appears that a large proportion of the protein exists in these foci, compared to any cytoplasmic pools. So if these proteins are potentially active, the inheritance, or lack thereof, sets up a large degree of asymmetric partitioning of protein activity between mother and daughter cells.

It should be emphasized that not every aging mother cell contained an observable aggregate or focus. Further, not every mother cell that contained a focus retained the focus for her entire lifespan. There was some heterogeneity in the distribution of these aggregates. It is possible that this heterogeneity in the presence and distribution of these LARP foci can explain some of the stochasticity in the aging process. If these foci are toxic and damaging to a cell, the cells that contain a focus could be the cells that die earlier than the average cell. Where the cells that do not have a focus (or distribute it to a daughter cell) are the ones that live longer than average. Extending this idea, perhaps daughter cells that inherit a focus are not as completely rejuvenated as daughter cells that do not.

Several of the questions posed about the LARPs that form foci can be answered by microfluidic analysis (Lee et al., 2012; Xie et al., 2012). This technology will eventually allow for the following of many cells throughout their lifespan while simultaneously tracking the inheritance of these LARP foci. Unfortunately, at the time of this study, this technology is not quite established enough to answer these questions.

5.1.6 **Plasma membrane LARPs**

Several of the proteins that we identified and characterized in our study are localized to the plasma membrane (Pma1, Sur7, and Mrh1)(Huh et al., 2003). Pma1, the major

regulator of cellular pH, was shown to be a pool of functional protein that has a direct effect on the aging process (Henderson et al., 2014). Unfortunately, the exact function of the other plasma membrane LARPs is not known. As functional information about the other plasma membrane LARPs, these proteins and their effects on the aging process will be much more tractable to study.

5.1.7 How are LARPs maintained and retained?

By definition LARPs have two properties. 1) They are long-lived proteins. 2) They are asymmetrically distributed between mother and daughter cells. There are a number of proteins that meet one, but not both of these criteria. Recently, several studies have tried to define these proteins in yeast (long-lived proteins or asymmetrically retained proteins)(Belle et al., 2006; Eldakak et al., 2010; Yang et al., 2015). And expectedly, they have found a partially overlapping set of proteins compared to those we defined as LARPs. While most of the proteins identified in these studies are, by definition, not LARPs, they may share some of the same properties that makes a LARP either long-lived or asymmetrically retained.

Several mechanisms have been proposed for the asymmetric retention of nuclear, cytoplasmic, organelle-associated and plasma membrane components (Eldakak et al., 2010; Gehlen et al., 2011; Liu et al., 2011; Shcheprova et al., 2008; Spokoini et al., 2012). These mechanisms can be categorized into two groups, active retention and passive retention. Active retention relies on cellular processes to recognize, tether and/or return these proteins to the mother cell. Passive retention relies upon these proteins existing as part of a larger structure with relatively slow diffusion rates within the cell. And because cell division is a relatively rapid process, limited to a small region of the cell, there is a low likelihood for a significant amount of these proteins to diffuse into the daughter cells. There has been convincing evidence for each of these models, and they are not mutually exclusive. It is likely that the mechanism of retention of various LARP proteins may be a combination of these two models.

Recently, our lab has begun a genome-wide screen for genes essential for the asymmetry of several plasma membrane LARPs. While this work is still preliminary, it has been

relatively successful, identifying several components necessary for LARP behavior. While technically less difficult than looking at the distribution of LARP proteins that form foci, these studies of plasma membrane LARPs may serve as a template to identify factors and cellular processes responsible for the retention of these long-lived proteins.

5.1.8 How are LARPs modified?

During the characterization of several LARP proteins, we noted that there was an age-dependent modification of the protein. While the exact biochemical nature of these modifications remains unclear, it could be an important mechanism by which LARPs contribute to the aging process. Several modifications are known to accumulate in aging cells (Schöneich, 2006). Proteins are oxidized with age, possibly as a result of accumulating reactive oxygen species. Proteins are also known to be glycosylated in aging cells. Each of these modifications, among others, could contribute to the biochemical behavior of these proteins in old cells. Further biochemical characterization of these modifications will no doubt contribute to understanding the behavior of LARPs and how they contribute to the aging process.

5.1.9 How do the proteins found in this study compare to aging studies carried out in other organisms?

A few years prior to the completion of this study, Toyama et al. used a similar heavy-isotope labeling strategy to identify long-lived proteins in a different model system, the rat brain (Toyama et al., 2013). Despite the technical similarities in the approaches used between the two studies, there are several differences that would influence the types of proteins identified in each study. Mainly, the cells in the aging rat brain are mostly in a non-dividing state, whereas replicatively aged yeast cells are, by definition, repeatedly dividing. The major group of proteins that Toyama et al. identified were components of the nuclear-pore complex. While our study did not identify any components of the nuclear pore or nuclear proteins, we did find a component of the eisosome, Sur7 (Walther et al., 2006). While sharing no functional similarities, these proteins are both part of large multi-protein complexes that are inserted into lipid membranes. It is possible that this feature

is a property of long-lived proteins in aging cells; they are part of large complexes, a context in which turnover would require rebuilding large parts of the complex.

Toyama et al. also identified several other types of proteins with similar properties to some LARP proteins. They identified several components of the Extra Cellular Matrix, with has similar functionality to the yeast cell wall (discussed above). They also identified what is thought to be a cytoplasmic metabolic enzyme, Asrgl1 (Dieterich et al., 2003). While not directly related to the metabolic enzymes we identified (Thr1), they may share similar properties which lead to their extended retention in aging cells.

Due to differences in the experimental protocol, their study would not have been sensitive to the detection of long-lived protein fragments. It would be interesting to repeat this experiment, as well as extend it into other aging models, to find if proteins similar to the fragmented LARPs can be identified.

5.1.10 How do LARPs affect the aging process?

There are several possible ways that LARP proteins could influence the aging process. I will discuss several possibilities, but this list is not exhaustive nor is each example mutually exclusive. LARP proteins likely influence the aging process through a combination of these and other mechanisms.

Active LARP protein accumulates with age – One possibility is that a LARP, because it is long-lived, asymmetrically retained, and continued to be expressed, accumulates in aging cells. This increased activity is potentially incompatible with other aspects of the aging process and this protein activity then limits lifespan. This is the mechanism by which Pma1 affects how a cell ages, where lowering Pma1 activity in aging cells leads to increased lifespan (Henderson et al., 2014). Conversely, it is also theoretically possible that this accumulated activity is beneficial to an aging cell and removing it would shorten lifespan.

LARP protein is damaged and changes activity – Several LARP proteins are maintained in a mother cell throughout lifespan, as a result they are subject to several possible sources of damage. Damage could cause a loss of activity or regulation that is required

for a cell to continue to divide (Kikis et al., 2010). If this activity could be replaced in an old cell, it is possible that this would extend lifespan.

LARP protein acquires damage that is toxic to a cell – As discussed above, LARP proteins are subject to several forms of protein damage. Accumulation of some forms of damaged proteins are known to be toxic to a cell (Squier, 2001). It is possible this damage is what limits lifespan in some cells, not necessarily the loss of protein's activity. Damaged proteins that have become aggregated or modified with a reactive oxygen species could potentially affect the young and healthy protein in the cell. If the damage protein could be repaired or removed, a cell may have extended lifespan.

These are just a few examples of how LARP proteins could possibly influence the aging process and determine the absolute lifespan of a cell. It is also possible that some LARPs are simply present in aging cells and do not explicitly alter or influence the aging process. The ability to modulate these protein's behavior (presence, asymmetry, longevity) in aging cells will help identify roles in various aging pathways. More work is needed to identify all proteins that act similarly and to further understand their role in aging. However, this study demonstrated the existence of this novel class of proteins.

5.2 DISCUSSION ON METHODS TO MEASURE LIFESPAN

The ability to quickly and easily identify altered lifespan is a critical tool necessary to study the aging process. First, it is useful to test if particular processes or activities are able to alter the ultimate lifespan of an organism. Second, it is it absolutely required for unbiased screening for effectors of lifespan. Discussed below, the lifespan assay presented in Chapter III of this dissertation addresses several needs that were not met by existing methods used to study aging cells.

5.2.1 **Comparison to other lifespan assays**

The observation that a yeast cell has a finite lifespan was first made nearly 60 years ago (Mortimer and Johnston, 1959). However, the traditional assay to measure a cell's lifespan was extremely tedious and has limited many attempts to leverage the powers of

the yeast system to explore this phenomenon. The idea to create a tractable lifespan assay is not novel, and there have been several attempts to create alternative assays.

Micromanipulation assay – The traditional micromanipulation assay requires an experimentalist to intervene approximately every 90 minutes, manually separating daughter cells from mother cells after each cell division (Steffen et al., 2009). This manual intervention is continued throughout the lifespan of the cells. Because this process is tedious and time consuming, approximately 50-100 cells can be assayed for lifespan at once. It has been suggested that these low sample number are responsible for generating lifespan data that is difficult to repeat using other techniques (Huberts et al., 2014). Using this technique, there have been attempts to screen the yeast deletion collection for altered lifespan with some success (Kaeberlein et al., 2005a; McCormick et al., 2015). However, these studies made several compromises during initial screening (extremely low sample numbers) and required a huge amount of time and resources to complete. It is hard to envision repeating these screens under multiple environmental conditions or in different genetic backgrounds.

Microfluidic devices – Recently, there have been several attempts to create a microfluidic device capable of automatically separating daughter cells from mother cells (Jo et al., 2015; Lee et al., 2012; Xie et al., 2012). While removing the need for experimentalist intervention, these devices still require relatively expensive technology in order to monitor the cells throughout their lifespan. Additionally, the current devices retain cells by physically trapping them, possibly introducing bias by trapping only certain cells. This method of retention may also harm aging cells, physically crushing them or limiting access to nutrients (Lee et al., 2012; Liu et al., 2015). Ultimately, I feel that technical advances will eventually lead to microfluidic devices being the standard platform for measuring replicative lifespan; however, they may be limited to relatively low throughput screening. A system in which pools of strains comprised of many different genotypes are all screened for lifespan or age-related phenotypes should be far more amenable to genome-wide screening.

Mother Enrichment Program – There have been several genetic systems designed in order to study aging cells, one of which is the Mother Enrichment Program (MEP)(Jarolim

et al., 2004; Lindstrom and Gottschling, 2009). The MEP is an inducible genetic system that can selectively make daughter cells inviable. While this system has been successfully used to distinguish the lifespan of a long-lived strain, this analysis required tedious colony counting, and the assay could be skewed by random mutations that altered the effectiveness of the MEP machinery. The MEP is not sufficient to be used as a high-throughput assay for lifespan. However, the MEP is a useful tool that allows culturing of a large number of mother cells for their entire lifespan. The assay described in this thesis would not be possible without utilizing the MEP.

Alternative culturing methods – In addition to genetic systems, there have been several tools developed that allow experimentalists to obtain significant numbers of aged cells. Usually using magnetic beads coupled to original mother cells, these systems have obtained populations of cells suitable for biochemical and cell biological characterization of these aged cells (Laun et al., 2001; Smeal et al., 1996). However, these systems are not really designed, nor easily adaptable, to identify mutants with altered lifespan.

Similar fluorescent labeling approaches. Previous studies have used fluorescent labeling techniques similar to those that I used. In principle, coupling a fluorescent molecule to the cell wall is very similar to the magnetic purification strategies and has been used to track the original cells in a population (McFaline-Figueroa et al., 2011). Additionally, there are several stains that are specific for the budscars that accumulate in a mother cell wall after each division (WGA-FITC and calcofluor-white)(Chen et al., 2003; Janssens et al., 2015). The intensity of these fluorescent stains can be used as a rough measure of age, but lacks the resolution to distinguish the age of cells more than approximately 10 divisions old. These techniques are also limited by the fact that daughter cells will quickly crowd out cells of any significant age, limiting observations to middle age – not near the end of lifespan.

I feel that the assay described in Chapter III of this dissertation provides a useful and novel tool to screen for mutants and conditions that alter lifespan. It requires minimal experimentalist intervention, uses technology that is available to most modern laboratories, is based upon large numbers of cells, and should be amenable for genome-wide screening.

5.2.2 The absence of Caloric Restriction effects

As demonstrated in Chapter III, the method was able to detect the effects of several previously reported long- and short-lived mutants. Additionally, the method was able to detect altered lifespan of several other mutants and genetic backgrounds (data were not shown). However, the method was not able to detect the expected effects from several different implementations of Caloric Restriction (CR). While a number of variables remain untested, this surprising result, does not appear to be due to the method of implementation, media type, temperature, osmotic stresses, or the absence of specific excreted metabolites.

While there is potentially an issue with how the method measures lifespan, a recent report has also claimed difficulties observing lifespan extension under CR conditions, even using multiple methods to determine lifespan (Huberts et al., 2014). In this report, Huberts et al. discuss several possibilities to explain the differences between their findings and several previously published works. Ultimately, they suggest that there is no lifespan extension due to CR, and the previous studies were biased by under-sampling the population of aging cells. While my findings are in agreement with this conclusion, as my assay monitors the viability of thousands of cells and should not suffer from under-sampling the population, I feel it may be too early to conclude that there is no lifespan extension under CR conditions. There continues to be reports of CR conditions extending lifespan and altering various aging phenotypes (Jo et al., 2015; Mei and Brenner, 2015). Perhaps the effects of CR are modulated by specific metabolites, as suggested by Mei et al., or altered by some unknown environmental variable (like those observed in Chapter IV).

I suggest that there is no lifespan extension of yeast cells from CR under the specific environmental conditions tested. The mechanism by which CR extends lifespan has never been established and there may be several environmental dependencies that are not realized. As CR is reported to be the most widely conserved method to extend lifespan, it may warrant further study to identify the specific conditions required to observe lifespan extension by CR.

5.2.3 A genome-wide screen to identify modulators of lifespan

Originally, I believed the inability to detect lifespan extension under CR conditions was a limitation of the assay. A great deal of effort was dedicated to identifying a variable responsible for the absence of CR effects. As a result, I was unable to proceed with the originally intended genome-wide screen for effectors of lifespan. However, after recent reports, I am more confident that the assay is accurately reporting the lifespan under these conditions (Huberts et al., 2014; Mei and Brenner, 2015). Due to certain time limitations, it ended up not being feasible to complete a screen for the modulators of lifespan. However, I feel the tools presented in this dissertation will allow for such approaches to be taken in the near future. Additionally, the assay presented in this dissertation may be the ideal system to test for the environmental or genetic requirements for lifespan extension by CR.

5.3 Discussion on exploring the genetics regulating age-associated phenotypes

In Chapter IV of this dissertation, I introduced a genome-wide screen for the age-associated decline in mitochondrial membrane potential ($\Delta\psi^{mito}$) and the specific results of the screen were discussed in that chapter. Here, I will discuss some of the more general findings, issues encountered and future directions resulting from this project.

5.3.1 Many potential suppressors identified by primary screen

The primary screen identified many putative suppressors of the age-associated loss of $\Delta\psi^{mito}$, or more specifically an age-associated loss of DiOC6(3) staining intensity. I found that 79 genotypes were enriched in a population that apparently suppressed the loss of DiOC6(3) staining. Unfortunately, due to technical limitations and complications (several of which are discussed below), I was not able to further characterize all of the suppressors identified in the primary screen. As more tools become available to quickly and accurately characterize mitochondrial phenotypes in old cells, the effects of these putative suppressors should be further investigated. It is possible that many of these candidates

are true suppressors of this aging phenotype and are potentially capable of altering the aging process of the cell.

5.3.2 Several suppressors of $\Delta\psi^{mito}$ also affect vacuole acidity.

During the initial characterization of the age-associated loss of $\Delta\psi^{mito}$, Hughes and Gottschling found that this event is preceded by a loss of vacuole acidity (2013). They found that one way of suppressing $\Delta\psi^{mito}$ loss is to prevent the loss of vacuole acidity. It appears that a number of $\Delta\psi^{mito}$ suppressors that I identified during this study act by preventing or delaying the loss of vacuole acidity (still by an unknown mechanism). It may require alternative approaches to identify the factors connecting these two age-associated phenotypes.

Hughes and Gottschling found that a chemical induction of vacuole acidity, by Concanamycin A treatment, is sufficient to cause mitochondrial dysfunction. This dysfunction appears qualitatively similar to the dysfunction seen in the context of aging. A screen for suppressors of mitochondrial dysfunction after Concanamycin A treatment may yield effectors acting specifically between vacuole acidity loss and mitochondrial dysfunction. Concanamycin A was not used in this study because it induces vacuole acidity loss more severe than that seen during aging; however, it may be required to identify the processes that connect these aging phenotypes.

5.3.3 Do the suppressors of the age-associated phenotype affect lifespan?

One outstanding question is – do the suppressors of the age-associated loss of $\Delta\psi^{mito}$ also extend lifespan? The suppressors identified by Hughes and Gottschling did in fact extend lifespan, so one might expect the suppressors identified in the study to as well. However, several of the mutants identified in this study appear to rescue $\Delta\psi^{mito}$, without altering the fragmentation of the mitochondrial network that also occurs with age. At this point, it is not known which of these phenotypes (loss of $\Delta\psi^{mito}$ or fragmentation) is the limiter of lifespan. The suppressors identified by Hughes and Gottschling were selected for their suppression of the change in mitochondrial morphology. Additionally, it is

possible that the mutants in Chapter IV rescue $\Delta\psi^{mito}$ in a manner that is detrimental to other cellular processes, possibly shortening lifespan.

5.3.4 Issues encountered during the screen

During this project I encountered several issues in the screen, as it was designed. I will discuss several of the specific issues here so as to explain several caveats of this study. This information may prove useful for any future studies attempting to use similar techniques.

The deletion collection that was screened was incomplete – The MEP was an important tool for this project that allowed me to culture large numbers of aging cells to significant ages. In order to screen the deletion collection for aging phenotypes, we first had to introduce the deletion collection in the MEP genetic background (Lindstrom and Gottschling, 2009). The MEP consists of three components each marked with a unique genetic marker (*HphMX, NatMX,* and *LEU2*) and the deletion from the deletion collection is marked with *KanMX* (Bähler et al., 1998). During construction of the library, these four markers were selected for simultaneously. However, I soon discovered that many of the strains in the library did not contain the MEP component marked with *HphMX*. Through careful analysis, I found that strains lacking *HphMX* cassette are able to grow in the presence of Hygromycin and G418 in synthetic medium (strains lacking the *HphMX* cassette are not able to grow on Hygromycin + and G418+ in YPD medium). These were the conditions that our lab and collaborators used during library construction (SC+Hygromycin+G418+Natamycin). After taking each strain in the collection and sequentially selecting for each marker, I was left with approximately 60% of the deletion collection containing all of the required MEP components.

DiOC6 is not entirely specific for $\Delta\psi^{mito}$ – During characterization of several hits from my primary screen, it became apparent that DiOC6(3) was staining some cellular structures in a seemingly $\Delta\psi^{mito}$ independent manner. This was only true in certain mutants and suggests these mutants may have altered $\Delta\psi$ across other membranes or altered permeability to the dye. I was able to overcome this complication using an alternative measure of $\Delta\psi^{mito}$ in a secondary screen; however, the number of false positives from the

primary screen appeared relatively high. It is possible that the primary screen could have been made more accurate and specific by using an alternative measure of $\Delta\psi^{mito}$.

Subtle environmental changes alter normal aging phenotypes – During this study I discovered that subtle changes in the environment can alter the normal onset of some age-associated phenotypes. The realization that there are batch-to-batch differences in rich media inspired a switch to synthetic defined medium (discussed in more detail below). While cells aged in this synthetic medium still showed an age-associated loss of $\Delta\psi^{mito}$, it is possible that some suppressors are only able to alter aging phenotypes in certain environmental conditions. This could possibly explain why some hits from the primary screen (performed in rich medium) failed to suppress loss of $\Delta\psi^{mito}$ during further characterization (performed in synthetic medium).

5.3.5 This approach can be used to study other age-associated phenotypes

The screening protocol, as described in Chapter IV, only requires that an aging phenotype be characterizable by a change in fluorescence. A number of aging phenotypes can be coupled to a reporter by a change in fluorescence. These reporters can be other dyes that report on the health or state of particular organelles (Greenspan et al., 1985). They could be transcription reporters that provide a readout of the activity of particular stress response that is normally activated in old cells (Xie et al., 2012). They could be fluorescent fusions to particular proteins that are known to accumulate or decline with age. Simply, many aging phenotypes, both those previously known and those yet to be identified, can be characterized by a change in fluorescence, and the screening protocol should be easily adaptable to study any of these phenotypes.

5.3.6 Other collections that can be screened using a similar approach

Further, the screening protocol is not specific to the Yeast Deletion Collection and only requires that each genotype be marked with a unique sequence barcode. These barcodes are a common feature of many genome-wide, and other, collections of yeast strains. One such collection, the MoBY, contains a collection of 2μ plasmids each containing a single gene to be overexpressed (Ho et al., 2009). A screen of this collection could identify

specific factors that become limiting during the aging process and lead to the onset of a particular age-associated phenotype. Overexpression of various cellular components can also act as a dominant negative, generating phenotypes not seen in the deletion collection (Prelich, 2012).

5.3.7 **Not all variables that affect the aging process are known and/or controlled**

The aging process is inherently incredibly complex and we, as a field, do not know everything that could potentially alter how a cell ages. It is accepted, however, that the cell's interaction with its environment has dramatic consequences for the aging process and lifespan (Finch and Ruvkun, 2001). Yet, yeast aging studies are traditionally conducted in an environment that may vary from lab to lab (or even experiment to experiment, discussed above). This variation could explain some controversies in the field, potentially even why some labs observe lifespan extension from CR and others do not (Huberts et al., 2014).

I argue that there needs to be an effort to reduce the number of variables in these aging experiments. Primarily, aging experiments should be conducted in a defined synthetic media in which the concentration of every nutrient is known and controlled. There are simply too many things that remain unknown about the aging process and if we continue to not control for possible effectors and environmental variables, there will continue to be controversy.

5.4 CONCLUDING STATEMENTS.

For a number of years, studies of the replicative aging process in yeast were limited to relatively low-throughput approaches. Still, several benefits of the yeast system allowed this model to be an attractive system in which to study how a cell ages (e.g. relatively short lifespan, tractable genetics, fully sequenced genome). However, many of the more powerful approaches available in the yeast system could not be applied to studying the aging process because of the technical limitations in measuring lifespan and obtaining populations of aged cells. This dissertation presented three tools that allowed unbiased genome-wide screening to explore and identify effectors of the aging process. It is my

hope that the approaches described here will facilitate the full utilization of the power of the yeast system and lead to a better understanding of the aging process in all organisms.

BIBLIOGRAPHY

Aguilaniu, H., Gustafsson, L., Rigoulet, M., and Nyström, T. (2003). Asymmetric inheritance of oxidatively damaged proteins during cytokinesis. Science *299*, 1751–1753.

Al-Regaiey, K.A., Masternak, M.M., Bonkowski, M., Sun, L., and Bartke, A. (2005). Long-lived growth hormone receptor knockout mice: interaction of reduced insulin-like growth factor i/insulin signaling and caloric restriction. Endocrinology *146*, 851–860.

Amberg, D.C., Burke, D.J., and Strathern, J.N. (2005). Methods in Yeast Genetics: A Cold Spring Harbor Laboratory COurse Manual (Cold Spring Harbor, NY: Cold Spring Harbor Laboratory Press).

Aström, S.U., Cline, T.W., and Rine, J. (2003). The Drosophila melanogaster sir2+ gene is nonessential and has only minor effects on position-effect variegation. Genetics *163*, 931–937.

Austad, S.N. (2010). Cats, "rats," and bats: the comparative biology of aging in the 21st century. Integr. Comp. Biol. *50*, 783–792.

Bähler, J., Wu, J.Q., Longtine, M.S., Shah, N.G., McKenzie, a, Steever, a B., Wach, a, Philippsen, P., and Pringle, J.R. (1998). Heterologous modules for efficient and versatile PCR-based gene targeting in Schizosaccharomyces pombe. Yeast *14*, 943–951.

Balch, W.E., Morimoto, R.I., Dillin, A., and Kelly, J.W. (2008). Adapting proteostasis for disease intervention. Science *319*, 916–919.

Ballou, C.E. (1982). Yeast cell wall and cell surface. In The Molecular Biology of The Yeast Saccharomyces, (Cold Spring Harbor, NY: Cold Spring Harbor Laboratory Press),.

Bank, R.A., Bayliss, M.T., Lafeber, F.P., Maroudas, A., and Tekoppele, J.M. (1998). Ageing and zonal variation in post-translational modification of collagen in normal human articular cartilage. The age-related increase in non-enzymatic glycation affects biomechanical properties of cartilage. Biochem. J. *330 (Pt 1*, 345–351.

Belle, A., Tanay, A., Bitincka, L., Shamir, R., and O'Shea, E.K. (2006). Quantification of protein half-lives in the budding yeast proteome. Proc. Natl. Acad. Sci. U. S. A. *103*, 13004–13009.

Bergman, L.W. (2001). Growth and Maintenance of Yeast. In Methods in Molecular Biology, Vol.

177, Two-Hybrid Systems: Methods and Protocols, P.N. MacDonald, ed. (Totowa, NJ: Humana Press),.

Bi, E., and Park, H.-O. (2012). Cell polarization and cytokinesis in budding yeast. Genetics *191*, 347–387.

Botstein, D., and Fink, G.R. (2011). Yeast: an experimental organism for 21st Century biology. Genetics *189*, 695–704.

Bouquin, N., Barral, Y., Courbeyrette, R., Blondel, M., Snyder, M., and Mann, C. (2000). Regulation of cytokinesis by the Elm1 protein kinase in Saccharomyces cerevisiae. J. Cell Sci. *113 (Pt 8*, 1435–1445.

Brachmann, C.B., Davies, a, Cost, G.J., Caputo, E., Li, J., Hieter, P., and Boeke, J.D. (1998). Designer deletion strains derived from Saccharomyces cerevisiae S288C: a useful set of strains and plasmids for PCR-mediated gene disruption and other applications. Yeast *14*, 115–132.

Bratic, A., and Larsson, N.-G. (2013). The role of mitochondria in aging. J. Clin. Invest. *123*, 951–957.

Bricker, D.K., Taylor, E.B., Schell, J.C., Orsak, T., Boutron, A., Chen, Y.-C., Cox, J.E., Cardon, C.M., Van Vranken, J.G., Dephoure, N., et al. (2012). A Mitochondrial Pyruvate Carrier Required for Pyruvate Uptake in Yeast, Drosophila, and Humans. Science (80-.). *337*, 96–100.

Brown, K., Xie, S., Qiu, X., Mohrin, M., Shin, J., Liu, Y., Zhang, D., Scadden, D.T., and Chen, D. (2013). SIRT3 reverses aging-associated degeneration. Cell Rep. *3*, 319–327.

Bufalino, M.R., DeVeale, B., and van der Kooy, D. (2013). The asymmetric segregation of damaged proteins is stem cell-type dependent. J. Cell Biol. *201*, 523–530.

Burnett, C., Valentini, S., Cabreiro, F., Goss, M., Somogyvári, M., Piper, M.D., Hoddinott, M., Sutphin, G.L., Leko, V., McElwee, J.J., et al. (2011). Absence of effects of Sir2 overexpression on lifespan in C. elegans and Drosophila. Nature *477*, 482–485.

Cappellaro, C., Mrsa, V., and Tanner, W. (1998). New potential cell wall glucanases of Saccharomyces cerevisiae and their involvement in mating. J. Bacteriol. *180*, 5030–5037.

Carter, M., and Brunet, A. (2005). Quick Guide: FOXO transcription factors. Curr. Biol. *17*, R113–R114.

Cashikar, A.G., Duennwald, M., and Lindquist, S.L. (2005). A chaperone pathway in protein disaggregation. Hsp26 alters the nature of protein aggregates to facilitate reactivation by Hsp104. J. Biol. Chem. *280*, 23869–23875.

Caudron, F., and Barral, Y. (2009). Septins and the lateral compartmentalization of eukaryotic membranes. Dev. Cell *16*, 493–506.

Chen, L.B. (1988). Mitochondrial membrane potential in living cells. Annu. Rev. Cell Biol. *4*, 155–181.

Chen, C., and Contreras, R. (2007). Identifying genes that extend life span using a high-throughput screening system. Methods Mol. Biol. *371*, 237–248.

Chen, C., Dewaele, S., Braeckman, B., Desmyter, L., Verstraelen, J., Borgonie, G., Vanfleteren, J., and Contreras, R. (2003). A high-throughput screening system for genes extending life-span. Exp. Gerontol. *38*, 1051–1063.

Chondrogianni, N., Petropoulos, I., Grimm, S., Georgila, K., Catalgol, B., Friguet, B., Grune, T., and Gonos, E.S. (2014). Protein damage, repair and proteolysis. Mol. Aspects Med. *35*, 1–71.

Clancy, D.J., Gems, D., Hafen, E., Leevers, S.J., and Partridge, L. (2002). Dietary restriction in long-lived dwarf flies. Science *296*, 319.

Coelho, M., Dereli, A., Haese, A., Kühn, S., Malinovska, L., DeSantis, M.E.E., Shorter, J., Alberti, S., Gross, T., and Tolić-Nørrelykke, I.M.M. (2013). Fission yeast does not age under favorable conditions, but does so after stress. Curr. Biol. *23*, 1844–1852.

Costanzo, M., Baryshnikova, A., Bellay, J., Kim, Y., Spear, E.D., Sevier, C.S., Ding, H., Koh, J.L.Y., Toufighi, K., Mostafavi, S., et al. (2010). The genetic landscape of a cell. Science *327*, 425–431.

Craig, R., Cortens, J.P., and Beavis, R.C. Open source system for analyzing, validating, and storing protein identification data. J. Proteome Res. *3*, 1234–1242.

Croft, D.P., Brent, L.J.N., Franks, D.W., and Cant, M. a. (2015). The evolution of prolonged life after reproduction. Trends Ecol. Evol. 1–10.

D'Angelo, M.A., Raices, M., Panowski, S.H., and Hetzer, M.W. (2009). Age-dependent deterioration of nuclear pore complexes causes a loss of nuclear integrity in postmitotic cells. Cell

136, 284–295.

D'Aquino, K.E., Monje-Casas, F., Paulson, J., Reiser, V., Charles, G.M., Lai, L., Shokat, K.M., and Amon, A. (2005). The protein kinase Kin4 inhibits exit from mitosis in response to spindle position defects. Mol. Cell *19*, 223–234.

Davey, H.M., Kell, D.B., Weichart, D.H., and Kaprelyants, A.S. (2004). Estimation of Microbial Viability Using Flow Cytometry. In Current Protocols in Cytometry, (Hoboken, NJ, USA: John Wiley & Sons, Inc.), p. Unit 11.3.

Defossez, P. a, Prusty, R., Kaeberlein, M., Lin, S.J., Ferrigno, P., Silver, P. a, Keil, R.L., and Guarente, L. (1999). Elimination of replication block protein Fob1 extends the life span of yeast mother cells. Mol. Cell *3*, 447–455.

Denoth Lippuner, A., Julou, T., and Barral, Y. (2014). Budding yeast as a model organism to study the effects of age. FEMS Microbiol. Rev. *38*, 300–325.

DeRisi, J.L., Iyer, V.R., and Brown, P.O. (1997). Exploring the metabolic and genetic control of gene expression on a genomic scale. Science *278*, 680–686.

Dickinson, B.C., and Chang, C.J. (2011). Chemistry and biology of reactive oxygen species in signaling or stress responses. Nat. Chem. Biol. *7*, 504–511.

Dieterich, D.C., Landwehr, M., Reissner, C., Smalla, K.-H., Richter, K., Wolf, G., Böckers, T.M., Gundelfinger, E.D., and Kreutz, M.R. (2003). Gliap--a novel untypical L-asparaginase localized to rat brain astrocytes. J. Neurochem. *85*, 1117–1125.

Douglas, L.M., Wang, H.X., Li, L., and Konopka, J.B. (2011). Membrane Compartment Occupied by Can1 (MCC) and Eisosome Subdomains of the Fungal Plasma Membrane. Membranes (Basel). *1*, 394–411.

Dunham, M.J., Gartenberg, M.R., and Brown, G.W. (2015). Methods in Yeast Genetics and Genomics, 2015 Edition: A CSHL Course Manual (Cold Spring Harbor, NY: Cold Spring Harbor Laboratory Press).

Durieux, J., Wolff, S., and Dillin, A. (2011). The cell-non-autonomous nature of electron transport chain-mediated longevity. Cell *144*, 79–91.

Edgar, D., and Trifunovic, A. (2009). The mtDNA mutator mouse: Dissecting mitochondrial

involvement in aging. Aging (Albany. NY). *1*, 1028–1032.

Efron, B., and Tibshirani, R. (1993). An Introduction to the Bootstrap (New York, NY: Chapman and Hall).

Egilmez, N.K., and Jazwinski, S.M. (1989). Evidence for the involvement of a cytoplasmic factor in the aging of the yeast Saccharomyces cerevisiae. J. Bacteriol. *171*, 37–42.

Eldakak, A., Rancati, G., Rubinstein, B., Paul, P., and V (2010). Asymmetrically inherited multidrug resistance transporters are recessive determinants in cellular replicative ageing. Nat. Cell *12*, 798–805.

Erjavec, N., Larsson, L., Grantham, J., and Nyström, T. (2007). Accelerated aging and failure to segregate damaged proteins in Sir2 mutants can be suppressed by overproducing the protein aggregation-remodeling factor Hsp104p. Genes Dev. *21*, 2410–2421.

Erjavec, N., Bayot, A., Gareil, M., Camougrand, N., Nystrom, T., Friguet, B., and Bulteau, A.-L. (2012). Deletion of the mitochondrial Pim1/Lon protease in yeast results in accelerated aging and impairment of the proteasome. Free Radic. Biol. Med.

Escusa-Toret, S., Vonk, W.I.M., and Frydman, J. (2013). Spatial sequestration of misfolded proteins by a dynamic chaperone pathway enhances cellular fitness during stress. Nat. Cell Biol. *15*, 1231–1243.

Fabrizio, P., and Longo, V.D. (2007). The chronological life span of Saccharomyces cerevisiae. Methods Mol. Biol. *371*, 89–95.

Faca, V., Coram, M., Phanstiel, D., Glukhova, V., Zhang, Q., Fitzgibbon, M., McIntosh, M., and Hanash, S. (2006). Quantitative analysis of acrylamide labeled serum proteins by LC-MS/MS. J. Proteome Res. *5*, 2009–2018.

Falcón, A. a, and Aris, J.P. (2003). Plasmid accumulation reduces life span in Saccharomyces cerevisiae. J. Biol. Chem. *278*, 41607–41617.

Faty, M., Fink, M., and Barral, Y. (2002). Septins: a ring to part mother and daughter. Curr. Genet. *41*, 123–131.

Fehrmann, S., Paoletti, C., Goulev, Y., Ungureanu, A., Aguilaniu, H., and Charvin, G. (2013). Aging Yeast Cells Undergo a Sharp Entry into Senescence Unrelated to the Loss of Mitochondrial

Membrane Potential. Cell Rep. *5*, 1589–1599.

Finch, C., and Kirkwood, T.B.L. (2000). Chance, Development and Aging (New York, NY: University of Oxford Press).

Finch, C.E., and Ruvkun, G. (2001). The genetics of aging. Annu. Rev. Genomics Hum. Genet. *2*, 435–462.

Finkel, T., Deng, C.-X., and Mostoslavsky, R. (2009). Recent progress in the biology and physiology of sirtuins. Nature *460*, 587–591.

Fröhlich, F., Moreira, K., Aguilar, P.S., Hubner, N.C., Mann, M., Walter, P., and Walther, T.C. (2009). A genome-wide screen for genes affecting eisosomes reveals Nce102 function in sphingolipid signaling. J. Cell Biol. *185*, 1227–1242.

Garinis, G.A., van der Horst, G.T.J., Vijg, J., and Hoeijmakers, J.H.J. (2008). DNA damage and ageing: new-age ideas for an age-old problem. Nat. Cell Biol. *10*, 1241–1247.

Gehlen, L.R., Nagai, S., Shimada, K., Meister, P., Taddei, A., and Gasser, S.M. (2011). Nuclear geometry and rapid mitosis ensure asymmetric episome segregation in yeast. Curr. Biol. *21*, 25–33.

Gershon, H., and Gershon, D. (2001). Critical assessment of paradigms in aging research. Exp. Gerontol. *36*, 1035–1047.

Gershon, H., and Gershon, D. (2002). Caenorhabditis elegans--a paradigm for aging research: advantages and limitations. Mech. Ageing Dev. *123*, 261–274.

Ghaemmaghami, S., Huh, W.-K., Bower, K., Howson, R.W., Belle, A., Dephoure, N., O'Shea, E.K., and Weissman, J.S. (2003). Global analysis of protein expression in yeast. Nature *425*, 737–741.

Giaever, G., Chu, A.M., Ni, L., Connelly, C., Riles, L., Véronneau, S., Dow, S., Lucau-Danila, A., Anderson, K., André, B., et al. (2002). Functional profiling of the Saccharomyces cerevisiae genome. Nature *418*, 387–391.

Giannakou, M.E., Goss, M., Jacobson, J., Vinti, G., Leevers, S.J., and Partridge, L. (2007). Dynamics of the action of dFOXO on adult mortality in Drosophila. Aging Cell *6*, 429–438.

Gibson, D.G., Young, L., Chuang, R.-Y., Venter, J.C., Hutchison, C.A., and Smith, H.O. (2009). Enzymatic assembly of DNA molecules up to several hundred kilobases. Nat. Methods *6*, 343–345.

de Godoy, L.M.F., Olsen, J. V, de Souza, G.A., Li, G., Mortensen, P., and Mann, M. (2006). Status of complete proteome analysis by mass spectrometry: SILAC labeled yeast as a model system. Genome Biol. *7*, R50.

de Godoy, L.M.F., Olsen, J. V., Cox, J., Nielsen, M.L., Hubner, N.C., Fröhlich, F., Walther, T.C., and Mann, M. (2008). Comprehensive mass-spectrometry-based proteome quantification of haploid versus diploid yeast. Nature *455*, 1251–1254.

Goldberg, A.L. (2003). Protein degradation and protection against misfolded or damaged proteins. Nature *426*, 895–899.

Grandison, R.C., Piper, M.D.W., and Partridge, L. (2009). Amino-acid imbalance explains extension of lifespan by dietary restriction in Drosophila. Nature *462*, 1061–1064.

Greenberg, M.L., and Axelrod, D. (1993). Anomalously slow mobility of fluorescent lipid probes in the plasma membrane of the yeast Saccharomyces cerevisiae. J. Membr. Biol. *131*, 115–127.

Greenspan, P., Mayer, E.P., and Fowler, S.D. (1985). Nile red: a selective fluorescent stain for intracellular lipid droplets. J. Cell Biol. *100*, 965–973.

Grossmann, G., Malinsky, J., Stahlschmidt, W., Loibl, M., Weig-Meckl, I., Frommer, W.B., Opekarová, M., and Tanner, W. (2008). Plasma membrane microdomains regulate turnover of transport proteins in yeast. J. Cell Biol. *183*, 1075–1088.

Gruhler, A., Olsen, J. V, Mohammed, S., Mortensen, P., Faergeman, N.J., Mann, M., and Jensen, O.N. (2005). Quantitative phosphoproteomics applied to the yeast pheromone signaling pathway. Mol. Cell. Proteomics *4*, 310–327.

Guarente, L., and Kenyon, C. (2000). Genetic pathways that regulate ageing in model organisms. Nature *408*, 255–262.

Hahn-Hägerdal, B., Karhumaa, K., Larsson, C.U., Gorwa-Grauslund, M., Görgens, J., and van Zyl, W.H. (2005). Role of cultivation media in the development of yeast strains for large scale industrial use. Microb. Cell Fact. *4*, 31.

Halestrap, A.P. (1975). The mitochondrial pyruvate carrier. Kinetics and specificity for substrates and inhibitors. Biochem. J. *148*, 85–96.

Hamilton, W.D. (1966). The moulding of senescence by natural selection. J. Theor. Biol. *12*, 12–45.

Hamilton, B., Dong, Y., Shindo, M., Liu, W., Odell, I., Ruvkun, G., and Lee, S.S. (2005). A systematic RNAi screen for longevity genes in C. elegans. Genes Dev. *19*, 1544–1555.

Hansen, M., Taubert, S., Crawford, D., Libina, N., Lee, S.-J., and Kenyon, C. (2007). Lifespan extension by conditions that inhibit translation in Caenorhabditis elegans. Aging Cell *6*, 95–110.

Hansen, M., Chandra, A., Mitic, L.L., Onken, B., Driscoll, M., and Kenyon, C. (2008). A role for autophagy in the extension of lifespan by dietary restriction in C. elegans. PLoS Genet. *4*, e24.

Harman, D. (1991). The aging process: major risk factor for disease and death. Proc. Natl. Acad. Sci. U. S. A. *88*, 5360–5363.

Hartl, F.-U., Pfanner, N., Nicholson, D.W., and Neupert, W. (1989). Mitochondrial protein import. Biochim. Biophys. Acta (BBA)-Reviews Biomembr. *988*, 1–45.

Hartwell, L. (1971). Genetic control of the cell division cycle in yeast *1IV. Genes controlling bud emergence and cytokinesis. Exp. Cell Res. *69*, 265–276.

Haslbeck, M., Miess, A., Stromer, T., Walter, S., and Buchner, J. (2005). Disassembling protein aggregates in the yeast cytosol. The cooperation of Hsp26 with Ssa1 and Hsp104. J. Biol. Chem. *280*, 23861–23868.

Hay, N., and Sonenberg, N. (2004). Upstream and downstream of mTOR. Genes Dev. *18*, 1926–1945.

Haynes, C.M., and Ron, D. (2010). The mitochondrial UPR - protecting organelle protein homeostasis. J. Cell Sci. *123*, 3849–3855.

Henderson, K. a, and Gottschling, D.E. (2008). A mother's sacrifice: what is she keeping for herself? Curr. Opin. Cell Biol. *20*, 723–728.

Henderson, K. a, Hughes, A.L., and Gottschling, D.E. (2014). Mother-daughter asymmetry of pH underlies aging and rejuvenation in yeast. Elife *3*, e03504.

Henderson, S.T., Bonafè, M., and Johnson, T.E. (2006). daf-16 protects the nematode Caenorhabditis elegans during food deprivation. J. Gerontol. A. Biol. Sci. Med. Sci. *61*, 444–460.

Heo, J.-M., Livnat-Levanon, N., Taylor, E.B., Jones, K.T., Dephoure, N., Ring, J., Xie, J., Brodsky, J.L., Madeo, F., Gygi, S.P., et al. (2010). A stress-responsive system for mitochondrial protein degradation. Mol. Cell *40*, 465–480.

Herskowitz, I. (1987). Functional inactivation of genes by dominant negative mutations. Nature *329*, 219–222.

Herzig, S., Raemy, E., Montessuit, S., Veuthey, J.-L., Zamboni, N., Westermann, B., Kunji, E.R.S., and Martinou, J.-C. (2012). Identification and functional expression of the mitochondrial pyruvate carrier. Science *337*, 93–96.

Hjortmo, S., Patring, J., and Andlid, T. (2008). Growth rate and medium composition strongly affect folate content in Saccharomyces cerevisiae. Int. J. Food Microbiol. *123*, 93–100.

Ho, C.H., Magtanong, L., Barker, S.L., Gresham, D., Nishimura, S., Natarajan, P., Koh, J.L.Y., Porter, J., Gray, C. a, Andersen, R.J., et al. (2009). A molecular barcoded yeast ORF library enables mode-of-action analysis of bioactive compounds. Nat. Biotechnol. *27*, 369–377.

Horwitz, J. (1992). Alpha-crystallin can function as a molecular chaperone. Proc. Natl. Acad. Sci. U. S. A. *89*, 10449–10453.

Houthoofd, K., Braeckman, B.P., Lenaerts, I., Brys, K., De Vreese, A., Van Eygen, S., and Vanfleteren, J.R. (2002a). Axenic growth up-regulates mass-specific metabolic rate, stress resistance, and extends life span in Caenorhabditis elegans. Exp. Gerontol. *37*, 1371–1378.

Houthoofd, K., Braeckman, B.P., Lenaerts, I., Brys, K., De Vreese, A., Van Eygen, S., and Vanfleteren, J.R. (2002b). No reduction of metabolic rate in food restricted Caenorhabditis elegans. Exp. Gerontol. *37*, 1359–1369.

Huberts, D.H.E.W., Sik Lee, S., Gonzáles, J., Janssens, G.E., Vizcarra, I.A., and Heinemann, M. (2013). Construction and use of a microfluidic dissection platform for long-term imaging of cellular processes in budding yeast. Nat. Protoc. *8*, 1019–1027.

Huberts, D.H.E.W., González, J., Lee, S.S., Litsios, A., Hubmann, G., Wit, E.C., and Heinemann, M. (2014). Calorie restriction does not elicit a robust extension of replicative lifespan in

Saccharomyces cerevisiae. Proc. Natl. Acad. Sci. U. S. A. *111*, 11727–11731.

Hughes, A.L., and Gottschling, D.E. (2012). An early age increase in vacuolar pH limits mitochondrial function and lifespan in yeast. Nature *492*, 261–265.

Huh, W.-K., Falvo, J. V, Gerke, L.C., Carroll, A.S., Howson, R.W., Weissman, J.S., and O'Shea, E.K. (2003). Global analysis of protein localization in budding yeast. Nature *425*, 686–691.

Janssens, G.E., Meinema, A.C., González, J., Wolters, J.C., Schmidt, A., Guryev, V., Bischoff, R., Wit, E.C., Veenhoff, L.M., and Heinemann, M. (2015). Protein biogenesis machinery is a driver of replicative aging in yeast. Elife *4*.

Jarolim, S., Millen, J., Heeren, G., Laun, P., Goldfarb, D.S., and Breitenbach, M. (2004). A novel assay for replicative lifespan in Saccharomyces cerevisiae. FEMS Yeast Res. *5*, 169–177.

Jiang, J.C., Jaruga, E., Repnevskaya, M. V, and Jazwinski, S.M. (2000). An intervention resembling caloric restriction prolongs life span and retards aging in yeast. FASEB J. *14*, 2135–2137.

Jo, M.C., Liu, W., Gu, L., Dang, W., and Qin, L. (2015). High-throughput analysis of yeast replicative aging using a microfluidic system. Proc. Natl. Acad. Sci. U. S. A. *112*, 9364–9369.

Johnson, T.E. (1990). Increased life-span of age-1 mutants in Caenorhabditis elegans and lower Gompertz rate of aging. Science *249*, 908–912.

Jones, D.L., and Rando, T.A. (2011). Emerging models and paradigms for stem cell ageing. Nat. Cell Biol. *13*, 506–512.

Kaeberlein, M. (2010). Lessons on longevity from budding yeast. Nature *464*, 513–519.

Kaeberlein, M., and Kennedy, B.K. (2005). Large-scale identification in yeast of conserved ageing genes. Mech. Ageing Dev. *126*, 17–21.

Kaeberlein, M., McVey, M., and Guarente, L. (1999). The SIR2/3/4 complex and SIR2 alone promote longevity in Saccharomyces cerevisiae by two different mechanisms. Genes Dev. *13*, 2570–2580.

Kaeberlein, M., Andalis, A.A., Fink, G.R., and Guarente, L. (2002). High osmolarity extends life span in Saccharomyces cerevisiae by a mechanism related to calorie restriction. Mol. Cell. Biol.

22, 8056–8066.

Kaeberlein, M., Kirkland, K.T., Fields, S., and Kennedy, B.K. (2004). Sir2-independent life span extension by calorie restriction in yeast. PLoS Biol. *2*, E296.

Kaeberlein, M., Powers, R.W., Steffen, K.K., Westman, E. a, Hu, D., Dang, N., Kerr, E.O., Kirkland, K.T., Fields, S., and Kennedy, B.K. (2005a). Regulation of yeast replicative life span by TOR and Sch9 in response to nutrients. Science *310*, 1193–1196.

Kaeberlein, M., Kirkland, K.T., Fields, S., and Kennedy, B.K. (2005b). Genes determining yeast replicative life span in a long-lived genetic background.

Kaeberlein, M., Burtner, C.R., and Kennedy, B.K. (2007). Recent developments in yeast aging. PLoS Genet. *3*, e84.

Kaganovich, D., Kopito, R., and Frydman, J. (2008). Misfolded proteins partition between two distinct quality control compartments. Nature *454*, 1088–1095.

Kane, P.M., and Smardon, A.M. (2003). Assembly and regulation of the yeast vacuolar H+-ATPase. J. Bioenerg. Biomembr. *35*, 313–321.

Kanfi, Y., Naiman, S., Amir, G., Peshti, V., Zinman, G., Nahum, L., Bar-Joseph, Z., and Cohen, H.Y. (2012). The sirtuin SIRT6 regulates lifespan in male mice. Nature *05*, 3–6.

Kapahi, P., Zid, B.M., Harper, T., Koslover, D., Sapin, V., and Benzer, S. (2004). Regulation of Lifespan in Drosophila by Modulation of Genes in the TOR Signaling Pathway. Current *14*, 885–890.

Karotki, L., Huiskonen, J.T., Stefan, C.J., Ziółkowska, N.E., Roth, R., Surma, M.A., Krogan, N.J., Emr, S.D., Heuser, J., Grünewald, K., et al. (2011). Eisosome proteins assemble into a membrane scaffold. J. Cell Biol. *195*, 889–902.

Keller, A., Nesvizhskii, A.I., Kolker, E., and Aebersold, R. (2002). Empirical statistical model to estimate the accuracy of peptide identifications made by MS/MS and database search. Anal. Chem. *74*, 5383–5392.

Kennedy, B.K. (2008). The genetics of ageing: insight from genome-wide approaches in invertebrate model organisms. J. Intern. Med. *263*, 142–152.

Kennedy, B.K., Austriaco, N.R., and Guarente, L. (1994). Daughter cells of Saccharomyces cerevisiae from old mothers display a reduced life span. J. Cell Biol. *127*, 1985–1993.

Kennedy, B.K., Austriaco, N.R., Zhang, J., and Guarente, L. (1995). Mutation in the silencing gene SIR4 can delay aging in S. cerevisiae. Cell *80*, 485–496.

Kennedy, B.K., Gotta, M., Sinclair, D. a, Mills, K., McNabb, D.S., Murthy, M., Pak, S.M., Laroche, T., Gasser, S.M., and Guarente, L. (1997). Redistribution of silencing proteins from telomeres to the nucleolus is associated with extension of life span in S. cerevisiae. Cell *89*, 381–391.

Kennedy, B.K., Steffen, K.K., and Kaeberlein, M. (2007). Ruminations on dietary restriction and aging. Cell. Mol. Life Sci. *64*, 1323–1328.

Khmelinskii, A., Keller, P.J., Lorenz, H., Schiebel, E., and Knop, M. (2010). Segregation of yeast nuclear pores. Nature *466*, E1.

Khmelinskii, A., Keller, P.J., Bartosik, A., Meurer, M., Barry, J.D., Mardin, B.R., Kaufmann, A., Trautmann, S., Wachsmuth, M., Pereira, G., et al. (2012). Tandem fluorescent protein timers for in vivo analysis of protein dynamics. Nat. Biotechnol. *30*, 708–714.

Kikis, E.A., Gidalevitz, T., and Morimoto, R.I. (2010). Protein homeostasis in models of aging and age-related conformational disease. Adv. Exp. Med. Biol. *694*, 138–159.

Kim, Y.E., Hipp, M.S., Bracher, A., Hayer-Hartl, M., and Hartl, F.U. (2013). Molecular chaperone functions in protein folding and proteostasis. Annu. Rev. Biochem. *82*, 323–355.

Kimura, K.D. (1997). daf-2, an Insulin Receptor-Like Gene That Regulates Longevity and Diapause in Caenorhabditis elegans. Science (80-.). *277*, 942–946.

Kirkwood, T.B.L. (2002). Evolution of ageing. Mech. Ageing Dev. *123*, 737–745.

Kirkwood, T.B.L. (2008). A systematic look at an old problem. Nature *451*, 644–647.

Kirkwood, T.B.L., and Melov, S. (2011). On the Programmed/Non-Programmed Nature of Ageing within the Life History. Curr. Biol. *21*, R701–R707.

Klebl, F., and Tanner, W. (1989). Molecular cloning of a cell wall exo-beta-1,3-glucanase from Saccharomyces cerevisiae. J. Bacteriol. *171*, 6259–6264.

Kruegel, U., Robison, B., Dange, T., Kahlert, G., Delaney, J.R., Kotireddy, S., Tsuchiya, M., Tsuchiyama, S., Murakami, C.J., Schleit, J., et al. (2011). Elevated Proteasome Capacity Extends Replicative Lifespan in Saccharomyces cerevisiae. PLoS Genet. *7*, e1002253.

Kurtz, A., and Oh, S.-J. (2012). Age related changes of the extracellular matrix and stem cell maintenance. Prev. Med. (Baltim). *54 Suppl*, S50–S56.

Kushnirov, V. V (2000). Rapid and reliable protein extraction from yeast. Yeast *16*, 857–860.

Kysela, D.T., Brown, P.J.B., Huang, K.C., and Brun, Y. V (2013). Biological consequences and advantages of asymmetric bacterial growth. Annu. Rev. Microbiol. *67*, 417–435.

Laabs, T.L., Markwardt, D.D., Slattery, M.G., Newcomb, L.L., Stillman, D.J., and Heideman, W. (2003). ACE2 is required for daughter cell-specific G1 delay in Saccharomyces cerevisiae. Proc. Natl. Acad. Sci. U. S. A. *100*, 10275–10280.

Lakowski, B., and Hekimi, S. (1998). The genetics of caloric restriction in Caenorhabditis elegans. Proc. Natl. Acad. Sci. U. S. A. *95*, 13091–13096.

Lam, Y.T., Aung-Htut, M.T., Lim, Y.L., Yang, H., and Dawes, I.W. (2011). Changes in reactive oxygen species begin early during replicative aging of Saccharomyces cerevisiae cells. Free Radic. Biol. Med. *50*, 963–970.

Laun, P., Pichova, A., Madeo, F., Fuchs, J., Ellinger, A., Kohlwein, S., Dawes, I., Fröhlich, K.U., and Breitenbach, M. (2001). Aged mother cells of Saccharomyces cerevisiae show markers of oxidative stress and apoptosis. Mol. Microbiol. *39*, 1166–1173.

Laun, P., Bruschi, C. V, Dickinson, J.R., Rinnerthaler, M., Heeren, G., Schwimbersky, R., Rid, R., and Breitenbach, M. (2007). Yeast mother cell-specific ageing, genetic (in)stability, and the somatic mutation theory of ageing. Nucleic Acids Res. *35*, 7514–7526.

Lee, S., Lim, W.A., and Thorn, K.S. (2013). Improved Blue, Green, and Red Fluorescent Protein Tagging Vectors for S. cerevisiae. PLoS One *8*, e67902.

Lee, S.S., Vizcarra, I.A., Huberts, D.H.E.W., Lee, L.P., and Heinemann, M. (2012). Whole lifespan microscopic observation of budding yeast aging through a microfluidic dissection platform. Proc. Natl. Acad. Sci. U. S. A. 4–8.

van Leeuwen, F., and Gottschling, D.E. (2002). Assays for gene silencing in yeast. Methods

Enzymol. *350*, 165–186.

Li, R. (2013). The Art of Choreographing Asymmetric Cell Division. Dev. Cell *25*, 439–450.

Li, S.C., and Kane, P.M. (2009). The yeast lysosome-like vacuole: endpoint and crossroads. Biochim. Biophys. Acta *1793*, 650–663.

Libert, S., Zwiener, J., Chu, X., Vanvoorhies, W., Roman, G., and Pletcher, S.D. (2007). Regulation of Drosophila life span by olfaction and food-derived odors. Science *315*, 1133–1137.

Licklider, L.J., Thoreen, C.C., Peng, J., and Gygi, S.P. (2002). Automation of nanoscale microcapillary liquid chromatography-tandem mass spectrometry with a vented column. Anal. Chem. *74*, 3076–3083.

Lin, S., Kaeberlein, M., Andalis, A.A., Sturtz, L.A., Defossez, P.-A., Culotta, V.C., Fink, G.R., and Guarente, L. (2002). Calorie restriction extends Saccharomyces cerevisiae lifespan by increasing respiration. Nature *418*, 344–348.

Lin, S.J., Defossez, P.A., and Guarente, L. (2000). Requirement of NAD and SIR2 for life-span extension by calorie restriction in Saccharomyces cerevisiae. Science *289*, 2126–2128.

Lin, S.S., Manchester, J.K., and Gordon, J.I. (2001). Enhanced gluconeogenesis and increased energy storage as hallmarks of aging in Saccharomyces cerevisiae. J. Biol. Chem. *276*, 36000–36007.

Lindstrom, D.L., and Gottschling, D.E. (2009). The mother enrichment program: a genetic system for facile replicative life span analysis in Saccharomyces cerevisiae. Genetics *183*, 413–422, 1SI – 13SI.

Liu, H.P., and Bretscher, A. (1989). Disruption of the single tropomyosin gene in yeast results in the disappearance of actin cables from the cytoskeleton. Cell *57*, 233–242.

Liu, B., Larsson, L., Caballero, A., Hao, X., Oling, D., Grantham, J., and Nyström, T. (2010). The polarisome is required for segregation and retrograde transport of protein aggregates. Cell *140*, 257–267.

Liu, B., Larsson, L., Franssens, V., Hao, X., Hill, S.M., Andersson, V., Höglund, D., Song, J., Yang, X., Öling, D., et al. (2011). Segregation of protein aggregates involves actin and the polarity machinery. Cell *147*, 959–961.

Liu, P., Young, T.Z., and Acar, M. (2015). Yeast Replicator: A High-Throughput Multiplexed Microfluidics Platform for Automated Measurements of Single-Cell Aging. Cell Rep. *13*, 634–644.

Lynnerup, N., Kjeldsen, H., Heegaard, S., Jacobsen, C., and Heinemeier, J. (2008). Radiocarbon dating of the human eye lens crystallines reveal proteins without carbon turnover throughout life. PLoS One *3*, e1529.

Macara, I.G., and Mili, S. (2008). Polarity and Differential Inheritance—Universal Attributes of Life? Cell *135*, 801–812.

MacGurn, J.A., Hsu, P.-C., and Emr, S.D. (2012). Ubiquitin and Membrane Protein Turnover: From Cradle to Grave. Annu. Rev. Biochem. *81*, 231–259.

MacLean, B., Eng, J.K., Beavis, R.C., and McIntosh, M. (2006). General framework for developing and evaluating database scoring algorithms using the TANDEM search engine. Bioinformatics *22*, 2830–2832.

Mair, W., Goymer, P., Pletcher, S.D., and Partridge, L. (2003). Demography of dietary restriction and death in Drosophila. Science *301*, 1731–1733.

Manivannan, S., Scheckhuber, C.Q., Veenhuis, M., and van der Klei, I.J. (2012). The impact of peroxisomes on cellular aging and death. Front. Oncol. *2*, 50.

Martins-de-Souza, D. (2014). Shotgun Proteomics (New York, NY: Springer New York).

McCay, C.M., Crowell, M.F., and Maynard, L.A. (1935). The effect of retarded growth upon the length of life span and upon the ultimate body size. Nutr. Burbank Los Angeles Cty. Calif *5*, 155–171; discussion 172.

McCormick, M.A., Delaney, J.R., Tsuchiya, M., Tsuchiyama, S., Shemorry, A., Sim, S., Chou, A.C.-Z., Ahmed, U., Carr, D., Murakami, C.J., et al. (2015). A Comprehensive Analysis of Replicative Lifespan in 4,698 Single-Gene Deletion Strains Uncovers Conserved Mechanisms of Aging. Cell Metab. *22*, 895–906.

McFaline-Figueroa, J.R., Vevea, J., Swayne, T.C., Zhou, C., Liu, C., Leung, G., Boldogh, I.R., and Pon, L. a (2011). Mitochondrial quality control during inheritance is associated with lifespan and mother-daughter age asymmetry in budding yeast. Aging Cell 885–895.

Medvedev, Z.A. (1990). An attempt at a rational classification of theories of ageing. Biol. Rev. Camb. Philos. Soc. *65*, 375–398.

Mei, S.-C., and Brenner, C. (2015). Calorie restriction-mediated replicative lifespan extension in yeast is non-cell autonomous. PLoS Biol. *13*, e1002048.

Meissner, B., Boll, M., Daniel, H., and Baumeister, R. (2004). Deletion of the intestinal peptide transporter affects insulin and TOR signaling in Caenorhabditis elegans. J. Biol. Chem. *279*, 36739–36745.

Meitinger, F., Khmelinskii, A., Morlot, S., Kurtulmus, B., Palani, S., Andres-Pons, A., Hub, B., Knop, M., Charvin, G., and Pereira, G. (2014). A memory system of negative polarity cues prevents replicative aging. Cell *159*, 1056–1069.

Menendez-Benito, V., van Deventer, S.J., Jimenez-Garcia, V., Roy-Luzarraga, M., van Leeuwen, F., and Neefjes, J. (2013). Spatiotemporal analysis of organelle and macromolecular complex inheritance. Proc. Natl. Acad. Sci. U. S. A. *110*, 175–180.

Merzendorfer, H., and Heinisch, J.J. (2013). Microcompartments within the yeast plasma membrane. Biol. Chem. *394*.

Miller, R. a, Buehner, G., Chang, Y., Harper, J.M., Sigler, R., and Smith-Wheelock, M. (2005). Methionine-deficient diet extends mouse lifespan, slows immune and lens aging, alters glucose, T4, IGF-I and insulin levels, and increases hepatocyte MIF levels and stress resistance. Aging Cell *4*, 119–125.

Mnaimneh, S., Davierwala, A.P., Haynes, J., Moffat, J., Peng, W.-T., Zhang, W., Yang, X., Pootoolal, J., Chua, G., Lopez, A., et al. (2004). Exploration of essential gene functions via titratable promoter alleles. Cell *118*, 31–44.

Molin, M., Yang, J., Hanzén, S., Toledano, M.B., Labarre, J., and Nyström, T. (2011). Life Span Extension and H(2)O(2) Resistance Elicited by Caloric Restriction Require the Peroxiredoxin Tsa1 in Saccharomyces cerevisiae. Mol. Cell *43*, 823–833.

Montecino-Rodriguez, E., Berent-Maoz, B., and Dorshkind, K. (2013). Causes, consequences, and reversal of immune system aging. J. Clin. Invest. *123*, 958–965.

Moreira, K.E., Schuck, S., Schrul, B., Fröhlich, F., Moseley, J.B., Walther, T.C., and Walter, P.

(2012). Seg1 controls eisosome assembly and shape. J. Cell Biol. *198*, 405–420.

Morris, J.Z., Tissenbaum, H.A., and Ruvkun, G. (1996). A phosphatidylinositol-3-OH kinase family member regulating longevity and diapause in Caenorhabditis elegans. Nature *382*, 536–539.

Mortimer, R.K., and Johnston, J.R. (1959). Life Span of Individual Yeast Cells. Nature *183*, 1751–1752.

Müller, I. (1985). Parental age and the life-span of zygotes of Saccharomyces cerevisiae. Antonie Van Leeuwenhoek *51*, 1–10.

Nahnsen, S., Bielow, C., Reinert, K., and Kohlbacher, O. (2013). Tools for label-free peptide quantification. Mol. Cell. Proteomics *12*, 549–556.

Narayanaswamy, R., Levy, M., Tsechansky, M., Stovall, G.M., O'Connell, J.D., Mirrielees, J., Ellington, A.D., and Marcotte, E.M. (2009). Widespread reorganization of metabolic enzymes into reversible assemblies upon nutrient starvation. Proc. Natl. Acad. Sci. U. S. A. *106*, 10147–10152.

Nishimura, K., Fukagawa, T., Takisawa, H., Kakimoto, T., and Kanemaki, M. (2009). An auxin-based degron system for the rapid depletion of proteins in nonplant cells. Nat. Methods *6*, 917–922.

Noree, C., Sato, B.K., Broyer, R.M., and Wilhelm, J.E. (2010). Identification of novel filament-forming proteins in Saccharomyces cerevisiae and Drosophila melanogaster. J. Cell Biol. *190*, 541–551.

North, B.J., and Verdin, E. (2004). Sirtuins: Sir2-related NAD-dependent protein deacetylases. Genome Biol. *5*, 224.

Nyström, T., and Liu, B. (2014). The mystery of aging and rejuvenation—a budding topic. Curr. Opin. Microbiol. *18*, 61–67.

O'Connell, J.D., Zhao, A., Ellington, A.D., and Marcotte, E.M. (2012). Dynamic reorganization of metabolic enzymes into intracellular bodies. Annu. Rev. Cell Dev. Biol. *28*, 89–111.

Ogg, S., Paradis, S., Gottlieb, S., Patterson, G.I., Lee, L., Tissenbaum, H. a, and Ruvkun, G. (1997). The Fork head transcription factor DAF-16 transduces insulin-like metabolic and longevity signals in C. elegans. Nature *389*, 994–999.

Oldham, S., and Hafen, E. (2003). Insulin/IGF and target of rapamycin signaling: a TOR de force in growth control. Trends Cell Biol. *13*, 79–85.

Orlean, P. (2012). Architecture and biosynthesis of the Saccharomyces cerevisiae cell wall. Genetics *192*, 775–818.

Ortells, M.C., and Keyes, W.M. (2014). New insights into skin stem cell aging and cancer. Biochem. Soc. Trans. *42*, 663–669.

Pacifici, R.E., and Davies, K.J. (1991). Protein, lipid and DNA repair systems in oxidative stress: the free-radical theory of aging revisited. Gerontology *37*, 166–180.

Partridge, L. (2010). The new biology of ageing. Philos. Trans. R. Soc. Lond. B. Biol. Sci. *365*, 147–154.

Partridge, L., Alic, N., Bjedov, I., and Piper, M.D.W. (2011). Ageing in Drosophila: the role of the insulin/Igf and TOR signalling network. Exp. Gerontol. *46*, 376–381.

Pereira, G., and Schiebel, E. (2005). Kin4 kinase delays mitotic exit in response to spindle alignment defects. Mol. Cell *19*, 209–221.

Pletcher, S.D., Macdonald, S.J., Marguerie, R., Certa, U., Stearns, S.C., Goldstein, D.B., and Partridge, L. (2002). Genome-wide transcript profiles in aging and calorically restricted Drosophila melanogaster. Curr. Biol. *12*, 712–723.

Poole, A.C., Thomas, R.E., Andrews, L.A., McBride, H.M., Whitworth, A.J., and Pallanck, L.J. (2008). The PINK1/Parkin pathway regulates mitochondrial morphology. Proc. Natl. Acad. Sci. U. S. A. *105*, 1638–1643.

Prelich, G. (2012). Gene overexpression: uses, mechanisms, and interpretation. Genetics *190*, 841–854.

Pringle, J.R., Preston, R.A., Adams, A.E.M., Stearns, T., Drubin, D.G., Haarer, B.K., and Jones, E.W. (1989). Fluorescence microscopy methods for yeast. Methods Cell Biol *31*, 357–435.

Pronk, J.T.J.J.T., Yde Steensma, H., Van Dijken, J.P., Steensma, H.Y.H.H.Y., and Dijken, J. Van (1996). Pyruvate Metabolism in Saccharomyces cerevisiae. Yeast *12*, 1607–1633.

Rath, A., Glibowicka, M., Nadeau, V.G., Chen, G., and Deber, C.M. (2009). Detergent binding

explains anomalous SDS-PAGE migration of membrane proteins. Proc. Natl. Acad. Sci. U. S. A. *106*, 1760–1765.

Richie, J.P., Komninou, D., Leutzinger, Y., Kleinman, W., Orentreich, N., Malloy, V., and Zimmerman, J. a (2004). Tissue glutathione and cysteine levels in methionine-restricted rats. Nutrition *20*, 800–805.

Riesen, M., and Morgan, A. (2009). Calorie restriction reduces rDNA recombination independently of rDNA silencing. Aging Cell *8*, 624–632.

Rikans, L.E., and Hornbrook, K.R. (1997). Lipid peroxidation, antioxidant protection and aging. Biochim. Biophys. Acta *1362*, 116–127.

Rogina, B., and Helfand, S.L. (2004). Sir2 mediates longevity in the fly through a pathway related to calorie restriction. Proc. Natl. Acad. Sci. U. S. A. *101*, 15998–16003.

Rose, G., Dato, S., Altomare, K., Bellizzi, D., Garasto, S., Greco, V., Passarino, G., Feraco, E., Mari, V., Barbi, C., et al. (2003). Variability of the SIRT3 gene, human silent information regulator Sir2 homologue, and survivorship in the elderly. Exp. Gerontol. *38*, 1065–1070.

Ross, C.A., and Poirier, M.A. (2004). Protein aggregation and neurodegenerative disease. Nat. Med. *10 Suppl*, S10–S17.

Russnak, R., Konczal, D., and McIntire, S.L. (2001). A family of yeast proteins mediating bidirectional vacuolar amino acid transport. J. Biol. Chem. *276*, 23849–23857.

Sacksteder, K.A., and Gould, S.J. (2000). The genetics of peroxisome biogenesis. Annu. Rev. Genet. *34*, 623–652.

Salvioli, S., Ardizzoni, A., Franceschi, C., and Cossarizza, A. (1997). JC-1, but not DiOC6(3) or rhodamine 123, is a reliable fluorescent probe to assess delta psi changes in intact cells: implications for studies on mitochondrial functionality during apoptosis. FEBS Lett. *411*, 77–82.

Savas, J.N., Toyama, B.H., Xu, T., Yates, J.R., and Hetzer, M.W. (2012). Extremely Long-Lived Nuclear Pore Proteins in the Rat Brain. Science (80-.). 1–3.

Schaffitzel, E., and Hertweck, M. (2006). Recent aging research in Caenorhabditis elegans. Exp. Gerontol. *41*, 557–563.

Scheckhuber, C.Q., Erjavec, N., Tinazli, a, Hamann, a, Nyström, T., and Osiewacz, H.D. (2007). Reducing mitochondrial fission results in increased life span and fitness of two fungal ageing models. Nat. Cell Biol. *9*, 99–105.

Scheckhuber, C.Q., Wanger, R.A., Mignat, C.A., and Osiewacz, H.D. (2011). Unopposed mitochondrial fission leads to severe lifespan shortening.

Schindelin, J., Arganda-Carreras, I., Frise, E., Kaynig, V., Longair, M., Pietzsch, T., Preibisch, S., Rueden, C., Saalfeld, S., Schmid, B., et al. (2012). Fiji: an open-source platform for biological-image analysis. Nat. Methods *9*, 676–682.

Schlüter, A., Real-Chicharro, A., Gabaldón, T., Sánchez-Jiménez, F., and Pujol, A. (2010). PeroxisomeDB 2.0: an integrative view of the global peroxisomal metabolome. Nucleic Acids Res. *38*, D800–D805.

Schöneich, C. (2006). Protein modification in aging: an update. Exp. Gerontol. *41*, 807–812.

Schreiber, A., and Peter, M. (2014). Substrate recognition in selective autophagy and the ubiquitin-proteasome system. Biochim. Biophys. Acta *1843*, 163–181.

Schwikowski, B., Uetz, P., and Fields, S. (2000). A network of protein-protein interactions in yeast. Nat. Biotechnol. *18*, 1257–1261.

Selman, C., Lingard, S., Choudhury, A.I., Batterham, R.L., Claret, M., Clements, M., Ramadani, F., Okkenhaug, K., Schuster, E., Blanc, E., et al. (2008). Evidence for lifespan extension and delayed age-related biomarkers in insulin receptor substrate 1 null mice. FASEB J. *22*, 807–818.

Seo, A.Y., Joseph, A.-M., Dutta, D., Hwang, J.C.Y., Aris, J.P., and Leeuwenburgh, C. (2010). New insights into the role of mitochondria in aging: mitochondrial dynamics and more. J. Cell Sci. *123*, 2533–2542.

Shaner, N.C., Lambert, G.G., Chammas, A., Ni, Y., Cranfill, P.J., Baird, M.A., Sell, B.R., Allen, J.R., Day, R.N., Israelsson, M., et al. (2013). A bright monomeric green fluorescent protein derived from Branchiostoma lanceolatum. Nat. Methods *10*, 407–409.

Shapiro, S.D., Endicott, S.K., Province, M.A., Pierce, J.A., and Campbell, E.J. (1991). Marked longevity of human lung parenchymal elastic fibers deduced from prevalence of D-aspartate and nuclear weapons-related radiocarbon. J. Clin. Invest. *87*, 1828–1834.

Shcheprova, Z., Baldi, S., Frei, S.B., Gonnet, G., and Barral, Y. (2008). A mechanism for asymmetric segregation of age during yeast budding. Nature *454*, 728–734.

Sheff, M.A., and Thorn, K.S. (2004). Optimized cassettes for fluorescent protein tagging in Saccharomyces cerevisiae. Yeast *21*, 661–670.

Shnyreva, M.G., Petrova, E.V., Egorov, S.N., and Hinnen, A. (1996). Biochemical properties and excretion behavior of repressible acid phosphatases with altered subunit composition. Microbiol. Res. *151*, 291–300.

Signer, R.A.J., and Morrison, S.J. (2013). Mechanisms that Regulate Stem Cell Aging and Life Span. Cell Stem Cell *12*, 152–165.

Sinclair, D. a, and Guarente, L. (1997). Extrachromosomal rDNA circles--a cause of aging in yeast. Cell *91*, 1033–1042.

Sinclair, D., Mills, K., and Guarente, L. (1998). Aging in Saccharomyces cerevisiae. Annu. Rev. Microbiol. *52*, 533–560.

Smeal, T., Claus, J., Kennedy, B., Cole, F., and Guarente, L. (1996). Loss of transcriptional silencing causes sterility in old mother cells of S. cerevisiae. Cell *84*, 633–642.

Smith, A.M., Heisler, L.E., Mellor, J., Kaper, F., Thompson, M.J., Chee, M., Roth, F.P., Giaever, G., and Nislow, C. (2009a). Quantitative phenotyping via deep barcode sequencing. Genome Res. *19*, 1836.

Smith, A.M., Heisler, L.E., St Onge, R.P., Farias-Hesson, E., Wallace, I.M., Bodeau, J., Harris, A.N., Perry, K.M., Giaever, G., Pourmand, N., et al. (2010). Highly-multiplexed barcode sequencing: an efficient method for parallel analysis of pooled samples. Nucleic Acids Res. *38*, e142.

Smith, D.L., Li, C., Matecic, M., Maqani, N., Bryk, M., and Smith, J.S. (2009b). Calorie restriction effects on silencing and recombination at the yeast rDNA. Aging Cell *8*, 633–642.

Smith, J.S., Brachmann, C.B., Pillus, L., and Boeke, J.D. (1998). Distribution of a limited Sir2 protein pool regulates the strength of yeast rDNA silencing and is modulated by Sir4p. Genetics *149*, 1205–1219.

Spokoini, R., Moldavski, O., Nahmias, Y., England, J.L., Schuldiner, M., and Kaganovich, D.

(2012). Confinement to Organelle-Associated Inclusion Structures Mediates Asymmetric Inheritance of Aggregated Protein in Budding Yeast. Cell Rep. *2*, 738–747.

Squier, T.C. (2001). Oxidative stress and protein aggregation during biological aging. Exp. Gerontol. *36*, 1539–1550.

Stefani, M., and Dobson, C.M. (2003). Protein aggregation and aggregate toxicity: new insights into protein folding, misfolding diseases and biological evolution. J. Mol. Med. (Berl). *81*, 678–699.

Steffen, K.K., Kennedy, B.K., and Kaeberlein, M. (2009). Measuring replicative life span in the budding yeast. J. Vis. Exp. e1209.

Steinkraus, K. a, Kaeberlein, M., and Kennedy, B.K. (2008). Replicative aging in yeast: the means to the end. Annu. Rev. Cell Dev. Biol. *24*, 29–54.

Stewart, C.C., and Steinkamp, J.A. (1982). Quantitation of cell concentration using the flow cytometer. Cytometry *2*, 238–243.

Stewart, B.W., Kleihues, P., for Research on Cancer, I.A., and others (2003). World cancer report (IARC press Lyon).

Stumpferl, S.W., Brand, S.E., Jiang, J.C., Korona, B., Tiwari, A., Dai, J., Seo, J.-G., and Jazwinski, S.M. (2012). Natural genetic variation in yeast longevity. Genome Res.

Tatar, M. (2007). Diet restriction in Drosophila melanogaster. Design and analysis. Interdiscip. Top. Gerontol. *35*, 115–136.

Tatar, M. (2011). The plate half-full: status of research on the mechanisms of dietary restriction in Drosophila melanogaster. Exp. Gerontol. *46*, 363–368.

Timón-Gómez, A., Proft, M., and Pascual-Ahuir, A. (2013). Differential regulation of mitochondrial pyruvate carrier genes modulates respiratory capacity and stress tolerance in yeast. PLoS One *8*, e79405.

Tissenbaum, H. a, and Guarente, L. (2001). Increased dosage of a sir-2 gene extends lifespan in Caenorhabditis elegans. Nature *410*, 227–230.

Tissenbaum, H. a, and Guarente, L. (2002). Model organisms as a guide to mammalian aging. Dev.

Cell *2*, 9–19.

Tone, J., Yoshimura, A., Manabe, K., Murao, N., Sekito, T., Kawano-Kawada, M., and Kakinuma, Y. (2015). Characterization of Avt1p as a vacuolar proton/amino acid antiporter in Saccharomyces cerevisiae. Biosci. Biotechnol. Biochem. *79*, 782–789.

Toyama, B.H., and Hetzer, M.W. (2013). Protein homeostasis: live long, won't prosper. Nat. Rev. Mol. Cell Biol. *14*, 55–61.

Toyama, B.H., Savas, J.N., Park, S.K., Harris, M.S., Ingolia, N.T., Yates, J.R., and Hetzer, M.W. (2013). Identification of Long-Lived Proteins Reveals Exceptional Stability of Essential Cellular Structures. Cell *154*, 971–982.

Tran, J.R., Tomsic, L.R., and Brodsky, J.L. (2011). A Cdc48p-associated factor modulates endoplasmic reticulum-associated degradation, cell stress, and ubiquitinated protein homeostasis. J. Biol. Chem. *286*, 5744–5755.

Tran, P.T., Paoletti, A., and Chang, F. (2004). Imaging green fluorescent protein fusions in living fission yeast cells. Methods *33*, 220–225.

Truscott, R.J.W. (2010). Are Ancient Proteins Responsible for the Age-Related Decline in Health and Fitness? Rejuvenation Res. *13*, 83–89.

Truscott, R.J.W. (2011). Macromolecular deterioration as the ultimate constraint on human lifespan. Ageing Res. Rev. *10*, 397–403.

Veatch, J.R., McMurray, M. a, Nelson, Z.W., and Gottschling, D.E. (2009). Mitochondrial dysfunction leads to nuclear genome instability via an iron-sulfur cluster defect. Cell *137*, 1247–1258.

Verzijl, N., DeGroot, J., Thorpe, S.R., Bank, R.A., Shaw, J.N., Lyons, T.J., Bijlsma, J.W., Lafeber, F.P., Baynes, J.W., and TeKoppele, J.M. (2000). Effect of collagen turnover on the accumulation of advanced glycation end products. J. Biol. Chem. *275*, 39027–39031.

Verzijlbergen, K.F., Menendez-Benito, V., van Welsem, T., van Deventer, S.J., Lindstrom, D.L., Ovaa, H., Neefjes, J., Gottschling, D.E., and van Leeuwen, F. (2010). Recombination-induced tag exchange to track old and new proteins. Proc. Natl. Acad. Sci. U. S. A. *107*, 64–68.

Vizcaíno, J.A., Deutsch, E.W., Wang, R., Csordas, A., Reisinger, F., Ríos, D., Dianes, J.A., Sun,

Z., Farrah, T., Bandeira, N., et al. (2014). ProteomeXchange provides globally coordinated proteomics data submission and dissemination. Nat. Biotechnol. *32*, 223–226.

Vowinckel, J., Hartl, J., Butler, R., and Ralser, M. (2015). MitoLoc: A method for the simultaneous quantification of mitochondrial network morphology and membrane potential in single cells. Mitochondrion *24*, 77–86.

Walker, G., Houthoofd, K., Vanfleteren, J.R., and Gems, D. (2005). Dietary restriction in C. elegans: from rate-of-living effects to nutrient sensing pathways. Mech. Ageing Dev. *126*, 929–937.

Walther, T.C., Brickner, J.H., Aguilar, P.S., Bernales, S., Pantoja, C., and Walter, P. (2006). Eisosomes mark static sites of endocytosis. Nature *439*, 998–1003.

Weisman, L.S., Bacallao, R., and Wickner, W. (1987). Multiple methods of visualizing the yeast vacuole permit evaluation of its morphology and inheritance during the cell cycle. J. Cell Biol. *105*, 1539–1547.

World Health Organization (2010). The World Health Report (Geneva, Switzerland: WHO Press).

Xie, Z., Zhang, Y., Zou, K., Brandman, O., Luo, C., Ouyang, Q., and Li, H. (2012). Molecular Phenotyping of Aging in Single Yeast Cells Using a Novel Microfluidic Device. Aging Cell.

Yang, J., Dungrawala, H., Hua, H., Manukyan, A., Abraham, L., Lane, W., Mead, H., Wright, J., and Schneider, B.L. (2011). Cell size and growth rate are major determinants of replicative lifespan. Cell Cycle *10*, 144–155.

Yang, J., McCormick, M.A., Zheng, J., Xie, Z., Tsuchiya, M., Tsuchiyama, S., El-Samad, H., Ouyang, Q., Kaeberlein, M., Kennedy, B.K., et al. (2015). Systematic analysis of asymmetric partitioning of yeast proteome between mother and daughter cells reveals “aging factors” and mechanism of lifespan asymmetry. Proc. Natl. Acad. Sci. U. S. A. *112*, 11977–11982.

Zhou, C., Slaughter, B.D., Unruh, J.R., Eldakak, A., Rubinstein, B., and Li, R. (2011). Motility and segregation of Hsp104-associated protein aggregates in budding yeast. Cell *147*, 1186–1196.

Zimmerman, J. a, Malloy, V., Krajcik, R., and Orentreich, N. (2003). Nutritional control of aging. Exp. Gerontol. *38*, 47–52.

APPENDIX – LIFESPAN ASSAY PROTOCOL

Materials Needed:
NHS-Rhodamine – kept as dry powder
NHS-Fluorescein – kept as dry powder
NHS-Dylight680 – kept as 1mg/ml stock in DMSO
Growth Media – Media should be prewarmed to 30
37% Formaldehyde
****This protocol is written as if a FACS protocol already exists. If you need to create a new protocol be sure to prepare all necessary single stained controls. ****
Day -2:

- Start 1-5 ml cultures. Grow overnight to reach saturation.
    - one strain is to be tested for life span
    - other strain is a strain of “normal life span”

Day -1:

- Start 50ml cultures from .5ul-2ul of saturated culture. Grow for 14-17 hours.
- Keep the rest of the saturated culture on your bench to use the next day during cell pelleting.

Day 1:
==Labelling Cells==

- Count cell density of overnight culture -- should between 1E6 and 1E7 cells/ml
- Spin down 50ml log cultures, resuspend in 1x PBS and transfer to eppendorf tube
- Wash cells several times with PBS to remove traces of YPD that will interfere with the labeling reaction (spins at 1800 g)
- Resuspend cells in 800ul PBS, then transfer 400ul to separate tube. 1 tube will be labeled with fluorescein, 1 tube will be labeled with rhodamine.
- Make NHS-Rhodamine and NHS-Fluorescein labeling solutions:
    - Weigh out ~1mg of each. Be extremely careful as anything this touches will be stained
    - Resuspend each in 1xPBS at 1mg/ml
    - Spin solutions at full speed on bench-top centrifuge to pellet any insoluble particles
- Add 400 ul of NHS-Rhodamine solution to 1 tube of each strain; add 400 ul NHS-fluorescein to the remaining tube of each strain.
    - Be sure to place pipet tip in center of the tube to avoid any pelleted stain as well as stain that forms a film on the surface.
- Stain cells for 15-20 minutes on rotator
- Wash cells in PBS until washes are near colorless
- Resuspend cells in YPD at 2E6 cells/ml
- Let cells recover at 30 for 2 hours

==Aging Cells==
After labeled cells have recovered for 2 hours:

- Inoculate 6 or 10-- 6ml YPD+ED(1uM)+Amp(50ug/ml)

- 1-3 – Strain#1-Rhodamine & Strain#2-Fluorescein --1e4 cells/ml each
- 4-6 – Strain#2-Rhodamine & Strain#1-Fluorescein--1e4 cells/ml each

--Optional--

- 7 – Strain #1-Rhodamine 2E4 cells/ml
- 8 – Strain #1-Fluorescien 2E4 cells/ml
- 9 – Strain #2-Rhodamine 2E4 cells/ml
- 10 – Strain #2- Fluorescein 2E4 cells/ml

**If using cell density and volumes suggested you can simply add 30ul of each recovery culture without recounting cells **

== Taking Samples ==

Timepoints suggested are 0,3,24,48. (Two early timepoints are important during data analysis)

For each sample:

- Remove 1ml of aging culture
- ==Optional==: Add 10-100ul of density standard (usually a population of fixed, double labeled cells. You want their final density to be around 2E4 /ml)
- Spin culture at 1,800g to pellet cells. Wash several times in PBS. Resuspend in 100ul of PBS.
  - For early timepoints (0 and 3) add 10ul of an unlabeled saturated culture. These cells help pellet the dilute labeled cells in the culture and prevent cell loss.
- Make Live/Dead cell stain:
  - Dilute 1mg/ml NHS-Dylight680 to 50ug/ml (2ul of 1mg/ml stock into 1ml of PBS)
- Add 100ul of Live/Dead stain to 100ul of cells in each sample
- Stain for 20 minutes on rotator
- Add 25ul of 37% formaldehyde and fix for 10-15 minutes (formaldehyle will quench excess stain and prevent it from staining cells during the fix step)
- Spin down cells, wash once with PBS, and suspend in 500ul to 1ml of PBS

== Preparing sample for FACS Analyzer ==

- Sonicate each sample
  - Setting 3 for 5 1-second pulse

==Flow cytometry analysis==

- Analyze samples on a flow cytometer capable of resolving each population of cells (Rhodamine+, Fluorescein+, Unlabeled daughter cells).
- Collect at least 1000 events from each population of interest – preferable 10,000.

VITA

RESEARCH EXPERIENCE

Gottschling Lab, 2010-2016

Basic Science Division, Fred Hutchinson Cancer Research Center

PhD Student – Using budding yeast to investigate the genetics and molecular mechanisms of the aging process.

Tompa Lab, 2010

Computer Science Department, University of Washington

Graduate Program Rotation – Using computational tools to identify the sequence motif and regulatory targets of TTK69, a transcription factor with important roles during *Drosophila* development.

Berg Lab, 2009

Genome Science Department, University of Washington

Graduate Program Rotation – Developing a fluorescent in situ hybridization technique to identify targets and quantify effects of the transcription factor, TTK69, during *Drosophila* tubulogenesis with single cell resolution.

Hunter Lab, 2006-2008

Microbiology Department, University of California, Davis

Undergraduate Researcher and Junior Specialist – Using budding yeast and mice to investigate the genetics and molecular dynamics of double-strand DNA break repair.

EDUCATION

PhD	University of Washington & FHCRC Molecular and Cell Biology	2009-2016
BS	University of California, Davis Biochemistry and Molecular Biology	2004-2008

FELLOWSHIPS, AWARDS and HONORS

NIH NRSA Predoctoral Fellowship F31 - F31AG041579, 2012 – 2016

Cellular and Molecular Biology Training Grant – T32 GM007270, 2011 – 2012

Graduated with High Honors in Biochemistry and Molecular Biology from UC Davis, 2008

Departmental Citation Award, Biochemistry and Molecular Biology, UC Davis, 2008

President's Undergraduate Research Fellowship, 2007

PUBLICATIONS

Thayer NH, Leverich CK, Fitzgibbon MP, Nelson ZW, Henderson KA, Gafken PR, Hsu JJ, Gottschling DE. *Identification of long-lived proteins retained in cells undergoing repeated asymmetric divisions*. *PNAS. 2014* doi: 10.1073/pnas.1416079111.

Highlighted by:

-Current Biology Dispatch – Zhou C, Li R, Kennedy BK. *Life History: Mother-Specific Proteins that Promote Aging* – doi: 10.1016/j.cub.2014.11.007.

-Faculty of 1000 Biology (http://f1000.com/prime/718879970)

Peters NC, Thayer NH, Kerr SA, Tompa M, Berg CA. *Following the 'tracks': Tramtrack69 regulates epithelial tube expansion in the Drosophila ovary through Paxillin, Dynamin, and the homeobox protein Mirror*. *Developmental Biology. 2013* doi: 10.1016/j.ydbio.2013.03.017.

Bzymek M, Thayer NH, Oh SD, Kleckner N, Hunter N. *Double Holliday junctions are intermediates of DNA break repair*. *Nature. 2010* doi: 10.1038/nature08868.

Highlighted by:

-Faculty of 1000 Biology (http://f1000.com/prime/2744956)